UNIVERSITA' DEGLI STUDI DELL'INSUBRIA

DOTTORATO DI RICERCA IN SCIENZE
DELLA VITA E BIOTECNOLOGIE

XXXIII CICLO

D-amino acids in Alzheimer's disease (with a special focus on D-aspartate catabolism)

D-amminoacidi nella malattia Alzheimer (con un focus speciale sul catabolismo del D-aspartato)

Docente guida: Prof. Luciano Piubelli
Tutor: Prof. Silvia Sacchi

Tesi di dottorato di:
Valentina Rabattoni
705688

Dip. Biotecnologie e Scienze della Vita - Università degli Studi dell'Insubria
Anno accademico 2019/2020

Contents

List of abbreviations

AD: Alzheimer's disease

ATP: adenosine triphosphate

CDR: clinical dementia rating

CHX: cycloheximide

CNS: central nervous system

CQ: chloroquine

CSF: cerebro spinal fluid

D-AAs: D-amino acids

D-Asp: D-aspartate

D-Glu: D-glutamate

D-Ser: D-serine

DAAO: D-amino acid oxidase

DASPO: D-aspartate oxidase

FAD: flavin adenine dinucleotide

H_2O_2: hydrogen peroxide

hDAAO: human D-amino acid oxidase

hDASPO: human D-aspartate oxidase

HS: healthy subjects

IP: immunoprecipitation

k_{cat}: turnover number

K_d: dissociation constant

K_i: inhibitory constant

K_m: Michaelis constant

LTD: long-term depression

LTP: long-term potentiation

MG132: benzyloxycarbonyl-L-leucyl-L-leucyl-L-leucinal

mGluR: Metabotropic glutamate receptor

NMDAr: N-methyl-D-aspartate receptor

PKA: protein kinase A

PTMs: post-translational modifications

PTS1: peroxisomal targeting signal 1

UPS: ubiquitin-proteasome system

Abstract

D-amino acids (D-AAs), the enantiomeric counterparts of L-amino acids, were long considered to be absent or non-functional in mammals. Today, they are acknowledged to be involved in numerous physiological processes and different pathologies. Several studies showed an alteration of both D-aspartate (D-Asp) and D-serine (D-Ser) levels in tissues and/or biological fluids of Alzheimer's disease (AD) patients, although controversial results have been published. Here, I investigated whether the levels of these two D-AAs are actually deregulated in the serum of AD patients by using a standardized, well-established analytical procedure. These studies highlighted a significant correlation between serum D-Ser level and AD, thus allowing to propose this parameter as a precocious and easily affordable biomarker for AD diagnosis.

Concerning D-Asp, this molecule is involved in important physiological functions, such as N-methyl-D-aspartate receptor (NMDAr)-mediated neurotransmission and the regulation of (neuro) endocrine processes. However, contrary to D-Ser, little is known about its metabolism in humans: the D-Asp synthetic pathway is still unclear and its levels are thought to be mainly regulated by the FAD dependent catabolic flavoenzyme human D-aspartate oxidase (hDASPO). Thus, my further studies aimed at shedding light on the molecular processes modulating the cellular levels of D-Asp by acting on its catabolic enzyme. In particular, I focused on two reported isoforms of the human enzyme, constituted by 341 and 369 amino acids: their functional properties, degradation kinetics and mechanisms involved in protein turnover were investigated by ectopically expressing hDASPO_341 and, for the first time, hDASPO_369 isoforms in a human cell line. These studies demonstrated that both isoforms are active (with a similar specific activity), localize to the peroxisomes, are highly stable and primarily degraded through the ubiquitin-proteasome system.

I further deep inside the mechanisms that might regulate the activity of hDASPO (and, in turn, D-Asp cellular levels) by evaluating the effects of specific post-translational modifications. hDASPO can be *in vitro* nitrosylated and, mildly, sulfhydrated but both

modifications do not seem to affect its catalytic activity, as also demonstrated at the cellular level.

The elucidation of the regulation mechanisms of this human flavoenzyme will permit to clarify important physiological processes and might allow the identification of novel targets for the treatment of human diseases in which the NMDAr mediated neurotransmission is likely to be affected by D-Asp levels.

1. Introduction

With the only exception of glycine, all amino acids are chiral molecules that naturally occur in two structures, conventionally called L- and D-enantiomers. Although the two stereoisomers show almost identical chemical and physical properties, only the L-amino acids were selected during biological evolution for ribosomal protein synthesis. For a long time, it was thus believed that D-amino acids (D-AAs) were unnatural, non-functional isomers, thought to only be present in the peptidoglycans of bacterial cell walls and certain antibiotic peptides. However, in the '90s the development of more sensitive and enantioselective analytical techniques revealed significant concentrations of D-AAs also in higher organisms, including mammals, both in free form or as components of peptides and proteins (Hashimoto et al., 1992; Powell et al., 1992; Armstrong et al., 1993; Schell et al., 1995).

In this PhD thesis, we focus on free D-AAs, which may originate from multiple sources. For humans, diet is considered the main source of D-AAs (Csapó et al., 2009). Indeed, D-AAs are naturally present in fermented products, deriving from the starting materials or from microbial activity during fermentation, as reviewed in (Marcone et al., 2020). They can also be produced during food processing by racemization of the L-enantiomers due to heat and alkaline pH treatments (Marcone et al., 2020). Beside this, it is estimated that approximately one-third of the total human D-AAs content derives from microbial synthesis (Friedman, 2010). Accordingly, a recent evidence has highlighted the role of gut microbiota as a key contributor to the systemic abundance of D-AAs in mammals. High concentrations of D-Ala, D-Asp, D-Glu, and D-Pro (~200–500 nmol/g) were detected in the cecal contents from adult mice with resident microbiota, whereas low levels of D-Asp were detected in germ-free mice (Sasabe et al., 2016). Furthermore, free D-AAs can derive from endogenous biosynthesis: the racemization of the L-enantiomer by the activity of racemases. Currently, two amino acid racemases have been found in animals: serine racemase (SR, EC 5.1.1.18) and aspartate racemase (AR, EC 5.1.1.13) (Wolosker et al., 1999; Kim et al., 2010), but only the first one has been detected in humans (Xia et al., 2004). Indeed, despite AR activity has been measured in numerous tissues of rats and mice (Topo et al., 2010a), the identity of the actual enzyme in mammals is still under debate (Kim et al., 2010; Matsuda et al., 2015; Tanaka-Hayashi et al., 2015). However,

D-Asp content in animal tissues undergoes significative variations during development (see below), suggesting that it can be endogenously synthesized: the presence of this D-AA cannot be explained as derived from exogenous sources, especially in the brain where D-AAs transport appears to be limited by the blood-brain barrier (Oldendorf, 1973).

D-serine (D-Ser) and D-Asp are the most abundant D-AAs in mammals (Ohide et al., 2011) and the most commonly studied in relation to human physiology. Indeed, both are involved in multiple processes in the central nervous system (CNS) as well as in various endocrine tissues. For reviews see (Fuchs et al., 2005; Kiriyama and Nochi, 2016; Sasabe and Suzuki, 2019). D-Ser is present at low concentrations in peripheral tissues (such as kidney, spleen, pituitary and adrenal glands) and physiological fluids (plasma, serum and urine), whereas high concentrations of this molecule have been detected in the brain (especially in the forebrain) (Nagata et al., 1994; Schell et al., 1995; Hashimoto and Oka, 1997). Here it acts as a key co-agonist of N-methyl-D-aspartate receptors (NMDAr): it binds to the glycine site on the NR1 subunit of the receptor, thus controlling its activation status together with the agonist L-glutamate (L-Glu) bound to the NR2 subunit (Mothet et al., 2000). These receptors are involved in brain development and play a crucial role in learning and memory formation, as reviewed in (Riedel et al., 2003; Ewald and Cline, 2008). According to its role, alterations in D-Ser signaling and metabolism have been related to several neurophysiological disorders such as schizophrenia, ischemia, epilepsy as well as neurodegenerative diseases in which NMDAr-mediated neurotransmission appears especially affected (Sasabe et al., 2007; Klatte et al., 2013; Cho et al., 2016).

On the other hand, the presence of endogenous free D-Asp has been described in several tissues, in particular in the endocrine system and in the CNS. In neuroendocrine and endocrine tissues (pineal gland, pituitary gland and testicles), D-Asp levels increase during the postnatal and adult phase together with their functional maturation and it has been showed to be involved in the synthesis and release of several hormones, such as glucocorticoids, prolactin, oxytocin and steroids, as reviewed by (D'Aniello, 2007). Also in the brain D-Asp undergoes a definite developmental regulation, intriguingly opposite to the endocrine glands one: it is present at high levels during embryonic and

early post-natal phases, then it markedly decreases in the subsequent phases, without further changes until adulthood (Dunlop et al., 1986; Hashimoto et al., 1993; Punzo et al., 2016), so it appears that in the brain this molecule is kept to relatively low concentrations.

In mammals, D-Asp has gained interest owing to its involvement in important physiological processes and pathological states, recently reviewed by (Katane and Homma, 2010; Ota et al., 2012). In the CNS, D-Asp behaves as a classical neurotransmitter (D'Aniello et al., 2011) and several studies suggest it can play a neuromodulatory role at glutamatergic synapses due to a relatively high affinity for the glutamate site on the NR2 subunit (Errico et al., 2011b). Indeed, D-Asp may act as an endogenous agonist of NMDAr, thereby activating this subclass of ionotropic glutamate receptors (Errico et al., 2008a; Errico et al., 2008b). D-Asp is also able to activate the metabotropic glutamate receptor 5 (mGluR5) in neonate rat hippocampal and cortical slices (Molinaro et al., 2010). Furthermore, recent studies have indicated that this D-AA induces the *in vivo* release of L-Glu in mice cortex (Cristino et al., 2015; Sacchi et al., 2017) through the presynaptic activation of NMDA, AMPA, and mGlu5 receptors (Sacchi et al., 2017).

Based on these findings, D-Asp has been proposed as a candidate signaling molecule involved in the cellular events related to neural development (such as neurogenesis, proliferation, and differentiation), and influencing brain morphology and behavior at adulthood. Indeed, many of these fundamental processes are critically regulated by the glutamatergic NMDA and mGlu5 receptors (Di Giorgi-Gerevini et al., 2005; Ikonomidou, 2009; Jansson and Åkerman, 2014).

Two flavoenzymes, i.e. D-aspartate oxidase (DASPO or DDO, EC 1.4.3.1) and D-amino acid oxidase (DAAO or DAO, EC 1.4.3.3), are responsible for the degradation of D-Asp and D-Ser, respectively. DASPO and DAAO share a high amino acid sequence identity and are thought to derive from a common ancestor (Negri et al., 1992; Takahashi et al., 2004).

DAAO was discovered first, 85 years ago in pig kidney by H. Krebs (Krebs, 1935). Whereas DASPO was discovered in rabbit 14 years later by J. L. Still, who described the activity of

an oxidase that specifically catalyzes the oxidation of D-Asp to oxaloacetic acid in kidney and liver extracts (Still et al., 1949).

Since then, the two flavoenzymes have been identified in a variety of organisms. They have been identified in all kingdoms with few exceptions: plants in the case of DAAO, bacteria and plants in the case of DASPO. Both enzymes' targeting is ensured by the presence of a type-1 peroxisomal targeting signal (PTS1) sequence at the C-terminal, and they are FAD-containing flavoproteins with cofactor non-covalently bound to the protein moiety.

DAAO catalyzes the specific oxidative deamination of hydrophobic, neutral, polar and basic D-AAs (Pollegioni et al., 2007), whereas DASPO is stereospecific for acidic D-AAs: in addition to D-Asp, DASPO can oxidize *in vitro* with high efficiency N-methyl-D-Asp (NMDA) and, to a lesser extent, D-glutamate (D-Glu) (Katane and Homma, 2010). The reactions catalyzed by the two flavoproteins follow the same scheme (reported for DASPO in Fig. 1) which involves two steps: i) the dehydrogenation of D-AAs to produce the corresponding imino acid, with the concomitant reduction of FAD (Fig. 1a); ii) the re-oxidation of reduced flavin by molecular oxygen, yielding hydrogen peroxide (Fig. 1b). In aqueous solutions the imino acid product spontaneously hydrolyzes to the corresponding 2-ketoacid and ammonia (Fig. 1c).

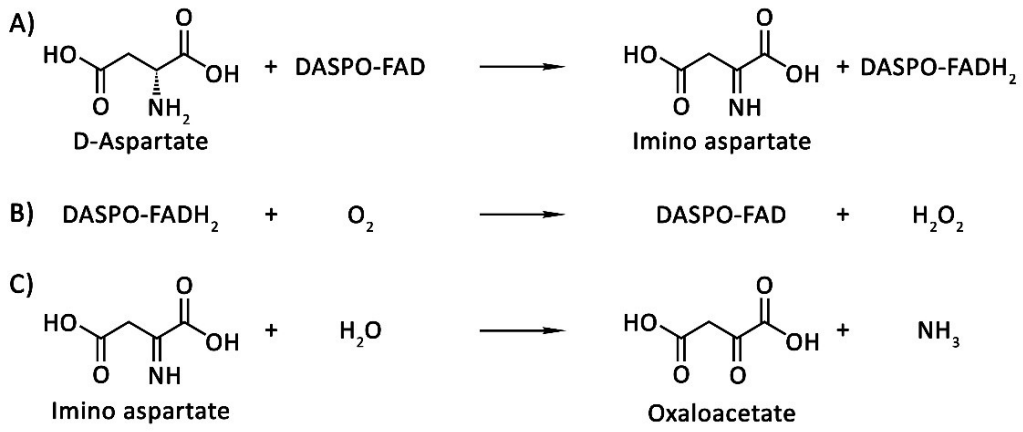

Fig. 1: Scheme of the reaction catalyzed by DASPO. (a) DASPO catalyzes the dehydrogenation of D-aspartate to generate the corresponding imino acid, coupled with the reduction of the flavin cofactor; (b) FAD then spontaneously reoxidizes in the presence of O_2, yielding H_2O_2; (c) Finally, the imino acid non-enzymatically hydrolyzes to the corresponding 2-oxo acid and NH_3.

By regulating D-Ser and D-Asp levels, DAAO and DASPO exert a pivotal role in important physiological processes in which these D-AAs are involved, including neuromodulation in the CNS of mammals.

DAAO has been extensively investigated: the chemical aspects of the flavoenzyme reactivity and its biochemical properties were described in detail between 1950 and 1980, and it soon became the prototype of FAD-dependent oxidases (Pilone, 2000). However, the biochemical properties and the structure-function relationships of the human enzyme (hDAAO) have been investigated more recently (Molla et al., 2006; Sacchi et al., 2012; Murtas et al., 2017) after the crystallographic structure was solved (Kawazoe et al., 2006), and several studies regarding the modulation of its activity are still ongoing.

On the other hand, although the biochemical properties of human DASPO have been studied since the second half of the 90s (Setoyama and Miura, 1997), the first three-dimensional structure of this enzyme was only published this year (Molla et al., 2020) and consequently, several of its fundamental properties are still poorly understood. Moreover, much remains to be uncovered concerning the regulation of the enzyme levels and activity at the cellular level. Investigating these processes is of utmost relevance since they will provide crucial information concerning the regulation exerted by hDASPO on D-Asp levels in the brain.

1.1. D-Aspartate oxidase: distribution and localization

DASPO activity has been detected in various organisms, such as yeasts, cephalopods, gastropods, amphibians, fishes, birds and mammals, including humans (D'Aniello et al., 1975; Daves and Johnston, 1975; Kera et al., 1992; Kera et al., 1996; Yamada et al., 1996; Parveen et al., 2001; Sarower et al., 2003).

In mammals, the enzyme is present in various tissues. The highest activity is found in the kidney, followed by liver and brain, while is relatively low in other peripheral tissues (Yamada et al., 1988; Van Veldhoven et al., 1991).

Immunohistochemical analysis in bovine kidney and liver revealed that the enzyme is localized to the epithelial cells of proximal renal tubules and to hepatocytes, respectively

(Zaar, 1996). DASPO content in kidney and liver of rodents is relatively low at birth and rapidly increase thereafter (Van Veldhoven et al., 1991; D'Aniello et al., 1993; Kera et al., 1993). Accordingly, D-Asp content in these tissues decreases as development proceeds (Dunlop et al., 1986; D'Aniello et al., 1993).

As reported in studies performed in mice and humans (Hashimoto et al., 1993), in the brain DASPO activity is very low during embryonic stages, but rapidly increases after birth until 6 weeks of life (Van Veldhoven et al., 1991), resulting in a substantial decrease in D-Asp levels (D'Aniello et al., 1993; Kera et al., 1993; Schell et al., 1997). Thus, it has been proposed that the onset and progressive increase of DASPO activity strictly controls the postnatal levels of D-Asp.

Recent findings indicate that the gradual decrease of D-Asp content between the fifteenth embryonic day (E15) and the sixty postnatal day (P60) (Fig. 2A) is paralleled by a complementary increased transcription of *Ddo* gene (Fig. 2B,D). This increased transcription has been shown to be due to a progressive demethylation in the CpG sites of the putative regulatory region of *Ddo* gene promoter (Fig. 2C), thus suggesting an epigenetic regulation mechanism (Punzo et al., 2016).

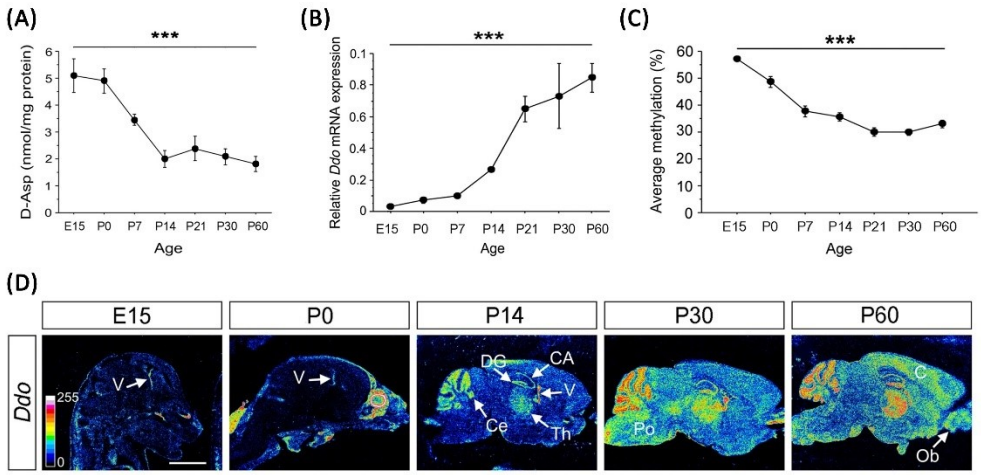

Fig. 2: Variation of D-Asp concentration and *Ddo* mRNA expression levels in mouse brain during ontogenesis. (A) Average content of D-Asp determined by HPLC analysis at different ages. (B) qRT-PCR analysis of the expression levels of the mRNA encoding DASPO in mice whole brain homogenates. (C) Average methylation degree of the eight CpG sites of *Ddo* gene regulatory region in mouse brain during ontogenesis. (D) Autoradiographs representing sagittal sections of mouse brain at E15, P0, P14, P30, and P60 showing *Ddo* mRNA expression pattern. V, Ependymal cell layer of the ventricle; CA, cornu ammonis area; Ce, cerebellum; DG, dentate gyrus; Th, thalamus; Po, pons; C, cortex; Ob, olfactory bulb. Modified from (Punzo et al., 2016).

According to the proposed physiological role in controlling free D-Asp endogenous levels, several studies reported that DASPO expression in different brain regions and cell populations is reciprocal to D-Asp localization: the enzyme concentration is higher in nerve cells, such as the pyramidal neurons in the cerebral cortex and hippocampus, and the olfactory epithelial neurons, in which D-Asp is barely detectable (Schell et al., 1997). In rat brain, DASPO activity is also present in the choroid plexus, ependyma, the granule cell layer and white matter (Schell et al., 1997). On the other hand, D-Asp is localized in the pituitary gland, in particular in the anterior and posterior lobes, while DASPO activity has been detected exclusively in the intermediate lobe (Schell et al., 1997). No DASPO activity has been instead detected in the pineal gland, where the D-Asp content is very high (Hamase et al., 1997).

The intracellular localization of DASPO in the peroxisomes has been demonstrated by electron-microscopic analyses of rat kidney and bovine kidney and liver, as well as rat and human brain (Beard, 1990; Zaar et al., 2002). This localization allows the elimination by catalase of the H_2O_2 produced by the enzyme which would be otherwise toxic to the cell.

Most organisms possess a single *Ddo* gene, an exception is represented by the nematode *Caenorhabditis elegans* which has three different genes (*Ddo-1, Ddo-2,* and *Ddo-3*) encoding functional DASPOs in its genome (Katane et al., 2010b). The gene product of *Ddo-1* (C47Ap) contains a PTS1 motif at the C-terminus, which is absent in *Ddo-2* (F18Ep) and *Ddo-3* (F20Hp) products. The latter in addition, shows a secretion signal at the N-terminus and was demonstrated to be secreted into *C. elegans* seminal fluid (Saitoh et al., 2019), while *Ddo-2* product lacks any known localization signal peptides and is supposed to localize to the cytoplasm.

In human, *Ddo* gene is present in a single copy located on chromosome 6 (region 6q21) and it likely encodes different mRNA forms. In fact, the UniProtKB database reports three different isoforms for hDASPO (Fig. 3, identifier Q99489): isoform 1 (hDASPO 341), referred to as the "canonical isoform", consists of 341 amino acid residues and is homologous to the only known protein form in rodents; isoform 2 (hDASPO 282), which

is identical to hDASPO 341 but lacks 59 residues in the central region (95-153 in the canonical isoform) and is probably originated by alternative splicing of the transcript; and isoform 3 (hDASPO 369), apparently highly preserved in primates and characterized by the presence of 28 additional N-terminal residues, probably originated by the recognition of an upstream alternative start codon in the protein encoding transcript.

To date, the functional properties of the "non canonical" protein isoforms have been poorly investigated: hDASPO 282 was expressed in *E. coli* but the recombinant protein was insoluble and fully produced as inclusion bodies (Setoyama and Miura, 1997); on the other hand, hDASPO 369 has never been expressed. Thus, the physiological role of these two protein isoforms has yet to be elucidated.

```
hDASPO_341      ----------------------------MDTARIAVVGAGVVGLSTAVCISKLVPRCSVT
hDASPO_369      MRPARHWETRFGARDFGGFQDCFFRDRLMDTARIAVVGAGVVGLSTAVCISKLVPRCSVT
hDASPO_282      ----------------------------MDTARIAVVGAGVVGLSTAVCISKLVPRCSVT
                                             ********************************

hDASPO_341      IISDKFTPDTTSDVAAGMLIPHTYPDTPIHTQKQWFRETFNHLFAIANSAEAGDAGVHLV
hDASPO_369      IISDKFTPDTTSDVAAGMLIPHTYPDTPIHTQKQWFRETFNHLFAIANSAEAGDAGVHLV
hDASPO_282      IISDKFTPDTTSDVAAGMLIPHTYPDTPIHTQKQWFRETFNHLFAIANSAEAGDAGVHLV
                ************************************************************

hDASPO_341      SGWQIFQSTPTEEVPFWADVVLGFRKMTEAELKKFPQYVFGQAFTTLKCECPAYLPWLEK
hDASPO_369      SGWQIFQSTPTEEVPFWADVVLGFRKMTEAELKKFPQYVFGQAFTTLKCECPAYLPWLEK
hDASPO_282      S-----------------------------------------------------------
                *

hDASPO_341      RIKGSGGWTLTRRIEDLWELHPSFDIVVNCSGLGSRQLAGDSKIFPVRGQVLQVQAPWVE
hDASPO_369      RIKGSGGWTLTRRIEDLWELHPSFDIVVNCSGLGSRQLAGDSKIFPVRGQVLQVQAPWVE
hDASPO_282      GIKGSGGWTLTRRIEDLWELHPSFDIVVNCSGLGSRQLAGDSKIFPVRGQVLQVQAPWVE
                 ************************************************************

hDASPO_341      HFIRDGSGLTYIYPGTSHVTLGGTRQKGDWNLSPDAENSREILSRCCALEPSLHGACNIR
hDASPO_369      HFIRDGSGLTYIYPGTSHVTLGGTRQKGDWNLSPDAENSREILSRCCALEPSLHGACNIR
hDASPO_282      HFIRDGSGLTYIYPGTSHVTLGGTRQKGDWNLSPDAENSREILSRCCALEPSLHGACNIR
                ************************************************************

hDASPO_341      EKVGLRPYRPGVRLQTELLARDGQRLPVVHHYGHGSGGISVHWGTALEAARLVSECVHAL
hDASPO_369      EKVGLRPYRPGVRLQTELLARDGQRLPVVHHYGHGSGGISVHWGTALEAARLVSECVHAL
hDASPO_282      EKVGLRPYRPGVRLQTELLARDGQRLPVVHHYGHGSGGISVHWGTALEAARLVSECVHAL
                ************************************************************

hDASPO_341      RTPIPKSNL
hDASPO_369      RTPIPKSNL
hDASPO_282      RTPIPKSNL
                *********
```

Fig. 3: Amino acid sequences alignment of the three known hDASPO isoforms (constituted by 341, 369 and 282 residues).

1.2. DASPO physiological role in mammals

The physiological role of DASPO in mammals remained elusive until the mid-80s, when substantial amounts of endogenous free D-Asp were detected in several tissues of mice, rats and humans (Dunlop et al., 1986; Neidle and Dunlop, 1990; Hashimoto et al., 1993). The physiological role of the enzyme was mainly investigated through the generation of DASPO-deficient mouse models in which the *Ddo* gene has been deleted (*Ddo*$^{-/-}$ mice) (Errico et al., 2006; Han et al., 2015): a markedly increased (up to 20-fold) endogenous free D-Asp level was present both in the whole brain and in the peripheral organs of these animals. In particular, the immunohistochemical analysis revealed a high D-Asp content in pinealocytes, cortical and hippocampal neurons, in the intermediate lobe of the pituitary gland, adrenals, ovaries and testes (Huang et al., 2006).

These findings, together with the previously described inverse correlation, both spatial and temporal, between D-Asp and DASPO (D'Aniello et al., 1993; Schell et al., 1997), strongly suggested that the mammalian enzyme degrades endogenous D-Asp as a physiological substrate *in vivo*, thereby regulating its cellular level.

In order to increase D-Asp levels, a pharmacological approach based on oral or intraperitoneal administration of D-Asp to C57BL/6J and DDY mice was also pursued. In these mouse models, HPLC analysis revealed a significant increase in D-Asp levels in the brain, albeit to a lesser extent than those detected in *Ddo*$^{-/-}$ mice (Yamada et al., 1989; Errico et al., 2008a; Errico et al., 2008b; Errico et al., 2011b). Taken together, these results strongly suggest that mammalian DASPO mediates the elimination of accumulated exogenous D-Asp, in addition to strictly regulating its endogenous levels.

Conversely, DASPO does not play a major role in the elimination of D-Glu: the *Ddo* gene knockout caused no significant increase in D-Glu levels (Han et al., 2015); accordingly, the catalytic efficiencies of mammalian DASPOs for D-Glu are considerably lower than those toward D-Asp (see Table 1, paragraph 1.5). Indeed, D-Glu is considered to be primarily metabolized by D-glutamate cyclase, which catalyzes the reversible reaction between D-Glu and 5-oxo-D-proline with H_2O (Ariyoshi et al., 2017).

In *Ddo*$^{-/-}$ mice, the dramatic increase of D-Asp in the intermediate lobe of the pituitary gland is paralleled with markedly lower levels of pituitary proopiomelanocortin (POMC)

and α-melanocyte-stimulating hormone (α-MSH). Accordingly, these animals showed altered α-MSH-related behaviors such as increased body mass, sexual deficits and decreased frequency of autogrooming (Huang et al., 2006).

On the other hand, exogenous D-Asp administration to rats induced a significant dose- and time-dependent release of serum prolactin (D'Aniello et al., 2000a), a rise in growth hormone level (D'Aniello et al., 2000b), and an increase in luteinizing hormone levels (D'Aniello et al., 1996, 2000b). Together, these findings strongly point to D-Asp as a physiological modulator of the neuroendocrine system and reproductive activity.

The *in vivo* consequences of the persistent deregulation of D-Asp levels in *Ddo*$^{-/-}$ and D-Asp-administered mouse models was further investigated through several electrophysiological and behavioural tests. Among the different brain areas, hippocampus represents an elective region for studying DASPO role and evaluating the effects of alterations in D-Asp catabolism. Indeed, very low concentrations of this D-AA are present in the adult hippocampus due to a high expression of DASPO (Schell et al., 1997; Zaar et al., 2002). The hippocampus is closely involved in learning and memory processes and is highly enriched in NMDArs, which could be activated by the non-physiological higher levels of D-Asp. Indeed, the electrophysiological analyses performed on hippocampal sections of both *Ddo*$^{-/-}$ and D-Asp- administered animals showed increased NMDAr-dependent long-term potentiation (LTP) (Errico et al., 2008a; Errico et al., 2008b; Errico et al., 2011a; Errico et al., 2011b; Errico et al., 2014): the higher D-Asp concentration in DASPO-deficient mice stabilizes the hippocampal LTP by preventing synaptic depotentiation (Errico et al., 2008a). These observations support the proposed role for D-Asp in the modulation of glutamatergic neurotransmission.

Among the different forms of synaptic plasticity, the hippocampal NMDAr-dependent LTP has a pivotal role in the processes involved in the spatial memory formation (Errico et al., 2012). Consistent with the D-Asp-dependent enhancement in the functional and structural synaptic plasticity, behavioral studies showed a significant improvement in spatial learning and memory abilities in both in *Ddo*$^{-/-}$ and D-Asp-treated animals, although in the latter to a lesser extent (Errico et al., 2011b; Errico et al., 2008a; Topo et al., 2010b).

Changes in synaptic functions are commonly associated with structural synaptic variations: accordingly, both mice models show increased dendritic length and spine density and greater dendritic complexity in pyramidal neurons of the prefrontal cortex and hippocampus (Errico et al., 2014).

However, it is known that if on the one hand NMDArs promote synaptic strength and connectivity, on the other they can cause neuronal death if their stimulation lasts too long (Hardingham and Bading, 2003). Indeed, subsequent studies have highlighted that the persistent deregulation of D-Asp levels causes age-dependent effects: an improvement of cognitive performances related to NMDAr-mediated neurotransmission in young *Ddo*$^{-/-}$ mice (4/5-month-old), followed by an abnormally precocious decay of these processes, leading to precocious brain aging, in individuals in late adulthood (13-/14-month-old). (Errico et al., 2011a; Errico et al., 2011b; Cristino et al., 2015). Similar results were also obtained by repeating the behavioral studies on mice chronically treated with D-Asp, although in this case the deterioration of the functions was shown to be reversible (Errico et al., 2011b).

Based on these findings, a neuroprotective role of DASPO has been proposed: the enzyme prevents NMDAr hyper-stimulation through the strict regulation of postnatal brain levels of D-Asp, thus preventing accelerated neurodegenerative processes (Cristino et al., 2015; Punzo et al., 2016).

1.3. Biochemical properties

The first DASPO to be purified and characterized *in vitro* was the one from bovine kidney (bDASPO) (Negri et al., 1987). Subsequently, the recombinant mouse (mDASPO), rat (rDASPO) and human (hDASPO) proteins were expressed in *E. coli* and partially characterized (Katane et al., 2007). In particular, several properties of the recombinant hDASPO have been investigated.

The enzyme exhibits the classical properties of the FAD-containing flavooxidases family: it shows the typical absorbance spectrum with absorption peaks at ~280, 370 and 455 nm; in anaerobic condition it is fully reduced after the addition of the substrate and it stabilizes the anionic red flavin semiquinone.

hDASPO enzymatic activity is optimal at alkaline pH values ranging from 8.3 and 12.5, while the enzyme is inactive at pH values below 6 and above 13 (Katane et al., 2015a). Other mammalian DASPOs share a very similar pH profile (Katane et al., 2018), with the only exception of the one from pig kidney, whose activity is higher at neutral pH (Yamamoto et al., 2007). The optimal temperature for hDASPO activity (on D-Asp at pH 8.3) is ~45 °C (Katane et al., 2015a), as for both rat and mouse DASPOs (Katane et al., 2018). The human enzyme is relatively stable at alkaline pHs (in the range 8 - 11) and at thermal denaturation (only 9% of the activity was lost after 30 minutes of incubation at 50 °C). Compared to hDASPO, the murine enzyme is stable at a wider range of pH values (in the 4-10 pH range) but is more sensitive to temperature: it gradually inactivates after 60 minutes of incubation at temperatures above 35 °C and completely inactivates at 55 °C (Puggioni et al., 2020).

Concerning the substrate preferences, mammalian DASPOs are highly specific for acidic D-AAs; however, the substrate preference and catalytic activities vary significantly across species (Table 1).

Table 1. Apparent kinetic parameters of recombinant mammalian DASPOs.

Enzyme source	K_m (mM)			k_{cat} (s^{-1})			k_{cat}/K_m ($mM^{-1}s^{-1}$)		
	D-Asp	**D-Glu**	**NMDA**	**D-Asp**	**D-Glu**	**NMDA**	**D-Asp**	**D-Glu**	**NMDA**
Human[a]	1.05	31.5	2.76	81.3	11.3	73.6	77.4	0.36	26.7
Rat[b]	2.26	-	-	31.1	-	-	14.1	-	-
Mouse[b]	7.37	-	-	9.83	-	-	1.35	-	-
Pig kidney[c]	2.52	66.9	0.853	37.5	9.36	45.1	14.9	0.14	52.9
Bovine kidney[d]	3.7	5.6	1.5	22.5	1.19	30.9	6.09	0.21	20.6

a) Data are from (Molla et al., 2020); b) Data are from (Katane et al., 2015a); c) Data are from (Yamamoto et al., 2007); d) Data are from (Negri et al., 1999)

Pig and bovine kidney DASPOs prefer NMDA to other acidic D-AAs, including D-Asp (Negri et al., 1999; Yamamoto et al., 2007). hDASPO instead is highly specific for both D-Asp and its derivative NMDA, while it shows a lower activity towards D-Glu and D-Asn (12.8% and 9.5% vs D-Asp, respectively). It also oxidizes D-Pro and D-His (~1%) and D-Ser, D-Gln, and Gly (0.1%-0.2% vs D-Asp) (Molla et al., 2020). hDASPO shows a 5-fold higher specific

activity compared to the homologous bovine enzyme (Negri et al., 1988) and >10-fold higher than hDAAO on D-Ser (Molla et al., 2006).

Although the substrate specificity profile of hDASPO is similar to that of mDASPO (Katane et al., 2011), the relative level of these activities is markedly lower for mDASPO compared to either human or rat DASPOs (Katane et al., 2018; Molla et al., 2020). When D-Asp is used as the substrate, the K_m value of hDASPO and rDASPO towards D-Asp are similar (1.05 mM and 2.26 mM, respectively), while that of mDASPO is higher (7.37 mM). In addition, the k_{cat} value and the catalytic efficiency (k_{cat}/K_m) of hDASPO are significantly higher than those of both murine enzymes (Katane et al., 2015a).

Overall, these results suggest that tiny changes in the active site of hDASPO result in an enzyme more efficient for catalyzing the oxidative deamination of D-Asp than other mammalian DASPOs.

Binding studies using either competitive (malonate, meso-tartrate, 5-aminonicotinic acid) or noncompetitive (aminooxyacetic acid) inhibitors, further support these findings: all the inhibitors show low inhibition constant (K_i) values (between 3.8 µM and 1.49 mM) (Katane et al., 2015a; Katane et al., 2015b), thus are effective in inhibiting the enzymatic activity; however, only in the case of aminooxyacetic acid, the K_i value determined for the three enzymes is comparable, while the values obtained for the other inhibitors significantly differ (Table 2) (Katane et al., 2015a).

Table 2. Ki values for several inhibitors against recombinant human, rat, and mouse DASPOs (Katane et al., 2015a; Katane et al., 2015b).

Inhibitor	K_i (µM)		
	hDASPO	**rDASPO**	**mDASPO**
Malonate	153 ± 26	1562 ± 120	1220 ± 133
meso-Tartrate	681 ± 48	472 ± 87	2089 ± 216
Aminooxyacetic acid	1492 ± 693	1416 ± 356	1915 ± 100
5-Aminonicotinic acid	3.80 ± 0.96	5.89 ± 0.61	8.69 ± 0.72

1.4. Kinetic mechanism

As for hDAAO, the oxidative deamination catalyzed by hDASPO follows a ternary complex mechanism (Molla et al., 2006; Molla et al., 2020). The dehydrogenation of the

substrate derives from the direct transfer of an hydride, i.e. the α-hydrogen from the α-carbon of the substrate, to the flavin N(5) (Pollegioni et al., 2018).

For mammalian DAAOs, and especially for hDAAO, the reductive-half reaction (the conversion of the D-AA into the planar imino acid together with the flavin reduction) is very fast (117 ± 6 s^{-1} on D-Ser), more than the turnover (6.3 ± 1.4 s^{-1}).

As already reported, the rate limiting step in hDAAO catalysis is the imino acid product release (< 1 s^{-1}) which is too slow to allow the reoxidation step to start from the free, reduced enzyme. Accordingly, reoxidation begins from the corresponding reduced enzyme-imino acid complex, with a second-order reaction corresponding to 1.25 x 10^5 $M^{-1}s^{-1}$ (Molla et al., 2006).

The rate limiting step identified in the catalysis of bovine DASPO consists instead into a conformational change related to the binding of a second molecule of D-Asp to the reduced enzyme form (Negri et al., 1988). Compared to the bovine counterpart, the kinetic parameters of hDASPO on D-Asp (i.e. K_m and k_{cat} values) are ~5-fold higher, thus suggesting a different rate-limiting step.

The reductive half-reaction of hDASPO seems to be reversible, and an equilibrium constant of 4.7 ± 1.3 was estimated for the overall process (oxidized-enzyme + D-Asp ↔ reduced-enzyme + imino aspartate). The substrate oxidation step is very fast and it is not rate limiting (1550 ± 206 s^{-1}), since it is much higher than the turnover number (229 ± 27 s^{-1}). Indeed, the rate-limiting step in hDASPO reaction is the reoxidation of the reduced flavin, which was observed to corresponds to a single exponential process with a rate constant of ~10 x 10^4 $M^{-1}s^{-1}$. Notably, the activity of hDASPO is significantly higher than that of hDAAO (as well as of bovine DASPO).

1.5. Structural properties

The “canonical isoform” of human DASPO and most of other mammalian DASPOs are identical in size (i.e. 341 AA, 38-39 kDa) and share a high amino acidic sequence identity (75 to 91%). They contain the FAD-binding consensus sequence (Gly-X-Gly-X-X-Gly) near the N-terminal end, and a type-1 peroxisomal targeting signal (PTS1) sequence (S/T/A/G/C/N- R/K/H- L/I/V/M/A/F/Y, PROSITE, PS00342) at the C-terminal end.

Although the PTS1 sequence (SNL) of the human enzyme does not match the canonical consensus sequence, hDASPO was shown to localize to peroxisomes in cultured mammalian cells (Setoyama and Miura, 1997; Amery et al., 1998).

Gel-permeation chromatography and native PAGE analyses demonstrated that the oligomerization state is different among the species: the human enzyme is monomeric (Katane et al., 2018; Molla et al., 2020), like the bovine one (Negri et al., 1987), while pig, rat, and mouse DASPOs are homotetramers (Yamamoto et al., 2007; Katane et al., 2018). Interestingly, it was hypothesized that the oligomerization state of mammalian DASPOs could depend on protein concentration, since mDASPO was reported to be a homodimer in solution at low concentrations (0.1 mg/mL) (Puggioni et al., 2020).

Even though mammalian DASPOs sequences are highly conserved their substrate-binding affinities, catalytic activities, and inhibitor sensitivities may differ (Table 1 and 2).

The first three-dimensional structure of the human flavoenzyme (PDB entry code 6RKF) has been recently published (Molla et al., 2020) and together with the substrate-docking simulations and the site-directed mutational analyses previously performed (Katane et al., 2011; Katane et al., 2017), it provides a powerful tool to understand the structure-functional relationships of this enzyme.

hDASPO structure is divided into two domains: a FAD-binding domain (FBD) (residues 1-46, 143-192, and 282-335) containing the Rossmann fold motif, typical of several flavoenzymes (Fraaije and Mattevi, 2000), and the substrate-binding domain (SBD) (residues 47-142, 193-281) characterized by a large, eight-stranded, mixed β-sheet (Fig. 4A).

The structural comparison performed with DALI software (Holm and Rosenström, 2010) indicates that the tertiary structure of hDASPO resembles that of other FAD-binding oxidoreductases, with the best match obtained with hDAAO (PDB code 5ZJA; identity of 41%). The major differences in the structures of these two human enzymes is represented by the presence of insertions/deletions and poor residue conservation at three loops in the substrate binding domain (highlighted in red in Fig. 4B) (Molla et al.,

2020), which highly impact on the structure at the entrance of the active site (as described in detail below).

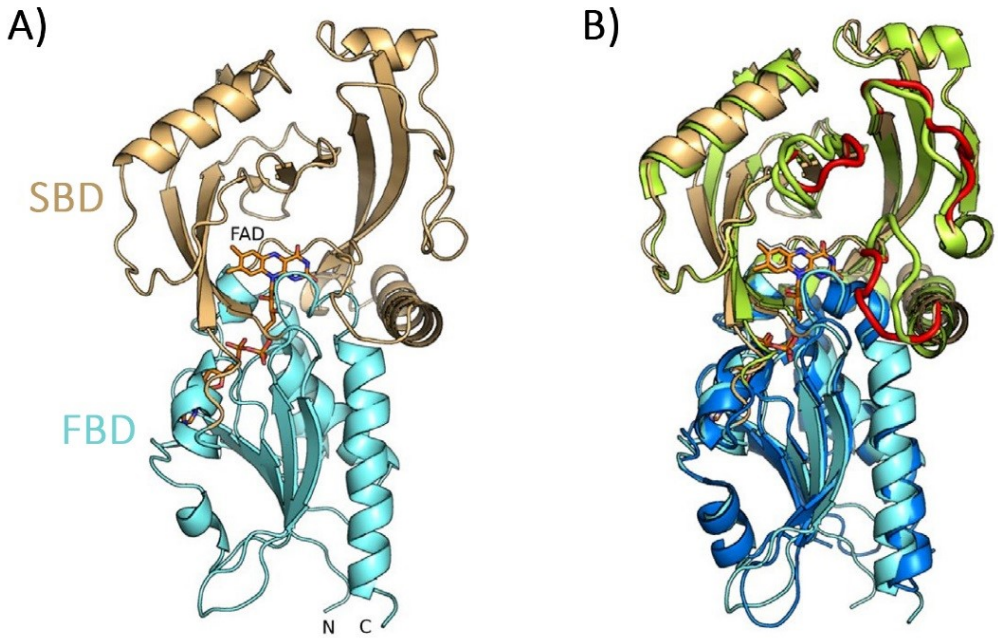

Fig.4: Structure of hDASPO. (A) Ribbon representation of the substrate-binding domain (SBD) and the FAD-binding domain (FBD), labeled and colored in gold and cyan, respectively. FAD molecule is represented as orange sticks and labeled; (B) Superimposition of hDASPO and hDAAO structures (SBD in green and FBD in blue). The major differences are highlighted as red loops in the hDASPO structure. Modified from (Molla et al., 2020).

However, while the tertiary structure of the two enzymes is very similar, hDAAO is dimeric in solution while hDASPO is monomeric: specific variations in the amino acidic sequence in the dimerization interface of hDAAO (i.e. decreased hydrophobicity and altered polar residue distribution) might account for the monomeric state of hDASPO (Molla et al., 2020).

Several amino acid residues involved in the catalytic activity, substrate binding, and substrate specificity of hDASPO have been identified. In the active site of the enzyme, an arginine (Arg278) and a tyrosine (Tyr223) are suggested to interact with the negatively charged α-carboxylic group of the substrate (Fig. 5A), similarly to what happens in hDAAO (Pollegioni et al., 2018). The substrate-binding network is completed by the formation of an hydrogen bond between the α-amino group of the substrate and the carbonyl oxygen of Ser308 and/or His54 side chain (Molla et al., 2020). Indeed, the

S308N SNP variant of hDASPO showed a 1.5 fold decreased specific activity on D-Asp compared to the wild type enzyme (Katane et al. 2017).

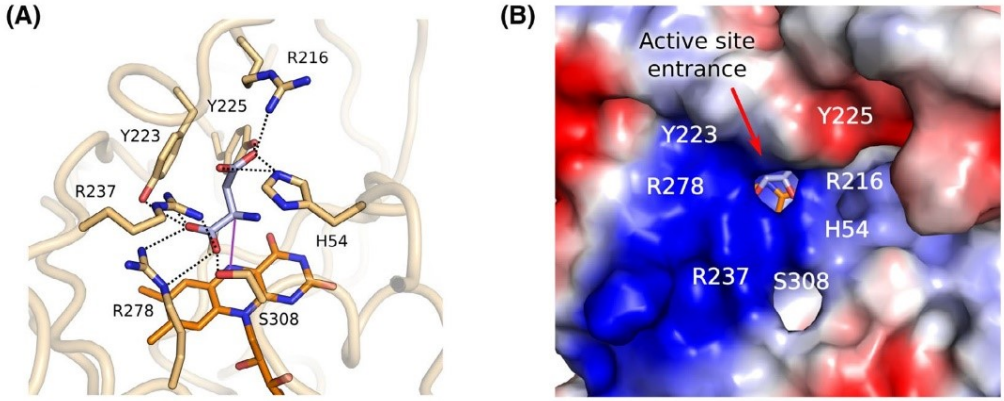

Fig.5: hDASPO active site. (A) Docking of D-Asp in the active site of hDASPO. The purple line indicates the distance (3.5 Å) between D-Asp αCa and the N(5) of FAD. Ligands and FAD are colored in pale blue and orange, respectively. Polar interactions are represented as dashed lines. (B) Electrostatic surface at the entrance of the active site (blue positively charged, and red negatively charged side chains). Modified from (Molla et al., 2020).

In addition to the residues described above, two other arginine residues (Arg216 and Arg237) seems to be involved in substrate specificity and/or catalytic activity, possibly by interacting with the carboxyl group of the substrate (Katane et al., 2011; Molla et al., 2020). These two arginine residues, together with His54, form a positively charged pocket at the entrance of the active site, thus creating an electrostatic funnel that facilitates the access of the negatively charged D-Asp (Fig. 5B) (Molla et al., 2020). The role in substrate selectivity assessed for Arg216 is confirmed by the dramatically lower kinetic efficiency on acidic D-AAs reported for R216Q hDASPO variant, which also acquired the ability to oxidize D-Ala (Katane et al., 2017). In the active site, the substrate side chain is further stabilized by the interaction with Arg237 and Arg278 (Molla et al., 2020).

This active site gating role proposed for the Arg-His residues (that forms a highly conserved region, specific to DASPO enzymes) is coupled with a drastic shortening in the loop region of hDASPO (residues 217-221) compared to hDAAO (residues 216-226) (Molla et al., 2020). In hDAAO this loop, which shapes the surface at the interface

between the active site and the solvent, forms a lid that limits the turnover number compared to yeast DAAOs, where it is absent (14.7 and 350 s^{-1}, respectively) (Pollegioni et al., 2002; Pollegioni et al., 2007). These structural differences limit the substrate range of hDASPO while they facilitate the substrate/product exchange, thus improving the activity of the enzyme in comparison to hDAAO.

The differences between hDASPO and hDAAO also extends to the cofactor-binding affinity; hDAAO shows a weak FAD interaction (K_d = 8.0 ± 2.0 μM) and thus it is present in solution as an equilibrium between the active holoenzyme and the inactive apoprotein (Molla et al., 2006; Caldinelli et al., 2010). On the other hand, hDASPO shows a strong interaction with the cofactor (K_d = 0.033 ± 0.003 μM) resulting into a stable holoenzyme (Molla et al., 2020).

Compared to other mammalian DASPOs, the FAD-binding affinity of the human enzyme is similar to the one from bovine kidney (K_d = 0.050 ± 0.002 μM) (Negri et al., 1987) and rat (K_d = 0.128 ± 0.036 μM) (Katane et al., 2018), while it is significantly higher compared to the mouse one (1.01 ± 0.05 μM) (Katane, et al., 2010a). Coherently, mDASPO is present in solution as an equilibrium between the holoenzyme and the apoprotein forms (80-90% and 10-20%, respectively) (Puggioni et al., 2020).

In hDASPO the flavin ring is located at the interface between the SBD and the FBD, with nearly all hydrogen-bond donors and acceptors of FAD interacting with protein atoms. Thirty-five amino acid residues are directly involved in FAD binding, of which eight establish polar or electrostatic interactions with the cofactor (Fig. 6). The N-terminal dipoles of helices A1 and A11 point toward the pyrophosphate group of FAD and the O_2 position of the isoalloxazine ring, respectively (Fig. 4A); this represents a typical structural fingerprint of glutathione reductase 2 family (Dym and Eisenberg, 2001). The flavin ring does not show any significant deviation from planarity, it largely interacts with the protein, and its two methyl groups are in van der Waals contact with Val203 and Gly276 (Molla et al., 2020).

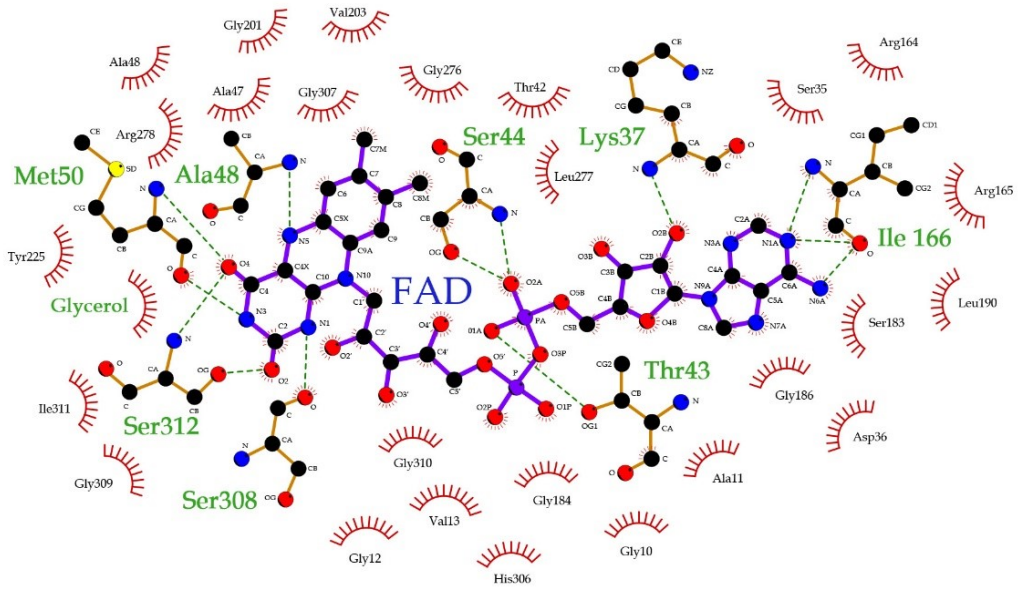

Fig.6: hDASPO-FAD interactions. The eight amino acid residues establishing polar or electrostatic interactions with the cofactor are labelled in green. The figure was rendered using the program LIGPLOT. Modified from (Molla et al., 2020).

Interestingly, from a structural viewpoint, the overall FAD-apoprotein interaction in hDASPO is very similar to the hDAAO one. The only remarkable difference can be found at the FAD ribose moiety and is mostly due to the presence of hDASPO Gly186 instead of the corresponding Trp185 in hDAAO (Molla et al., 2020).

Therefore, the different affinities for the cofactor could be due to distinct dynamics during the flavin binding process more than to specific interactions. Interestingly, the presence of a ligand in the active site of hDAAO results in a 20-fold decrease in the K_d for FAD binding and exerts a stabilizing effect by increasing the amount of holoenzyme in solution (Caldinelli et al., 2010).

The binding of the cofactor was reported to modulate the conformation and stability of hDASPO: gel permeation chromatography indicates that hDASPO apoprotein is present in solution as a monomer-trimer equilibrium (with a 2:1 molar ratio) and circular dichroism measurements indicate that both the secondary and tertiary structure of apoprotein are altered compared with the holoenzyme; moreover, the thermal stability of the enzyme is enhanced by the presence of the flavin, with an apparent synergistic

effect in the presence of both FAD and a ligand at the active site of the enzyme (Molla et al., 2020).

In conclusion, even though they share an overall similar tertiary structure, hDASPO shows peculiar features and appears to significantly differ from hDAAO: it shows a specific active site charge distribution, a different oligomerization state and a significantly higher cofactor binding affinity and activity (Molla et al., 2020).
These differences highlight a possible divergent evolution of the two orthologue flavoenzymes that reflects into a different modulation of the brain levels of D-Asp and D-Ser. While hDASPO is a specific and efficient catabolic enzyme that strictly controls D-Asp cellular level, hDAAO shows a low activity and differently affects D-Ser cellular concentration.

1.6. D-Aspartate and pathologies

Several experimental evidences indicate that altered D-Ser and / or D-Asp levels (frequently due to abnormal expression levels or activity of their catabolic enzymes) are related to NMDAr impaired activity (Katsuki et al., 2004; Shleper et al., 2005; Mothet et al., 2006; Errico et al., 2008a; 2011a; Turpin et al., 2011; Cristino et al., 2015). Given their major physiological role, it is not surprising that NMDAr dysfunctions are involved in several neurodegenerative diseases and neurological disorders. In particular, an excessive stimulation of NMDArs has been implicated in a large number of acute and chronic neurodegenerative conditions, including stroke, epilepsy, polyneuropathies, chronic pain, amyotrophic lateral sclerosis, Parkinson's disease (PD), Alzheimer's disease (AD), and Huntington's disease (HD), as recently reviewed by (Carvajal et al., 2016). On the other hand, an hypoactivation of these receptors has been linked to psychiatric conditions such as schizophrenia and bipolar disorder (Goff and Coyle, 2001; Ghasemi et al., 2014).
Schizophrenia is a severe chronic mental disorder that affects almost 1% of the population worldwide. Even though the etiology of this illness is uncertain, it is believed to be a neurodevelopmental disorder that results from a combination of environmental

risk factors and genetic vulnerabilities (Owen et al., 2011). NMDAr dysfunction is one of the main hypothesis of the pathophysiology of schizophrenia, as recently reviewed by (Hu et al., 2015; Balu, 2016). In particular, it is thought that abnormally reduced levels of the co-agonist D-Ser may cause the hypoactivation of NMDArs and therefore be a causal factor in the pathophysiology of this mental disorder (Coyle and Tsai, 2004; Javitt et al., 2012).

Given the potential influence exerted by D-Asp on NMDAr-mediated neurotransmission and its significant presence in the pre- and perinatal stages of neurological development, it has been recently hypothesized that this D-AA may play a role in the processes leading to the onset of schizophrenia (Errico et al., 2015a). Intriguingly, increased D-aspartate levels influence schizophrenia-like phenotypes in rodents, as indicated by improved fronto-hippocampal connectivity, reduced activation of neuronal circuitry and attenuated prepulse inhibition deficits induced by phencyclidine (de Bartolomeis et al., 2015; Errico et al., 2015b), a drug that models schizophrenia symptoms in both humans and rodents (Davies and Beech, 1960; Castañé et al., 2015).

Moreover, HPLC analyses on *post-mortem* brain samples have shown decreased D-Asp levels in the prefrontal cortex and striatum of schizophrenia-affected individuals compared to non-psychiatric controls (Errico et al., 2013). Interestingly, the observed decrease in D-Asp content (~30%) was associated to a significant increase in hDASPO activity that was not related to increased levels of *DDO* gene transcript (Nuzzo et al., 2017). This finding suggests that other processes (such as hDASPO post-translational modification and/or the interaction with regulatory proteins), or a pathological alteration of these processes, likely come into play to up-regulate the enzyme activity during schizophrenia onset.

In addition to its involvement in schizophrenia, altered D-Asp metabolism may play a role in the onset of AD. AD is a chronic and progressive neurodegenerative disease which pathophysiology is characterized by the accumulation of extracellular amyloid β (Aβ) plaques and the intraneuronal inclusions of the truncated and hyperphosphorylated forms of tau protein. These degenerative lesions are associated with glial activation, neuritic dystrophy and loss of synapses, and neuronal death, as recently reviewed by

(Serrano-Pozo et al., 2011). Consistent with the role of the glutamatergic system in learning and memory formation, alterations in NMDAr-mediated neurotransmission have been linked with the pathological processes underlying AD (Danysz and Parsons, 2012; Kocahan and Doğan, 2017; Liu et al., 2019).

As already reported, the long-lasting exposure to non-physiological, high concentration of D-Asp in *Ddo*$^{-/-}$ mice caused a precocious decay of synaptic plasticity and cognitive functions. Moreover, severe processes related to neuroinflammation were observed in this animal model, as indicated by the appearance of dystrophic microglia and reactive astrocytes (Punzo et al., 2016), characteristic features in neurodegenerative disorders (Liddelow et al., 2017; Yun et al., 2018). Very recently, high D-Asp levels in *Ddo*$^{-/-}$ mice were also shown to induce changes in tau phosphorylation (Nuzzo et al., 2019) and, intriguingly, D-Asp treatment seems to influence the process leading to Aβ40 and Aβ42 aggregation (D'Aniello et al., 2017).

In a murine model of neuropathic pain, D-Asp treatment reduced abnormal behaviours and normalized the Aβ expression, probably by increasing the steroids level in the prefrontal cortex and in the hippocampus (D'Aniello et al., 2017).

Notably, alterations in D-Asp levels have been also reported in patients with AD, although conflicting results were published and further studies are needed to corroborate these data. D-Asp levels were significantly higher in the cerebrospinal fluid of patients with AD (Fisher et al., 1994; Fisher et al., 1998), while in contrast, nearly halved D-Asp levels were detected in the white matter (Fisher et al., 1991) and in three neocortical regions, as well as hippocampus and amygdala, of AD patients compared to healthy subjects (D'Aniello et al., 1998). No alterations were instead measured in the cerebellum, an area which lacks the neuropathological changes of AD (D'Aniello et al., 1998). It is worth noting that all these studies were performed on a limited number of subjects (≤10 both for healthy individuals and AD patients).

I recently contributed to review the scientific literature concerning the role of D-AAs in Alzheimer's disease. This is reported at paragraph 3.1.

1.7. D-AAs as potential biomarkers for Alzheimer's disease

The identification and validation of biomarkers for diagnosing chronic neurodegenerative disorders such as AD are increasingly important. Biomarkers reflecting different types of pathophysiology in the brain can be used for clinical diagnosis, especially in the early stages of the disease, to predict progression and to monitor effects of novel drug candidates in clinical trials (Blennow et al., 2010).

During the past 25 years, three core cerebrospinal fluid (CSF) biomarkers for AD have been identified and tested. These are the 42-aminoacid isoform of β-amyloid (Aβ42), total tau (T-tau), and phosphorylated tau (P-tau) (Buerger et al., 2006; Tapiola et al., 2009; de Souza et al., 2012). These analytes reflect key aspects of disease pathogenesis, i.e., neuronal and axonal degeneration, phosphorylation of tau with cortical tangle formation, and oligomerization, aggregation and deposition of the Aβ42 peptide into plaques (Blennow, 2017).

However, CSF collection is regarded as a time-wasting, invasive and painful procedure, and the measurement of biomarkers in blood samples would be a more practical approach. Unfortunately, the levels of tau and Aβ in the plasma are dramatically lower compared to CSF (Khoury and Ghossoub, 2019). There is an extreme need for alternative, easily detectable biomarkers, which must be sensitive and specific (Blennow, 2017).

Due to their involvement in several pathological processes, D-AAs are increasingly recognized as promising candidate biomarkers for the diagnosis of several diseases (Kimura et al., 2016; Bastings et al., 2019). Moreover, even though the amount of these molecules is usually at trace level in human tissues and fluids, the recent technological advancements have enabled to measure their concentration with high sensitivity. As already mentioned, the outcomes of previous studies focused on differences in D-Asp levels between AD patients and healthy subjects were controversial (Fisher et al., 1991; Fisher et al., 1994; Nagata et al., 1995; D'Aniello et al., 1998; Madeira et al., 2015). However, these conflicting results can be ascribed to the absence of standardized protocols and suitable controls. For this reason, it would be challenging to further investigate whether the D-AA levels are deregulated in AD patients, and to assess their potential role as a new AD biomarker.

2. Aim of the research

Human D-aspartate oxidase (hDASPO) is a peroxisomal FAD-dependent enzyme responsible for the catabolism of acidic D-amino acids (D-AAs): it catalyzes their oxidative deamination to generate the corresponding α-ketoacids, along with the production of hydrogen peroxide and ammonia (Negri et al., 1987). Notably, DASPO is the only enzyme known to degrade D-aspartate (D-Asp), which in mammalian central nervous system (CNS) plays an important role in regulating brain functions by acting as an agonist of N-methyl-D-aspartate receptors (NMDAr) (Errico et al., 2011a).

Level of D-AAs have been related to different human pathological states. Recent studies showed an alteration of D-Asp and D-Ser levels in tissues and/or biological fluids of Alzheimer's disease (AD) patients, although controversial results have been published during the years. Accordingly, in the first part of this PhD project I decided to investigate whether D-Asp and D-Ser levels are deregulated in AD patients' serum by using an HPLC procedure based on the enzymatic degradation of the D-AAs. Blood is an easily affordable clinical sample to explore whether this parameter represents an early and easily detectable biomarker for AD precocious diagnosis.

Human *DDO* gene encodes different mRNA forms: three distinct isoforms of the enzyme, constituted by 341 (the "canonical" form), 369 and 282 amino acids, are reported in the UniProtKB database. The first three-dimensional structure of the 341 amino acids isoform (PDB entry code 6RKF) and an extensive characterization of its biochemical properties have been published recently (Molla et al., 2020), providing an insight into the structure-function relationships of this enzyme. Conversely, the functional properties of the "non canonical" protein isoforms have been poorly investigated: hDASPO 282 was produced as an insoluble recombinant protein in *E. coli* (Setoyama and Miura, 1997), while hDASPO 369 has never been expressed. Moreover, despite the increasing interest in hDASPO properties and physiological role, little is known concerning the processes involved in the regulation of the enzyme levels and activity at the cellular level.

For this reason, this PhD project was also aimed to the investigation of several of these processes using as a cellular model system the U87 human glioblastoma cells stably expressing hDASPO 341 and hDASPO 369 putative isoforms.

The project intends to study:

- the subcellular localization and specific activity of the longer putative isoform in comparison with the hDASPO 341 ones;
- the mechanisms that regulate the stationary levels of both hDASPO isoforms, focusing on their cellular stability and on the processes involved in their degradation;
- the presence of specific secondary modifications in hDASPO and the effect of these post-translational modifications on the enzyme's functionality.

3. Results

3.1. The role of D-AAs in Alzheimer's disease: a review

Submitted

The role of D-amino acids in Alzheimer's disease

Luciano **Piubelli**[a], Giulia **Murtas**[a], Valentina **Rabattoni**, Loredano **Pollegioni**

Department of Biotechnology and Life Sciences, University of Insubria, Varese, Italy

[*] Corresponding author: Luciano Piubelli, Department of Biotechnology and Life Sciences, University of Insubria, Via J. H. Dunant 3, 21100 Varese, Italy. e-mail address: luciano.piubelli@uninsubria.it. Tel: +39 0332 421 518. Fax: +39 0332 421 500.

[a] These authors contributed equally

Authors' e-mail addresses: luciano.piubelli@uninsubria.it; g.murtas@uninsubria.it; v.rabattoni@uninsubria.it; loredano.pollegioni@uninsubria.it

Running title: D-amino acids in Alzheimer's disease

Abstract

Alzheimer's disease (AD), the main cause of dementia worldwide, is characterized by a complex and multi-factorial etiology. In large part, excitatory neurotransmission in the central nervous system is mediated by glutamate and its receptors are involved in synaptic plasticity. The N-methyl-D-aspartate (NMDA) receptors, which require the agonist glutamate and a coagonist such as glycine or the D-enantiomer of serine for activation, play a main role here. A second D-amino acid, D-aspartate, acts as agonist of NMDA receptors. D-amino acids, present in low amounts in nature and long considered to be of bacterial origin, have distinctive functions in mammals. In recent years, alterations in physiological levels of various D-amino acids have been linked to various pathological states, ranging from chronic kidney disease to neurological disorders. Actually, the level of NMDA receptor signaling must be balanced to promote neuronal survival and prevent neurodegeneration: this signaling in AD is affected mainly by glutamate availability and modulation of the receptor's functions. Here, we report the experimental findings linking D-serine and D-aspartate, through NMDA receptor modulation, to AD and cognitive functions. Interestingly, AD progression has been also associated with the enzymes related to D-amino acid metabolism as well as with glucose and serine metabolism. Furthermore, the D-serine and D-/total serine ratio in serum have been recently proposed as biomarkers of AD progression. A greater understanding of the role of Damino acids in excitotoxicity related to the pathogenesis of AD will facilitate novel therapeutic treatments to cure the disease and improve life expectancy.

Keywords: D-serine; D-aspartate; NMDA receptor; excitotoxicity; amyloid beta

Introduction

Alzheimer's disease (AD) is the main cause of dementia: according to the World Health Organization it accounts for 60–70% of all cases. AD is characterized by a progressive decline in cognition, memory, and executive function, starting from early lack of memory to gradual worsening of language, orientation, and behavior and extending to severe loss of memory and some bodily functions. This chronic neurodegenerative disease is the result of synapse dysfunction, synapse loss, and, ultimately, neuronal death. The etiology of AD appears to be complex and multifactorial. Its pathophysiology includes both structural and functional abnormalities. Upstream initiators of AD are represented by the amyloid beta (Aβ) and tau proteins; as AD progresses, multiple brain lesions develop over time, such as senile plaques, consisting of Aβ and neurofibrillary tangles containing phosphorylated tau, and loss of synaptic profiles [1].

An open issue concerns the complex relationships between neurons, glia, microglia, and vasculature, which contribute to synapse and circuit dysfunction [2]. Acute brain insults (hypoglycemia, neurologic trauma, stroke, and epilepsy) result in disproportionate excitatory glutamatergic neurotransmission and trigger synapse dysfunction and massive cell death in the central nervous system. Cognitive impairment and dementia are commonly associated with recovery from such insults, suggesting shared pathological mechanisms among various forms of dementia, including AD. Aβ is thought to play a causal role in the pathogenesis of AD [3]. The action of Aβ on synapses engages glutamate receptors, especially the N-methyl-D-aspartate (NMDA) receptors, which act as common initiators of various forms of neuronal dysfunction/damage. Several single nucleotide polymorphisms in the genes encoding NMDA receptor subunits have been reported to be implicated in the pathophysiology of neurological disorders such as AD, schizophrenia, and depression.

To activate NMDA receptors, binding of the activator glutamate and a coagonist is required: this coagonist was originally proposed to be glycine (Gly) but in the last 15 years studies have established that D-serine (D-Ser) is frequently the preferred coagonist [4-6]. Owing to its critical role in the mammalian brain, the processes for D-Ser synthesis, transport, and degradation have been investigated in depth [7-9]. Furthermore, a second

D-amino acid (D-AA), D-aspartate (D-Asp), acts as a NMDA receptor agonist [10]. Indeed, D-Asp stimulates mGlu5 receptors and presynaptic AMPA receptors: it has been considered a signaling molecule involved in neural development, influencing brain morphology and behavior in adulthood [11, 12]. D-Asp is also involved in the synthesis of different hormones and of melatonin [11, 13].

D-AAs (Figure 1) are only present in low amounts in nature and were long considered to be of bacterial origin as they are key components of peptidoglycan in the bacterial cell wall and of certain antibiotics [14]. Now we know that D-AAs are constituents of biologically active peptides secreted by amphibians and are present in the cellular fluids of marine worms and invertebrates [15] and in foodstuffs of natural origin or that develop during processing [16]. D-AAs are also present in animals, originating from endogenous microbial flora, diet, or racemization of L-enantiomers. In 1992, Hashimoto and collaborators determined a relevant level of D-Asp and D-Ser in the central nervous system (CNS), making it then possible to ascribe a distinctive function to D-AAs in mammals [17, 18]. Here, we would like to note that D-Asp was detected in human brain about ten years before, being found in myelin-rich white matter: this was a relevant discovery as a correlation between the level of D-Asp in white matter and age was identified, although the presence of D-Asp was at first incorrectly attributed to the natural rate of racemization of L-Asp occurring in proteins with aging [19]. In recent years, alterations in physiological levels of different D-AAs have been related to various pathological states, e.g., chronic kidney disease [20] and neurological disorders such as AD, bipolar disorder, and schizophrenia [21-25].

NMDA receptors and Alzheimer's disease

In large part, excitatory neurotransmission in the mammalian CNS is mediated by glutamate: its receptors, mainly ligand-gated ionotropic glutamate receptors, are involved in synaptic plasticity, the mechanism underlying learning and memory [26]. On the one hand, the NMDA receptors, tetrameric channels constituted by two GluN1 subunits together with either two GluN2 subunits (selected among GluN2A-GluN2D isoforms) or a combination of GluN2 and GluN3 subunits (alternatively GluN3A or

GluN3B isoforms), play a main role [27], Figure 2. For activation, NMDA receptors require the principal agonist glutamate at the GluN2 subunit and a coagonist at the so-called "glycine-binding site" on the GluN1 subunit. The coagonist, which could be represented by D-Ser or Gly, plays an important modulatory role in NMDA receptor function [4-6, 28, 29]. At resting membrane potential (≈ −70 mV), Mg^{2+} blocks the Ca^{2+} channel of the NMDA receptor. Activated AMPA receptors remove this blockade by depolarization following the strong and prolonged release of glutamate from the presynaptic terminal during the induction of long-term potentiation (LTP): this promotes the influx of Ca^{2+} ion and, through the activation of Ca^{2+}/calmodulin-dependent protein kinase II-mediated signaling cascade, enhances synaptic strength. On the other hand, a modest activation of NMDA receptors induces a small increase in postsynaptic Ca^{2+} levels and elicits phosphatase activity yielding long-term depression (LTD) [30]. The interplay at the tripartite synapsis under physiological conditions is reported in Figure 3.

A classical view of AD pathogenesis proposes that an excessive stimulation of glutamate signaling results in excitotoxicity, which is mediated by increased calcium influx in post-synaptic neurons [31]. The prolonged calcium overload leads to gradual loss of synaptic functions followed by synaptotoxicity and neuronal cell death, which, in turn, correlates with the progressive decline in memory and cognition in AD [32, 33]. To give a complete picture, we would mention that recent literature suggests that AD results from presynaptic failures before postsynaptic dysfunction ensues [34-37].

The electrophysiological function of NMDA receptors is directly modulated by Aβ (Figure 4) since: i) it interacts with the receptors and, in cultured neurons, leads to internalization of synaptic NMDA receptors and the depression of related currents [38]; ii) it induces glutamate release from astrocytes, which, in turn, activates the pathological, extrasynaptic NMDA receptors on neurons and the ensuing decrease in miniature excitatory postsynaptic currents [39]; iii) its oligomers change the activation of NMDA receptor-dependent signaling pathway by impairing LTP and inducing LTD; and iv) NMDA receptors antagonists prevent the structural effects induced by Aβ. For reviews, see [31, 40].

NMDA receptors also play a major role in neuronal survival by activating the neuronal survival pathway [41, 42]: blocking NMDA receptor function causes neuronal apoptosis and degeneration [43, 44]. Neuronal cell survival is compromised both by insufficient synaptic NMDA receptor signaling and excessive stimulation of glutamatergic signaling, resulting in excitotoxicity by excessive Ca^{2+} entry, primarily through these receptors. The level of NMDA receptor signaling must be balanced to promote neuronal survival and prevent neurodegeneration: this signaling in AD is affected mainly by glutamate availability and modulation of the receptor's functions [31].

While the synaptic NMDA receptors are preferentially activated by the coagonist D-Ser, the extrasynaptic ones interact better with the coagonist Gly [45] and are preferentially targeted by the antagonist memantine [46]. Extrasynaptic NMDA receptor-induced responses seem to be tightly related to the physiological changes occurring in AD: Aβ specifically activated extrasynaptic NMDA receptors, which caused synaptic loss, an outcome that was antagonized by memantine [39, 40, 47].

AD has been also linked to the level of NMDA receptor coagonist D-Ser: in AD hippocampus or Aβ-treated cultured microglia, D-Ser levels increased due to a parallel increase in expression of serine racemase, the enzyme assigned to synthesize D-Ser (Figure 4) [48]. In addition, a decrease in forebrain D-Ser levels, obtained by knocking out serine racemase, ameliorated both NMDA- or Aβ-caused neurotoxicity [49]. Notably, six modulators acting at the glycine-binding site of NMDA receptors and showing procognitive and antidepressant properties were identified: three of them are D-AAs, namely, D-Ser, D-cyclo-serine, and D-alanine, reviewed in [50].

D-Asp levels have been also related to the modulation of excitatory neurotransmission. Knockout mice for the enzyme assigned to catabolize D-Asp, namely, D-aspartate oxidase [51], demonstrated that the persistently high levels of this amino acid caused age-dependent effects: spatial memory and cognitive ability improved in young individuals, followed by rapid deterioration of learning and memory abilities in the same animals, leading to precocious brain aging [52, 53]. Interestingly, the high D-Asp levels in these knockout mice resulted in changes in tau phosphorylation [54]. Degradation of D-Asp by D-aspartate oxidase prevented NMDA receptor hyperstimulation, while an

increase in D-Asp level rescued the age-related cognitive impairment [53]. In a murine model of neuropathic pain, D-Asp treatment reduced abnormal behaviors and normalized Aβ expression, probably by increasing steroid levels in the prefrontal cortex and in the hippocampus [55].

D-Amino acid levels in Alzheimer's patients

During the last 20 years, several studies aimed to quantify D-Asp and D-Ser in CNS and compare healthy subjects (HS) and AD patients. It should be noted, however, that most of this work, in particular that conducted before the 2000s, presents some issues. Firstly, different analytical methods were employed to determine amino acid levels (these included gas chromatography, enzymatic determinations, and diverse HPLC methodologies) and, in some cases, the analytical procedures employed were not described in detail. Secondly, all these studies were carried out on a limited number of subjects (often less than ten). Furthermore, the drugs used to treat these AD patients (kind and dosage) could also affect the D-AAs levels. These concerns resulted in contrasting and somewhat confusing results, also ascribable to the lack of standardized and accurate procedures and appropriate controls, as those proposed in [56]. Results obtained in these studies are summarized in Tables 1 and 2.

D-Ser. Similar levels of D-Ser in the frontal cortex of AD patients and HS were found by [57], whereas Madeira et al. [24] reported that D-Ser levels were significantly higher in hippocampus and parietal cortex of neuropathologically confirmed AD patients, but were the same as in HS in the occipital cortex. Concerning CSF, a 5-fold higher mean level of D-Ser and a 2.4-fold higher D-/(D+L)-Ser ratio were determined in the ventricular CSF of AD patients than in HS [58]. A 5-fold increase in D-Ser levels in probable AD patients as compared to HS was also observed in the lumbar CSF [24]. These authors reported a positive correlation between D-Ser levels and the progression of cognitive decline/impairment as assessed both by CDR and Mini-Mental Scale Examination (MMSE) scales. However, [59] did not confirm these findings; by employing an ultra-HPLC-tandem MS method, they found a 13% D-Ser increase in AD patients compared to HS only and no correlation with MMSE. Moreover, comparison of the mean value of D-

Ser observed in the lumbar CSF of AD patients revealed that the concentration in the study of [59] was about 8-fold lower than the value reported by [24]. A possible explanation for this discrepancy could be related to the different analytical methods employed, the different storage times of the samples, and the differences in MMSE values, in disease duration, and even in ethnic and genetic background of the two cohorts analyzed.

A slight decrease (-11%) in levels of L-Ser in serum of AD patients compared to HS, together with a moderate (-20%) and statistically significant decrease in D-/(D+L)-Ser ratio were reported in [21]. Different results were recently reported by [60] using a validated analytical method, where a moderately (+20%) and statistically significant increase both in D-Ser and in D-/(D+L)-Ser ratio were observed. Detailed analysis of these latter results showed a slight gender effect on serum D-Ser levels and a positive correlation between serum D-Ser levels and age of AD patients, which was not observed in HS. Most interestingly, a clearly increasing trend with disease progression (assessed by Clinical Dementia Rating, CDR, score, a scale used to characterize five domains of cognitive and functional performance in AD dementia, [61]) for both D-Ser and D-/(D+L)-Ser ratio was apparent. A statistically significant increase was found for serum D-Ser levels between HS and AD patients with a CDR score of 2 and for serum D-/(D+L)-Ser ratio between HS and AD patients with a CDR score of both 1 and 2. This latter result is in line with previous observations by [24].

D-Asp. The first paper reporting on D-Asp levels and AD stated that the D-/L-Asp ratio in white matter of human brain from HS increased during aging, from 1 to about 35 years, and that in the gray matter the average value of D-/L-Asp ratio was halved with respect to the one found in the white matter of the same subjects [62]. Moreover, no gender differences were observed. The D-/L-Asp ratio was the same in both white and gray matter of AD patients and in an age-matched cohort of HS [62]. In contrast, a different study reported that the free D-Asp level was more than twice as high in the white matter of AD patients than in HS, while a similar value was determined in gray matter between the two groups [63]. Notably, the same group one year later reported a significantly higher D-Asp/(D+L)-Asp level in both gray and white matter by using an enzymatic assay

on total protein hydrolyzed [64]. Later on, D'Aniello's group conducted a detailed analysis in different brain regions In this work, D-Asp levels in brain samples from AD patients were significantly lower than those observed in corresponding samples from HS in frontal, parietal, and temporal cortices and hippocampus and amygdala (43, 38, 35, 47, and 41%, respectively). In contrast, no significant differences were found in cerebellum, an area lacking the neuropathological changes of AD [65]. In addition to various brain tissues, D-Asp levels have been also assayed in lumbar and ventricular CSF. The mean values of D-Asp and D/(D+L)-Asp levels were 1.5- and 1.4-fold higher, respectively, in lumbar CSF of AD patients than in HS, and about 2.7-fold higher for both values in ventricular CSF [66].

Very recently, different results were reported based on HPLC analyses in which the identity and concentration of D-Asp was evaluated through selective enzymatic degradation. No difference in D-Asp levels and D/(D+L)-Asp ratio were reported in samples from the superior frontal gyrus of AD patients and HS [54]. Similarly, no significant modification in D-Asp concentration and D-/(D+L)-Asp ratio were found in serum from HS and AD patients [60]. Analyzing the latter results based on the CDR score, a moderately decreasing trend from HS (CDR 0) to patients with a CDR score of 2 (moderate dementia) was observed for the D-/(D+L)-Asp ratio [60]. Interestingly, a decreased mean value of D-/(D+L)-Asp ratio in AD patients was reported by [54], although the difference from HS was not statistically significant. The lack of statistical significance in both the two latter studies might be ascribed to the very low concentration of D-Asp, close to the limit of detection for the analytical method used.

Other D-amino acids. D-alanine (D-Ala) in gray and white matter was studied by [63]: comparison of data from HS and AD patients showed that D-Ala levels were similar in white matter, whereas doubled D-Ala levels were apparent in the gray matter of AD patients as compared to HS. No difference was found in the D-/(D+L)-Ala ratio. In ventricular CSF, both D-Ala and D-/(D+L)-Ala ratio were similar in AD patients and HS [58]. The same paper reported the presence of D-arginine (D-Arg) in ventricular CSF: in this case, D-Arg and D-/(D+L)-Arg ratio were lower in samples from AD patients, but the difference was not statistically significant. Concerning D-Ala, Lane's group concluded

that serum levels of the D-enantiomer of alanine in AD patients at different cognitive decline stage were unrelated to cognitive deficits when assessed by the CDR scale, while a positive correlation was evident when the Alzheimer's Disease Assessment Scale - Cognitive Subscale (ADAS-cog) was used, and relatively to the behavioral score only [67, 68].

Gly has been assayed in different brain areas by [24]. In parietal cortex Gly levels were significantly higher in AD patients than in HS (about 1.5-fold), whereas they were the same in occipital cortex and in hippocampus. The same paper also reported slightly higher Gly levels in lumbar CSF of probable AD patients than in HS (+15%), but this increment was not statistically significant.

D-Amino acid levels and cognition

NMDA receptors play a pivotal role in cognitive functions, particularly in learning and memory formation, development, behavior, and social interaction: they convert specific patterns of neuronal activity into long-term changes in synaptic structure and activity, processes considered to underlie higher cognitive functions [69, 70]. Their hypofunction or reduced activation can result in profound deficits in synaptic plasticity and cognitive processes. For example, $Grin1^{D481N}$ mice, in which behavioral phenotypes are relevant to schizophrenia and which possess a point mutation in the NR1 glycine binding site resulting in a 5-fold decrease in NMDA receptor affinity for the coagonist, showed impairments in long-term spatial learning and memory, abnormally persistent latent inhibition (reflecting a deficit in selective attention), and reduced social approach behaviors [71]. Notably, all these deficits were reversed by administering compounds that saturate the glycine-binding site of NMDA receptors, such as D-Ser [71]. A beneficial effect of a low dose of D-Ser (50 mg/kg/day) on reversal learning was observed in APPswe/PS1 mutant mice harboring Aβ plaques in the brain [72]. Interestingly, the same low-dose D-Ser treatment boosted memory consolidation, object recognition, and working memory in normal mice, too [73]. Indeed, oral administration of D-Ser rescued the cognitive deficit observed in APP knockout mice and also restored the observed deficits in spine dynamics, adaptative plasticity, and morphology [74]. Here, mice lacking

the enzyme responsible for D-Ser degradation (D-amino acid oxidase, DAAO, see below) underscore the crucial role of D-Ser in cognition and social behavior: in these animals, increased D-Ser levels were associated with better performance in both cognitive and behavioral tests [75-77]. Notably, increased DAAO levels were reported in peripheral blood of patients with AD or mild cognitive impairment, showing a positive correlation with the severity of the cognitive deficit and, in contrast with the known biological role of DAAO, with D-Ser levels [67]. This contradictory result requires further elucidation.

NMDA receptor hypofunction has been well documented in nonpathological brain aging and seems to arise from a reduction in D-Ser levels that should be mainly due to an impairment in the biosynthetic pathway [78, 79], while the affinity of D-Ser for NMDA receptor binding site should not be affected [78, 80]. Accordingly, exogenous D-Ser treatment enhanced synaptic plasticity in aged rats [80] and in a mouse model of accelerated senescence (SAMP8 mice) [81]. It is noteworthy that daily treatment with the well-known DAAO inhibitor sodium benzoate in individuals with amnestic mild cognitive impairment or mild AD produced significantly better improvement than placebo in several cognitive functions, such as processing speed and working memory [82]. The favorable effect of sodium benzoate in AD could be also ascribed to an antioxidant effect as DAAO inhibition prevents hydrogen peroxide from being generated during the enzymatic degradation of D-Ser [83]. The oxidative stress observed during aging can result in the oxidation of cysteines and alter dimeric, active conformation of serine racemase: this effect can be prevented by long-term treatment with the reducing agent N-acetyl cysteine, resulting in potent NMDA receptor activation [84].

However, if increased D-Ser levels can improve cognitive performance by enhancing glutamatergic transmission, then excessive stimulation of NMDA receptors can promote excitotoxicity, which is associated with AD onset [85, 86]. A recent clinical study highlighted a positive correlation between D-Ser (and D-Ala) blood levels and declined cognitive processes in AD patients [68]. This finding supports the increase in D-Ser levels reported in animal models of AD [24] and in blood/CSF of AD patients [24, 60], as well as the evidence that Aβ aggregates induced D-Ser release, Figure 4 [48]. However, the observed increase in D-Ser levels might also represent a protective mechanism to

counteract Aβ signaling and prevent AD pathology, as recently suggested by [83]. D-Ser enhances neurogenesis and neuronal survival [87] and regulates apoptosis, inhibiting this process at early phases and stimulating it at later phases [88]. The beneficial effect due to enhancement or attenuation of NMDA receptor neurotransmission may depend on the phase of the disease: increasing D-Ser levels might be therapeutically **beneficial** in the early phases of AD**.**

In agreement with its role as an endogenous agonist, D-Asp was also shown to affect NMDA receptor-dependent transmission, synaptic plasticity, dendritic morphology, and cognition. Studies performed on animal models with nonphysiologically high D-Asp levels (i.e., mice lacking the D-Asp-degrading enzyme D-aspartate oxidase or mice treated with D-Asp) showed an increase in NMDA receptor-dependent early- and late-phase hippocampal LTP [52, 89, 90] associated with structural synaptic variations: increased dendritic length and spine density and a greater dendritic complexity of hippocampal and cortical neurons [90]. Behavioral studies showed a significant improvement in spatial learning and memory formation in these animals [11, 91]. However, subsequent studies have highlighted that the persistent upregulation of D-Asp levels caused a precocious and progressive decay of synaptic transmission and hippocampal memory in 13/14-month-old mice [53], which was paralleled by a loss of excitatory glutamatergic synapses and reduction in synaptic GluN1 and GluN2B subunits [92]. Moreover, the deregulated D-Asp concentration in these mice was associated with precocious oxidative stress and caspase-3 activation, and ultimately leads to cell death, thus suggesting that D-aspartate oxidase, by strictly regulating D-Asp levels, plays a neuroprotective role and prevents early neurodegenerative processes triggered by excessive NMDA receptor stimulation [12].

A further D-AA, the partial agonist D-cycloserine, was shown to improve cognitive functions both in animal studies [93-95] and in patients with dementia [96, 97], although conflicting results were also reported [98, 99]. However, as several cognitive beneficial effects were observed in healthy individuals [100-102], it has been speculated that this molecule may have a different effect on mood and learning, depending on the stage of dementia [103].

Recently, a negative correlation between D-glutamate (D-Glu) blood levels and some cognitive functions (i.e., comprehension, naming objects, and following commands) was reported in AD patients [68], further confirming previous findings from the same group [67]. In contrast, D-Ala levels did not correlate with any of the cognitive functions analyzed, but higher D-Ala and lower D-Glu levels were associated with an increase in the ADAS-cog behavior scores, which reflect the severity of behavioral and psychological symptoms of dementia [68].

Metabolism of D-amino acids and Alzheimer's disease

As stated above, dysfunctional glutamatergic transmission mediated by altered NMDA receptor activity has been proposed to contribute to the pathogenesis of AD [40, 70, 104]. About 25 years ago, it was reported that D-cycloserine and D-Ser enhance memory performance in individuals with AD [96, 97] and restore retrograde memory in rats after perirhinal cortex injury [105], suggesting that D-Ser plays a complex and important role in the onset of AD. Thus, in the last two decades, the contribution of D-Ser in AD pathogenesis has been extensively investigated, also focusing on the enzymes involved in its metabolism.

In the brain, D-Ser is synthesized from the L-enantiomer by the PLP-dependent enzyme serine racemase (SR, EC 5.1.1.18) and is degraded either by SR itself or D-amino acid oxidase (DAAO, EC 1.4.3.3) [7]. SR is mainly expressed in neurons and to a lesser extent in astrocytes and microglia [106-109], while DAAO is expressed in astrocytes [110-113]. SR is functionally regulated by several mechanisms, including cofactor and ligand binding (Mg^{2+}, Ca^{2+} and ATP), protein interactors, oligomerization state, subcellular localization, and post-translational modifications [114-119]. DAAO activity is influenced by cofactor and ligand binding, protein mistargeting, post-translational modifications, and protein interactors (pLG72, Basson) [7, 120-124].

In 2004, Wu and collaborators reported that primary cultures of microglia treated with Aβ and the secreted forms of βAPP (sAPP) induced the release of an increased amount of D-Ser, which was coupled with an increase in transcription and protein level expression of the dimeric (active) form of SR [48, 125]. Moreover, it was reported that

primary cultures of hippocampal neurons responded to the conditioned medium from treated microglia with a rapid increase in Ca^{2+} levels, while the addition of DAAO reduced the ability of microglia-treated medium to induce the Ca^{2+} response, supporting the hypothesis that glial D-Ser is a cause of excitotoxicity, see Figure 4 [48, 125]. These conclusions were further confirmed as injecting Aβ in the hippocampus of SR knockout mice (showing a 90% decrease in D-Ser content in the brain compared to control mice) resulted in less degeneration than in wild-type animals [49]. Moreover, a strong upregulation of SR in reactive astrocytes in an AD rat model (TgF344-AD rats heterozygous for an APPsw/PS1ΔE9 transgene) and in human postmortem hippocampus and cortex samples from AD patients has been reported, supporting the notion that the increase in glial D-Ser may be associated with extrasynaptic NMDA receptor activation, thus playing an important role in excitotoxicity and neuronal damage, see Figure 4 [25]. Two studies conducted on postmortem AD brains, animal and cellular models of AD, and blood and CSF from probable to severe AD patients reported a significant increase in D-Ser levels [24, 68] and increased mRNA and protein levels of SR in homogenates from hippocampus or primary neuronal cultures treated with Aβ [24].

Similarly, DAAO has been related to AD progression, too. DAAO levels have been found to rise in the peripheral blood of patients with AD, with an increasing trend for severe AD [67]. Over the years, several studies focused on identifying and using DAAO inhibitors in different diseases [126], e.g., the inhibitor sodium benzoate was used for pain relief [127] and to treat early psychosis [128]. In randomized, double-blind placebo-controlled trials, sodium benzoate (250-750 mg/day for 24 weeks) improved the AD assessment scale (ADAS)-cog score, increasing neurocognitive function in patients with mild AD, without behavioral and psychological symptoms of dementia (DPSD) [82], while it did not show any efficacy in AD patients with DPSD treated with 622 mg benzoate/day for 6 weeks only [129].

A large percentage of AD patients show psychotic symptoms, such as delusions and hallucinations: linkage and association studies supported the hypothesis that psychiatric symptoms in AD could be due to genetic factors [130-132]. Interestingly, the *G72* gene, encoding a small protein (pLG72) that acts as a negative effector of DAAO [133-136], was

previously linked to schizophrenia, bipolar disorder, and psychotic illness [133, 136-138]. With the aim to clarify the role of the *G72* gene in the occurrence of psychosis in AD, 185 individuals with AD and depression in the early phase of disease were genotyped. This work identified an intronic mutation of the *G72* gene (rs2153674) associated with frequent and severe delusions [139]. Moreover, some years later, another intronic genetic mutation (rs778296) was associated with the early onset of AD, while the rs3391191 mutation encoding for the pLG72 R30K variant (associated to schizophrenia onset) [133] was found to influence the age of onset of the disease in PSE1 E280A AD patients [140, 141]. To confirm the hypothesis that pLG72 contributes to the pathogenesis of AD, the peripheral blood of patients with dementia (whose severity of cognitive deficit was evaluated based on the CDR scale) was analyzed, showing significantly higher pLG72 levels in mild cognitive impairment (MCI) and mild, moderate, and severe AD patients than in HS and the highest levels in patients with mild disease [142]. This work reported statistically significant differences in D-Ser levels and D-/(D+L)-Ser ratios among the five groups (values that increased with the dementia rating) and an association between pLG72 and L-Ser levels. These results support the view that pLG72 may contribute to AD onset by affecting DAAO activity [142].

A recent investigation highlighted a correlation between glucose metabolism, serine metabolism, and AD [143]. It is known that lower glucose metabolism is associated with early-stage AD and that mouse models of AD show reduced uptake and metabolism in the brain (probably depending on impaired vascular delivery) [144, 145]: a lack of ATP production affects ionic and neurotransmitter gradients. The astrocytic glucose metabolism is important for L-Ser production from the glycolytic intermediate 3-phosphoglycerate by phosphoglycerate dehydrogenase (PHGDH) belonging to the ‘‘phosphorylated pathway’’, see Figures 3 and 4 [146]. Notably, a lower level of both L- and D-Ser was reported in early-stage AD mice, resulting in a lower level of occupancy at the NMDA receptor coagonist site in hippocampal slices and impaired LTP: such a deficit was rescued by administering exogenous D-serine [143]. The dietary supplementation of D-Ser rescued impaired spatial memory at the whole-animal level, even for PHGDH knockout mice. Indeed, L-Ser administration rescued the same deficits

in the 3xTg-AD mice, which in any case did not show any alteration in PHGDH activity and serine metabolism. The lowered PHGDH level in late-stage AD (reactive) astrocytes may represent a further element affecting serine biosynthesis. This work proposed that oral L-Ser supplementation would be an effective therapy for AD by enhancing NMDA receptor activity [143]. However, such an activation might be potentially dangerous since NMDA receptor-dependent excitotoxic mechanisms have been proposed to contribute to synapse loss [147]. However, D-Ser is a coagonist for NMDA receptors frequently present at subsaturating levels, whose effects rely on the presence of the agonist glutamate: it has been proposed that increasing D-Ser levels "*could enhance signal to noise within AD circuits by improving the efficiency of phasic/synaptic NMDA receptor signaling, which mediates synaptic plasticity as well as neuroprotective signalling*" [148].

Conclusions

The tripartite glutamatergic synapses play an important role in the pathophysiology of AD [85]. Among the major factors affecting NMDA receptor-mediated neurotransmission in AD, availability of the agonist glutamate and modulation of the receptor's functions are extremely important [39, 149]. NMDA receptor function is modulated by both D-Ser and D-Asp and the noncompetitive antagonist memantine has been approved for treatment of moderate to advanced AD [85]. Here, the distinct preference of the coagonist for synaptic and extrasynaptic NMDA receptors makes it possible to identify separate neuronal outcomes, inducing cell survival or cell death. The possibility to selectively inhibit NMDA receptor-mediated excitotoxicity alone may delay the progression of synaptic disruption observed in AD. The pioneering work of the Joseph Coyle lab about 20 years ago demonstrated that AD patients receiving D-cycloserine, a molecule exhibiting partial agonist activity at the glycine site of NMDA receptors, resulted in a significant improvement in scores on the cognitive parameters [97]. Most recently, aged humans with impaired memory capacities in the Groton maze computer test showed an improvement in performance after receiving a D-Ser-enriched drink [150]. A greater understanding of the role of D-AAs in excitotoxicity related to the

pathogenesis of AD will facilitate novel therapeutic treatments for AD as well as for other acute and chronic diseases in which excitotoxicity is a core feature.

As current therapeutics do not cure the disease and do not improve life expectancy when administered in late-stage AD, the identification of early biomarkers is needed, especially related to NMDA receptors, which seem to be involved in synaptic dysfunction in early stages of AD. The potential use of both D-Ser and D-/(D+L)-Ser ratio in serum as biomarkers of AD was recently proposed by [60, 151] following the observation of a clearly increasing trend with progression of the disease (assessed by CDR score).

Acknowledgements

This work was supported by a grant from Ministero Università e Ricerca Scientifica PRIN 2017 (Grant 2017H4J3AS) to Loredano Pollegioni, and from Fondo di Ateneo per la Ricerca to Luciano Piubelli and Loredano Pollegioni. Valentina Rabattoni is a PhD student of the Life Sciences and Biotechnology course of University of Insubria.

Conflict of interest/Disclosure Statement

The authors have no conflict of interest to report.

References

[1] Perl DP (2010). Neuropathology of Alzheimer's disease. Mt Sinai J Med, 77(1):32-42.
[2] De Strooper B, Karran E (2016). The cellular phase of Alzheimer's disease. Cell, 164(4):603-615.
[3] Masters CL, Selkoe DJ (2012). Biochemistry of amyloid β-protein and amyloid deposits in Alzheimer disease. Cold Spring Harb Perspect Med, 2(6):a006262.
[4] Schell MJ, Molliver ME, Snyder SH (1995). D-serine, an endogenous synaptic modulator: localization to astrocytes and glutamate-stimulated release. Proc Natl Acad Sci U S A, 92(9):3948-3952.
[5] Mothet JP, Parent AT, Wolosker H, Brady RO Jr, Linden DJ, Ferris CD, Rogawski MA, Snyder SH (2000). D-serine is an endogenous ligand for the glycine site of the N-methyl-D-aspartate receptor. Proc Natl Acad Sci U S A, 97(9):4926-4931.
[6] Shleper M, Kartvelishvily E, Wolosker H (2005). D-serine is the dominant endogenous coagonist for NMDA receptor neurotoxicity in organotypic hippocampal slices. J Neurosci, 25(41):9413-9417.
[7] Pollegioni L, Sacchi S (2010). Metabolism of the neuromodulator D-serine. Cell Mol Life Sci, 67(14):2387-2404.
[8] Wolosker H (2011). Serine racemase and the serine shuttle between neurons and astrocytes. Biochim Biophys Acta,1814(11):1558-1566.
[9] Le Bail M, Martineau M, Sacchi S, Yatsenko N, Radzishevsky I, Conrod S, Ait Ouares K, Wolosker H, Pollegioni L, Billard JM, Mothet JP (2015). Identity of the NMDA receptor coagonist is synapse specific and developmentally regulated in the hippocampus. Proc Natl Acad Sci U S A, 112(2):E204-E213.
[10] Errico F, Napolitano F, Nisticò R, Centonze D, Usiello A (2009). D-aspartate: an atypical amino acid with neuromodulatory activity in mammals. Rev Neurosci, 20(5-6):429-440.

[11] Errico F, Napolitano F, Nisticò R, Usiello A (2012). New insights on the role of free D-aspartate in the mammalian brain. Amino Acids, 43(5):1861-1871.
[12] Punzo D, Errico F, Cristino L, Sacchi S, Keller S, Belardo C, Luongo L, Nuzzo T, Imperatore R, Florio E, De Novellis V, Affinito O, Migliarini S, Maddaloni G, Sisalli MJ, Pasqualetti M, Pollegioni L, Maione S, Chiariotti L, Usiello A (2016). Age-related changes in D-aspartate oxidase promoter methylation control extracellular D-aspartate levels and prevent precocious cell death during brain aging. J Neurosci, 36(10):3064-3078.
[13] Ota N, Shi T, Sweedler JV (2012). D-Aspartate acts as a signaling molecule in nervous and neuroendocrine systems. Amino Acids, 43(5):1873-1886.
[14] Aliashkevich A, Alvarez L, Cava F (2018). New insights into the mechanisms and biological roles of D-amino acids in complex eco-systems. Front Microbiol; 9:683.
[15] Genchi G (2017). An overview on D-amino acids. Amino Acids, 49(9):1521-1533.
[16] Marcone GL, Rosini E, Crespi E, Pollegioni L (2020). D-amino acids in foods. Appl Microbiol Biotechnol, 104(2):555-574.
[17] Hashimoto A, Nishikawa T, Hayashi T, Fujii N, Harada K, Oka T, Takahashi K (1992). The presence of free D-serine in rat brain. FEBS Lett, 296(1):33-36.
[18] Hashimoto A, Kumashiro S, Nishikawa T, Oka T, Takahashi K, Mito T, Takashima S, Doi N, Mizutani Y, Yamazaki T, Kaneko T, Ootomo E (1993). Embryonic development and postnatal changes in free D-aspartate and D-serine in the human prefrontal cortex. J Neurochem, 61(1):348-351.
[19] Man EH, Sandhouse ME, Burg J, Fisher GH (1983). Accumulation of D-aspartic acid with age in the human brain. Science, 220(4604):1407-1408.
[20] Kimura T, Hamase K, Miyoshi Y, Yamamoto R, Yasuda K, Mita M, Rakugi H, Hayashi T, Isaka Y (2016). Chiral amino acid metabolomics for novel biomarker screening in the prognosis of chronic kidney disease. Sci Rep, 6:26137.
[21] Hashimoto K, Fukushima T, Shimizu E, Okada S, Komatsu N, Okamura N, Koike K, Koizumi H, Kumakiri C, Imai K, Iyo M (2004). Possible role of D-serine in the pathophysiology of Alzheimer's disease. Prog Neuropsychopharmacol Biol Psychiatry, 28(2):385-388.
[22] Hashimoto K, Engberg G, Shimizu E, Nordin C, Lindström LH, Iyo M (2005). Reduced D-serine to total serine ratio in the cerebrospinal fluid of drug naive schizophrenic patients. Prog Neuropsychopharmacol Biol Psychiatry, 29(5):767-769.
[23] Errico F, Mothet JP, Usiello A (2015). D-Aspartate: an endogenous NMDA receptor agonist enriched in the developing brain with potential involvement in schizophrenia. J Pharm Biomed Anal, 116:7-17.
[24] Madeira C, Lourenco MV, Vargas-Lopes C, Suemoto CK, Brandão CO, Reis T, Leite RE, Laks J, Jacob-Filho W, Pasqualucci CA, Grinberg LT, Ferreira ST, Panizzutti R (2015). D-serine levels in Alzheimer's disease: implications for novel biomarker development. Transl Psychiatry, 5(5):e561.
[25] Balu DT, Pantazopoulos H, Huang CCY, Muszynski K, Harvey TL, Uno Y, Rorabaugh JM, Galloway CR, Botz-Zapp C, Berretta S, Weinshenker D, Coyle JT (2019). Neurotoxic astrocytes express the D-serine synthesizing enzyme, serine racemase, in Alzheimer's disease. Neurobiol Dis, 130:104511.
[26] Riedel G, Platt B, Micheau J (2003). Glutamate receptor function in learning and memory. Behav Brain Res, 140(1-2):1-47.
[27] Collingridge GL, Olsen RW, Peters J, Spedding M (2009). A nomenclature for ligand-gated ion channels. Neuropharmacology, 56(1):2-5.
[28] Johnson JW, Ascher P (1987). Glycine potentiates the NMDA response in cultured mouse brain neurons. Nature, 325(6104):529-531.
[29] Fuchs SA, Peeters-Scholte CM, de Barse MM, Roeleveld MW, Klomp LW, Berger R, de Koning TJ (2012). Increased concentrations of both NMDA receptor co-agonists D-serine and glycine in global ischemia: a potential novel treatment target for perinatal asphyxia. Amino Acids, 43(1):355-363.
[30] Lüscher C, Malenka RC (2012). NMDA receptor-dependent long-term potentiation and long-term depression (LTP/LTD). Cold Spring Harb Perspect Biol, 4(6):a005710.
[31] Wang R, Reddy PH (2017). Role of glutamate and NMDA receptors in Alzheimer's Disease. J Alzheimers Dis; 57(4):1041-1048.
[32] Wenk GL (2006). Neuropathologic changes in Alzheimer's disease: potential targets for treatment. J Clin Psychiatry; 67 Suppl 3:3-23.

[33] Danysz W, Parsons CG (2003). The NMDA receptor antagonist memantine as a symptomatological and neuroprotective treatment for Alzheimer's disease: preclinical evidence. Int J Geriatr Psychiatry, 18(Suppl 1):S23-S32.
[34] Barthet G, Jordà-Siquier T, Rumi-Masante J, Bernadou F, Müller U, Mulle C (2018). Presenilin-mediated cleavage of APP regulates synaptotagmin-7 and presynaptic plasticity. Nat Commun; 9(1):4780.
[35] He Y, Wei M, Wu Y, Qin H, Li W, Ma X, Cheng J, Ren J, Shen Y, Chen Z, Sun B, Huang FD, Shen Y, Zhou YD (2019). Amyloid β oligomers suppress excitatory transmitter release via presynaptic depletion of phosphatidylinositol-4,5-bisphosphate. Nat Commun, 10(1):1193.
[36] Chakroborty S, Hill ES, Christian DT, Helfrich R, Riley S, Schneider C, Kapecki N, Mustaly-Kalimi S, Seiler FA, Peterson DA, West AR, Vertel BM, Frost WN, Stutzmann GE (2019). Reduced presynaptic vesicle stores mediate cellular and network plasticity defects in an early-stage mouse model of Alzheimer's disease. Mol Neurodegener, 14(1):7.
[37] Barthet G, Mulle C (2020). Presynaptic failure in Alzheimer's disease. Prog Neurobiol, 101801.
[38] Snyder EM, Nong Y, Almeida CG, Paul S, Moran T, Choi EY, Nairn AC, Salter MW, Lombroso PJ, Gouras GK, Greengard P (2005). Regulation of NMDA receptor trafficking by amyloid-beta. Nat Neurosci, 8(8):1051-1058.
[39] Talantova M, Sanz-Blasco S, Zhang X, Xia P, Akhtar MW, Okamoto S, Dziewczapolski G, Nakamura T, Cao G, Pratt AE, Kang YJ, Tu S, Molokanova E, McKercher SR, Hires SA, Sason H, Stouffer DG, Buczynski MW, Solomon JP, Michael S, … Lipton SA (2013). Aβ induces astrocytic glutamate release, extrasynaptic NMDA receptor activation, and synaptic loss. Proc Natl Acad Sci U S A, 110(33):13691.
[40] Zhang Y, Li P, Feng J, Wu M (2016). Dysfunction of NMDA receptors in Alzheimer's disease. Neurol Sci, 37(7):1039-1047.
[41] Hardingham GE (2006). Pro-survival signalling from the NMDA receptor. Biochem Soc Trans, 34(Pt 5):936-938.
[42] Hetman M, Kharebava G (2006). Survival signaling pathways activated by NMDA receptors. Curr Top Med Chem, 6(8):787-799.
[43] Ikonomidou C, Bosch F, Miksa M, Bittigau P, Vöckler J, Dikranian K, Tenkova TI, Stefovska V, Turski L, Olney JW (1999). Blockade of NMDA receptors and apoptotic neurodegeneration in the developing brain. Science, 283(5398):70-74.
[44] Monti B, Contestabile A (2000). Blockade of the NMDA receptor increases developmental apoptotic elimination of granule neurons and activates caspases in the rat cerebellum. Eur J Neurosci, 12(9):3117-3123.
[45] Papouin T, Ladépêche L, Ruel J, Sacchi S, Labasque M, Hanini M, Groc L, Pollegioni L, Mothet JP, Oliet SH (2012). Synaptic and extrasynaptic NMDA receptors are gated by different endogenous coagonists. Cell, 150(3):633-646.
[46] Léveillé F, El Gaamouch F, Gouix E, Lecocq M, Lobner D, Nicole O, Buisson A (2008). Neuronal viability is controlled by a functional relation between synaptic and extrasynaptic NMDA receptors. FASEB J, 22(12):4258-4271.
[47] Hardingham GE, Bading H (2010). Synaptic versus extrasynaptic NMDA receptor signalling: implications for neurodegenerative disorders. Nat Rev Neurosci, 11(10):682-696.
[48] Wu SZ, Bodles AM, Porter MM, Griffin WS, Basile AS, Barger SW (2004). Induction of serine racemase expression and D-serine release from microglia by amyloid beta-peptide. J Neuroinflammation, 1(1):2.
[49] Inoue R, Hashimoto K, Harai T, Mori H (2008). NMDA- and beta-amyloid1-42-induced neurotoxicity is attenuated in serine racemase knock-out mice. J Neurosci, 28(53):14486-14491.
[50] Peyrovian B, Rosenblat JD, Pan Z, Iacobucci M, Brietzke E, McIntyre RS (2019). The glycine site of NMDA receptors: A target for cognitive enhancement in psychiatric disorders. Prog Neuropsychopharmacol Biol Psychiatry, 92:387-404.
[51] Molla G, Chaves-Sanjuan A, Savinelli A, Nardini M, Pollegioni L (2020). Structure and kinetic properties of human D-aspartate oxidase, the enzyme-controlling D-aspartate levels in brain. FASEB J, 34(1):1182-1197.
[52] Errico F, Nisticò R, Palma G, Federici M, Affuso A, Brilli E, Topo E, Centonze D, Bernardi G, Bozzi Y, D'Aniello A, Di Lauro R, Mercuri NB, Usiello A (2008). Increased levels of D-aspartate in the hippocampus enhance LTP but do not facilitate cognitive flexibility. Mol Cell Neurosci, 37(2):236-246.

[53] Errico F, Nisticò R, Napolitano F, Oliva AB, Romano R, Barbieri F, Florio T, Russo C, Mercuri NB, Usiello A (2011). Persistent increase of D-aspartate in D-aspartate oxidase mutant mice induces a precocious hippocampal age-dependent synaptic plasticity and spatial memory decay. Neurobiol Aging, 32(11):2061-2074.
[54] Nuzzo T, Feligioni M, Cristino L, Pagano I, Marcelli S, Iannuzzi F, Imperatore R, D'Angelo L, Petrella C, Carella M, Pollegioni L, Sacchi S, Punzo D, De Girolamo P, Errico F, Canu N, Usiello A (2019). Free D-aspartate triggers NMDA receptor-dependent cell death in primary cortical neurons and perturbs JNK activation, Tau phosphorylation, and protein SUMOylation in the cerebral cortex of mice lacking D-aspartate oxidase activity. Exp Neurol, 317:51-65.
[55] D'Aniello A, Luongo L, Romano R, Iannotta M, Marabese I, Boccella S, Belardo C, de Novellis V, Arra C, Barbieri A, D'Aniello B, Scandurra A, Magliozzi L, Fisher G, Guida F, Maione S (2017). D-Aspartic acid ameliorates painful and neuropsychiatric changes and reduces β-amyloid Aβ1-42 peptide in a long lasting model of neuropathic pain. Neurosci Lett, 651:151-158.
[56] Mothet JP, Billard JM, Pollegioni L, Coyle JT, Sweedler JV (2019). Investigating brain D-serine: Advocacy for good practices. Acta Physiol (Oxf), 226(1):e13257.
[57] Nagata Y, Borghi M, Fisher GH, D'Aniello A (1995). Free D-serine concentration in normal and Alzheimer human brain. Brain Res Bull, 38(2):181-183.
[58] Fisher G, Lorenzo N, Abe H, Fujita E, Frey WH, Emory C, Di Fiore MM, D' Aniello A (1998). Free D- and L-amino acids in ventricular cerebrospinal fluid from Alzheimer and normal subjects. Amino Acids, 15(3):263-269.
[59] Biemans EA, Verhoeven-Duif NM, Gerrits J, Claassen JA, Kuiperij HB, Verbeek MM (2016). CSF D-serine concentrations are similar in Alzheimer's disease, other dementias, and elderly controls. Neurobiol Aging, 42:213-216.
[60] Piubelli L, Pollegioni L, Rabattoni V, Mauri M, Princiotta-Cariddi L, Versino M, Sacchi S (2020). Serum D-serine levels are altered in early phases of Alzheimer's disease: towards a precocious biomarker. Transl Psych, in press.
[61] Hughes CP, Berg L, Danziger WL, Coben LA, Martin RL (1982). A new clinical scale for the staging of dementia. Br J Psychiatry, 140:566-572.
[62] Man EH, Fisher GH, Payan IL, Cadilla-Perezrios R, Garcia NM, Chemburkar R, Arends G, Frey WH 2nd (1987). D-aspartate in human brain. J Neurochem, 48(2):510-515.
[63] Fisher GH, D'Aniello A, Vetere A, Padula L, Cusano GP, Man EH (1991). Free D-aspartate and D-alanine in normal and Alzheimer brain. Brain Res Bull, 26(6):983-985.
[64] Fisher GH, D'Aniello A, Vetere A, Cusano GP, Chávez M, Petrucelli L (1992). Quantification of D-aspartate in normal and Alzheimer brains. Neurosci Lett, 143(1-2):215-218.
[65] D'Aniello A, Lee JM, Petrucelli L, Di Fiore MM (1998). Regional decreases of free D-aspartate levels in Alzheimer's disease. Neurosci Lett, 250(2):131-134.
[66] Fisher GH, Petrucelli L, Gardner C, Emory C, Frey WH 2nd, Amaducci L, Sorbi S, Sorrentino G, Borghi M, D'Aniello A (1994). Free D-amino acids in human cerebrospinal fluid of Alzheimer disease, multiple sclerosis, and healthy control subjects. Mol Chem Neuropathol, 23(2-3):115-124.
[67] Lin CH, Yang HT, Chiu CC, Lane HY (2017). Blood levels of D-amino acid oxidase vs. D-amino acids in reflecting cognitive aging. Sci Rep, 7(1):14849.
[68] Lin CH, Yang HT, Lane HY (2019). D-glutamate, D-serine, and D-alanine differ in their roles in cognitive decline in patients with Alzheimer's disease or mild cognitive impairment. Pharmacol Biochem Behav, 185:172760.
[69] Paoletti P, Bellone C, Zhou Q (2013). NMDA receptor subunit diversity: impact on receptor properties, synaptic plasticity and disease. Nat Rev Neurosci, 14(6):383-400.
[70] Liu J, Chang L, Song Y, Li H, Wu Y (2019). The role of NMDA receptors in Alzheimer's disease. Front Neurosci, 13:43.
[71] Labrie V, Lipina T, Roder JC (2008). Mice with reduced NMDA receptor glycine affinity model some of the negative and cognitive symptoms of schizophrenia. Psychopharmacology (Berl), 200(2):217-230.
[72] Filali M, Lalonde R (2013). The effects of subchronic D-serine on left-right discrimination learning, social interaction, and exploratory activity in APPswe/PS1 mice. Eur J Pharmacol, 701(1-3):152-158.

[73] Bado P, Madeira C, Vargas-Lopes C, Moulin TC, Wasilewska-Sampaio AP, Maretti L, de Oliveira RV, Amaral OB, Panizzutti R (2011). Effects of low-dose D-serine on recognition and working memory in mice. Psychopharmacology (Berl), 218(3):461-470.
[74] Zou C, Crux S, Marinesco S, Montagna E, Sgobio C, Shi Y, Shi S, Zhu K, Dorostkar MM, Müller UC, Herms J (2016). Amyloid precursor protein maintains constitutive and adaptive plasticity of dendritic spines in adult brain by regulating D-serine homeostasis. EMBO J, 35(20):2213-2222.
[75] Almond SL, Fradley RL, Armstrong EJ, Heavens RB, Rutter AR, Newman RJ, Chiu CS, Konno R, Hutson PH, Brandon NJ (2006). Behavioral and biochemical characterization of a mutant mouse strain lacking D-amino acid oxidase activity and its implications for schizophrenia. Mol Cell Neurosci, 32(4):324-334.
[76] Zhang M, Ballard ME, Basso AM, Bratcher N, Browman KE, Curzon P, Konno R, Meyer AH, Rueter LE (2011). Behavioral characterization of a mutant mouse strain lacking D-amino acid oxidase activity. Behav Brain Res, 217(1):81-87.
[77] Pritchett D, Hasan S, Tam SK, Engle SJ, Brandon NJ, Sharp T, Foster RG, Harrison PJ, Bannerman DM, Peirson SN (2015). D-amino acid oxidase knockout (Dao(-/-)) mice show enhanced short-term memory performance and heightened anxiety, but no sleep or circadian rhythm disruption. Eur J Neurosci, 41(9):1167-1179.
[78] Mothet JP, Rouaud E, Sinet PM, Potier B, Jouvenceau A, Dutar P, Videau C, Epelbaum J, Billard JM (2006). A critical role for the glial-derived neuromodulator D-serine in the age-related deficits of cellular mechanisms of learning and memory. Aging Cell, 5(3):267-274.
[79] Turpin FR, Potier B, Dulong JR, Sinet PM, Alliot J, Oliet SH, Dutar P, Epelbaum J, Mothet JP, Billard JM (2011). Reduced serine racemase expression contributes to age-related deficits in hippocampal cognitive function. Neurobiol Aging, 32(8):1495-1504.
[80] Potier B, Turpin FR, Sinet PM, Rouaud E, Mothet JP, Videau C, Epelbaum J, Dutar P, Billard JM (2010). Contribution of the D-serine-dependent pathway to the cellular mechanisms underlying cognitive aging. Front Aging Neurosci, 2:1.
[81] Yang S, Qiao H, Wen L, Zhou W, Zhang Y (2005). D-serine enhances impaired long-term potentiation in CA1 subfield of hippocampal slices from aged senescence-accelerated mouse prone/8. Neurosci Lett, 379(1):7-12.
[82] Lin CH, Chen PK, Chang YC, Chuo LJ, Chen YS, Tsai GE, Lane HY (2014). Benzoate, a D-amino acid oxidase inhibitor, for the treatment of early-phase Alzheimer disease: a randomized, double-blind, placebo-controlled trial. Biol Psychiatry,75(9):678-685.
[83] Guercio GD, Panizzutti R (2018). Potential and challenges for the clinical use of D-serine as a cognitive enhancer. Front Psychiatry, 9:14.
[84] Haxaire C, Turpin FR, Potier B, Kervern M, Sinet PM, Barbanel G, Mothet JP, Dutar P, Billard JM (2012). Reversal of age-related oxidative stress prevents hippocampal synaptic plasticity deficits by protecting D-serine-dependent NMDA receptor activation. Aging Cell, 11(2):336-344.
[85] Rudy CC, Hunsberger HC, Weitzner DS, Reed MN (2015). The role of the tripartite glutamatergic synapse in the pathophysiology of Alzheimer's disease. Aging Dis, 6(2):131-148.
[86] Hardingham GE, Bading H (2003). The Yin and Yang of NMDA receptor signalling. Trends Neurosci, 26(2):81-89.
[87] Sultan S, Gebara EG, Moullec K, Toni N (2013). D-serine increases adult hippocampal neurogenesis. Front Neurosci, 7:155.
[88] Esposito S, Pristerà A, Maresca G, Cavallaro S, Felsani A, Florenzano F, Manni L, Ciotti MT, Pollegioni L, Borsello T, Canu N (2012). Contribution of serine racemase/D-serine pathway to neuronal apoptosis. Aging Cell, 11(4):588-598.
[89] Errico F, Rossi S, Napolitano F, Catuogno V, Topo E, Fisone G, D'Aniello A, Centonze D, Usiello A (2008). D-aspartate prevents corticostriatal long-term depression and attenuates schizophrenia-like symptoms induced by amphetamine and MK-801. J Neurosci, 28(41):10404-10414.
[90] Errico F, Nisticò R, Di Giorgio A, Squillace M, Vitucci D, Galbusera A, Piccinin S, Mango D, Fazio L, Middei S, Trizio S, Mercuri NB, Teule MA, Centonze D, Gozzi A, Blasi G, Bertolino A, Usiello A (2014). Free D-aspartate regulates neuronal dendritic morphology, synaptic plasticity, gray matter volume and brain activity in mammals. Transl Psychiatry, 4(7):e417. Published 2014 Jul 29.
[91] Topo E, Soricelli A, Di Maio A, D'Aniello E, Di Fiore MM, D'Aniello A (2010). Evidence for the involvement of D-aspartic acid in learning and memory of rat. Amino Acids, 38(5):1561-1569.

[92] Cristino L, Luongo L, Squillace M, Paolone G, Mango D, Piccinin S, Zianni E, Imperatore R, Iannotta M, Longo F, Errico F, Vescovi AL, Morari M, Maione S, Gardoni F, Nisticò R, Usiello A (2015). D-Aspartate oxidase influences glutamatergic system homeostasis in mammalian brain. Neurobiol Aging, 36(5):1890-1902.
[93] Thompson LT, Moskal JR, Disterhoft JF (1992). Hippocampus-dependent learning facilitated by a monoclonal antibody or D-cycloserine. Nature, 359(6396):638-641.
[94] Baxter MG, Lanthorn TH, Frick KM, Golski S, Wan RQ, Olton DS (1994). D-cycloserine, a novel cognitive enhancer, improves spatial memory in aged rats. Neurobiol Aging, 15(2):207-213.
[95] Lelong V, Dauphin F, Boulouard M (2001). RS 67333 and D-cycloserine accelerate learning acquisition in the rat. Neuropharmacology, 41(4):517-522.
[96] Schwartz BL, Hashtroudi S, Herting RL, Schwartz P, Deutsch SI (1996). D-Cycloserine enhances implicit memory in Alzheimer patients. Neurology, 46(2):420-424.
[97] Tsai GE, Falk WE, Gunther J, Coyle JT (1999). Improved cognition in Alzheimer's disease with short-term D-cycloserine treatment. Am J Psychiatry, 156(3):467-469.
[98] Randolph C, Roberts JW, Tierney MC, Bravi D, Mouradian MM, Chase TN (1994). D-cycloserine treatment of Alzheimer disease. Alzheimer Dis Assoc Disord, 8(3):198-205.
[99] Fakouhi TD, Jhee SS, Sramek JJ, Benes C, Schwartz P, Hantsburger G, Herting R, Swabb EA, Cutler NR (1995). Evaluation of cycloserine in the treatment of Alzheimer's disease. J Geriatr Psychiatry Neurol, 8(4):226-230.
[100] Kalisch R, Holt B, Petrovic P, De Martino B, Klöppel S, Büchel C, Dolan RJ (2009). The NMDA agonist D-cycloserine facilitates fear memory consolidation in humans. Cereb Cortex, 19(1):187-196.
[101] Onur OA, Schlaepfer TE, Kukolja J, Bauer A, Jeung H, Patin A, Otte DM, Shah NJ, Maier W, Kendrick KM, Fink GR, Hurlemann R (2010). The N-methyl-D-aspartate receptor co-agonist D-cycloserine facilitates declarative learning and hippocampal activity in humans. Biol Psychiatry, 67(12):1205-1211.
[102] Feld GB, Lange T, Gais S, Born J (2013). Sleep-dependent declarative memory consolidation--unaffected after blocking NMDA or AMPA receptors but enhanced by NMDA coagonist D-cycloserine. Neuropsychopharmacology, 38(13):2688-2697.
[103] Lin CH, Lane HY (2019). The role of N-methyl-D-aspartate receptor neurotransmission and precision medicine in behavioral and psychological symptoms of dementia. Front Pharmacol, 10:540.
[104] Wang J, Gu BJ, Masters CL, Wang YJ (2017). A systemic view of Alzheimer disease - insights from amyloid-β metabolism beyond the brain. Nat Rev Neurol, 13(10):612-623.
[105] Andersen JM, Fonnum F, Myhrer T (2003). D-Serine alleviates retrograde amnesia of a visual discrimination task in rats with a lesion of the perirhinal cortex. Brain Res, 979(1-2):240–244.
[106] Wolosker H, Blackshaw S, Snyder SH (1999). Serine racemase: a glial enzyme synthesizing D-serine to regulate glutamate-N-methyl-D-aspartate neurotransmission. Proc Natl Acad Sci U S A, 96(23):13409–13414.
[107] Kartvelishvily E, Shleper M, Balan L, Dumin E, Wolosker H (2006). Neuron-derived D-serine release provides a novel means to activate N-methyl-D-aspartate receptors. J Biol Chem, 281(20):14151–14162.
[108] Miya K, Inoue R, Takata Y, Abe M, Natsume R, Sakimura K, Hongou K, Miyawaki T, Mori H (2008). Serine racemase is predominantly localized in neurons in mouse brain. J Comp Neurol, 510(6):641–654.
[109] Balu DT, Coyle JT (2012). Neuronal D-serine regulates dendritic architecture in the somatosensory cortex. Neurosci Lett, 517(2):77–81.
[110] Arnold G, Liscum L, Holtzman E (1979). Ultrastructural localization of D-amino acid oxidase in microperoxisomes of the rat nervous system. J Histochem Cytochem, 27(3):735–745.
[111] Horiike K, Tojo H, Arai R, Yamano T, Nozaki M, Maeda T (1987). Localization of D-amino acid oxidase in Bergmann glial cells and astrocytes of rat cerebellum. Brain Res Bull, 19(5):587–596.
[112] Horiike K, Tojo H, Arai R, Nozaki M, Maeda T (1994). D-amino-acid oxidase is confined to the lower brain stem and cerebellum in rat brain: regional differentiation of astrocytes. Brain Res, 652(2):297–303.
[113] Kappor R, Kapoor V (1997). Distribution of D-amino acid oxidase (DAO) activity in the medulla and thoracic spinal cord of the rat: implications for a role for D-serine in autonomic function. Brain Res, 771(2):351-355.

[114] Shoji K, Mariotto S, Ciampa AR, Suzuki H (2006). Regulation of serine racemase activity by D-serine and nitric oxide in human glioblastoma cells. Neurosci Lett, 392(1-2):75-78.
[115] Mustafa AK, van Rossum DB, Patterson RL, Maag D, Ehmsen JT, Gazi SK, Chakraborty A, Barrow RK, Amzel LM, Snyder SH (2009). Glutamatergic regulation of serine racemase via reversal of PIP2 inhibition. Proc Natl Acad Sci U S A, 106(8):2921-2926.
[116] Marchetti M, Bruno S, Campanini B, Bettati S, Peracchi A, Mozzarelli A. (2015) Regulation of human serine racemase activity and dynamics by halides, ATP and malonate. Amino Acids, 47(1):163-173.
[117] Kolodney G, Dumin E, Safory H, Rosenberg D, Mori H, Radzishevsky I, Wolosker H (2016). Nuclear compartmentalization of serine racemase regulates D-serine production: implications for N-methyl-D-aspartate (NMDA) receptor activation. J Biol Chem, 291(6):2630.
[118] Bruno S, Margiotta M, Marchesani F, Paredi G, Orlandi V, Faggiano S, Ronda L, Campanini B, Mozzarelli A (2017). Magnesium and calcium ions differentially affect human serine racemase activity and modulate its quaternary equilibrium toward a tetrameric form. Biochim Biophys Acta Proteins Proteom, 1865(4):381-387.
[119] Raboni S, Marchetti M, Faggiano S, Campanini B, Bruno S, Marchesani F, Margiotta M, Mozzarelli A (2019). The energy landscape of human serine racemase. Front Mol Biosci, 5:112.
[120] Caldinelli L, Molla G, Sacchi S, Pilone MS, Pollegioni L (2009). Relevance of weak flavin binding in human D-amino acid oxidase. Protein Sci, 18(4):801-810.
[121] Caldinelli L, Molla G, Bracci L, Lelli B, Pileri S, Cappelletti P, Sacchi S, Pollegioni L (2010). Effect of ligand binding on human D-amino acid oxidase: implications for the development of new drugs for schizophrenia treatment. Protein Sci, 19(8):1500-1512.
[122] Popiolek M, Ross JF, Charych E, Chanda P, Gundelfinger ED, Moss SJ, Brandon NJ, Pausch MH (2011). D-amino acid oxidase activity is inhibited by an interaction with bassoon protein at the presynaptic active zone. J Biol Chem, 286(33):28867-28875.
[123] Pollegioni L, Sacchi S, Murtas G (2018). Human D-amino acid oxidase: structure, function, and regulation. Front Mol Biosci, 5:107.
[124] Pollegioni L, Piubelli L, Molla G, Rosini E (2018). D-Amino acid oxidase-pLG72 interaction and D-serine modulation. Front Mol Biosci, 5:3.
[125] Wu S, Basile AS, Barger SW (2007). Induction of serine racemase expression and D-serine release from microglia by secreted amyloid precursor protein (sAPP). Curr Alzheimer Res, 4(3):243–251.
[126] Sacchi S, Rosini E, Pollegioni L, Molla G (2013). D-amino acid oxidase inhibitors as a novel class of drugs for schizophrenia therapy. Curr Pharm Des, 19(14):2499-2511.
[127] Hashimoto K, Fujita Y, Horio M, Kunitachi S, Iyo M, Ferraris D, Tsukamoto T (2009). Co-administration of a D-amino acid oxidase inhibitor potentiates the efficacy of D-serine in attenuating prepulse inhibition deficits after administration of dizocilpine. Biol Psychiatry, 65(12):1103–1106.
[128] Ryan A, Baker A, Dark F, Foley S, Gordon A, Hatherill S, Stathis S, Saha S, Bruxner G, Beckman M, Richardson D, Berk M, Dean O, McGrath J, Group CW, Scott J (2017). The efficacy of sodium benzoate as an adjunctive treatment in early psychosis - CADENCE-BZ: study protocol for a randomized controlled trial. Trials, 18(1):165.
[129] Lin CH, Chen PK, Wang SH, Lane HY (2019). Sodium benzoate for the treatment of behavioral and psychological symptoms of dementia (BPSD): A randomized, double-blind, placebo-controlled, 6-week trial. J Psychopharmacol, 33(8):1030-1033.
[130] Bacanu SA, Devlin B, Chowdari KV, DeKosky ST, Nimgaonkar VL, Sweet RA (2002). Linkage analysis of Alzheimer disease with psychosis. Neurology, 59(1):118-120.
[131] Bacanu SA, Devlin B, Chowdari KV, DeKosky ST, Nimgaonkar VL, Sweet RA (2005). Heritability of psychosis in Alzheimer disease. Am J Geriatr Psychiatry, 13(7):624-627.
[132] Hollingworth P, Hamshere ML, Holmans PA, O'Donovan MC, Sims R, Powell J, Lovestone S, Myers A, DeVrieze FW, Hardy J, Goate A, Owen M, Williams J (2007). Increased familial risk and genomewide significant linkage for Alzheimer's disease with psychosis. Am J Med Genet B Neuropsychiatr Genet, 144B(7):841-848.
[133] Chumakov I, Blumenfeld M, Guerassimenko O, Cavarec L, Palicio M, Abderrahim H, Bougueleret L, Barry C, Tanaka H, La Rosa P, Puech A, Tahri N, Cohen-Akenine A, Delabrosse S, Lissarrague S, Picard FP, Maurice K, Essioux L, Millasseau P, Grel P, … Cohen D (2002). Genetic and physiological data

implicating the new human gene G72 and the gene for D-amino acid oxidase in schizophrenia. Proc Natl Acad Sci U S A, 99(21):13675–13680.
[134] Sacchi S, Bernasconi M, Martineau M, Mothet JP, Ruzzene M, Pilone MS, Pollegioni L, Molla G (2008). pLG72 modulates intracellular D-serine levels through its interaction with D-amino acid oxidase: effect on schizophrenia susceptibility. J Biol Chem, 283(32):22244-22256.
[135] Sacchi S, Cappelletti P, Giovannardi S, Pollegioni L (2011). Evidence for the interaction of D-amino acid oxidase with pLG72 in a glial cell line. Mol Cell Neurosci, 48(1):20-28.
[136] Sacchi S, Binelli G, Pollegioni L (2016). G72 primate-specific gene: a still enigmatic element in psychiatric disorders. Cell Mol Life Sci, 73(10):2029-2039.
[137] Schumacher J, Jamra RA, Freudenberg J, Becker T, Ohlraun S, Otte AC, Tullius M, Kovalenko S, Bogaert AV, Maier W, Rietschel M, Propping P, Nöthen MM, Cichon S (2004). Examination of G72 and D-amino-acid oxidase as genetic risk factors for schizophrenia and bipolar affective disorder. Mol Psychiatry, 9(2):203–207.
[138] Addington AM, Gornick M, Sporn AL, Gogtay N, Greenstein D, Lenane M, Gochman P, Baker N, Balkissoon R, Vakkalanka RK, Weinberger DR, Straub RE, Rapoport JL (2004). Polymorphisms in the 13q33.2 gene G72/G30 are associated with childhood-onset schizophrenia and psychosis not otherwise specified. Biol Psychiatry, 55(10):976–980.
[139] Di Maria E, Bonvicini C, Bonomini C, Alberici A, Zanetti O, Gennarelli M (2009). Genetic variation in the G720/G30 gene locus (DAOA) influences the occurrence of psychotic symptoms in patients with Alzheimer's disease. J Alzheimers Dis, 18(4):953-960.
[140] Vélez JI, Chandrasekharappa SC, Henao E, Martinez AF, Harper U, Jones M, Solomon BD, Lopez L, Garcia G, Aguirre-Acevedo DC, Acosta-Baena N, Correa JC, Lopera-Gómez CM, Jaramillo-Elorza MC, Rivera D, Kosik KS, Schork NJ, Swanson JM, Lopera F, Arcos-Burgos M (2013). Pooling/bootstrap-based GWAS (pbGWAS) identifies new loci modifying the age of onset in PSEN1 p.Glu280Ala Alzheimer's disease. Mol Psychiatry, 18(5):568–575.
[141] Vélez JI, Rivera D, Mastronardi CA, Patel HR, Tobón C, Villegas A, Cai Y, Easteal S, Lopera F, Arcos-Burgos M (2016). A mutation in DAOA modifies the age of onset in PSEN1 E280A Alzheimer's disease. Neural Plast, 2016:9760314.
[142] Lin CH, Chiu CC, Huang CH, Yang HT, Lane HY (2019). pLG72 levels increase in early phase of Alzheimer's disease but decrease in late phase. Sci Rep, 9(1):13221.
[143] Le Douce J, Maugard M, Veran J, Matos M, Jégo P, Vigneron PA, Faivre E, Toussay X, Vandenberghe M, Balbastre Y, Piquet J, Guiot E, Tran NT, Taverna M, Marinesco S, Koyanagi A, Furuya S, Gaudin-Guérif M, Goutal S, Ghettas A, … Bonvento G (2020). Impairment of glycolysis-derived L-serine production in astrocytes contributes to cognitive deficits in Alzheimer's disease. Cell Metab, 31(3):503-517.e8.
[144] Sweeney MD, Kisler K, Montagne A, Toga AW, Zlokovic BV (2018). The role of brain vasculature in neurodegenerative disorders. Nat Neurosci, 21(10):1318-1331.
[145] Butterfield DA, Halliwell B (2019). Oxidative stress, dysfunctional glucose metabolism and Alzheimer disease. Nat Rev Neurosci, 20(3):148-160.
[146] Murtas G, Marcone GL, Sacchi S, Pollegioni L (2020). L-Serine synthesis via the phosphorylated pathway in humans. Cell. Mol. Life Sci, published online ahead of print.
[147] Ong WY, Tanaka K, Dawe GS, Ittner LM, Farooqui AA (2013). Slow excitotoxicity in Alzheimer's disease. J Alzheimers Dis, 35(4):643-668.
[148] Hardingham GE (2020). Targeting synaptic NMDA receptor co-agonism as a therapy for Alzheimer's disease?. Cell Metab, 31(3):439-440.
[149] Scott HA, Gebhardt FM, Mitrovic AD, Vandenberg RJ, Dodd PR (2011). Glutamate transporter variants reduce glutamate uptake in Alzheimer's disease. Neurobiol Aging, 32(3).
[150] Avellar M, Scoriels L, Madeira C, Vargas-Lopes C, Marques P, Dantas C, Manhães AC, Leite H, Panizzutti R (2016). The effect of D-serine administration on cognition and mood in older adults. Oncotarget, 7(11):11881-11888.
[151] Madeira C, Alheira FV, Calcia MA, Silva TCS, Tannos FM, Vargas-Lopes C, Fisher M, Goldenstein N, Brasil MA, Vinogradov S, Ferreira ST, Panizzutti R (2018). Blood levels of glutamate and glutamine in recent onset and chronic schizophrenia. Front Psychiatry. 2018;9:713.

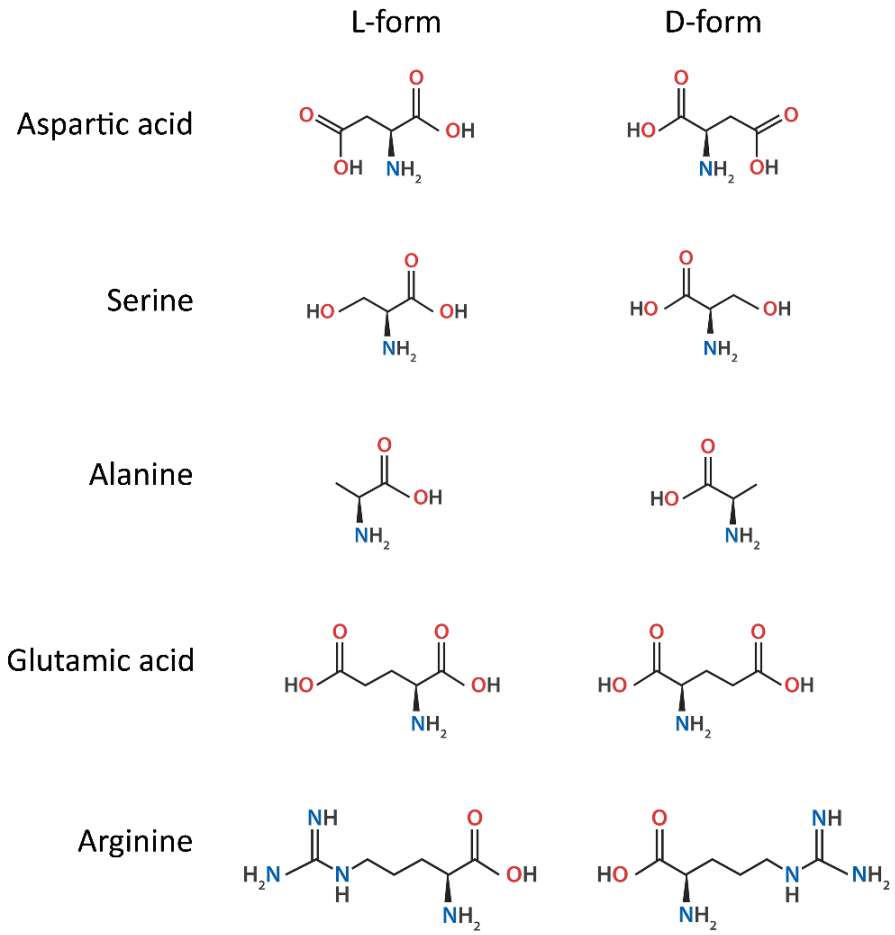

Figure 1. The mirror structure of the most relevant D-amino acids related to neuromodulation. Figure generated with Biorender.com.

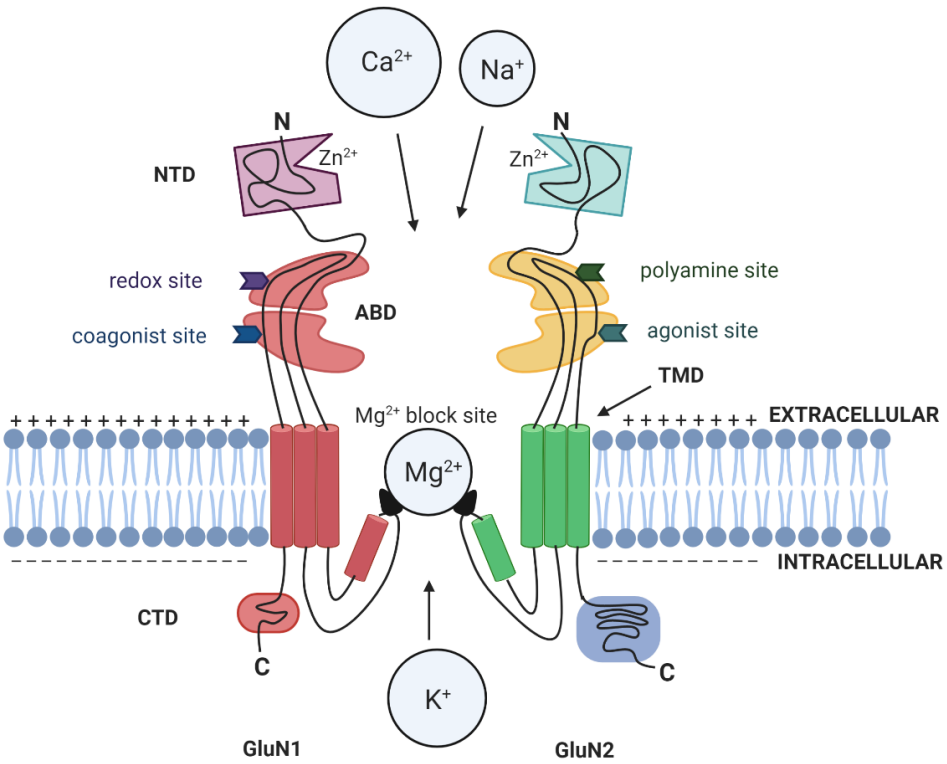

Figure 2. Scheme of the modular organization of NMDA receptors: heterotetramers are formed by two GluN1 subunits associated with the combination of two other subunits including GluN2(A-D) or a mixture of GluN2 and GluN3(A or B). The extracellular portion includes the NTD (N-terminal domain) and the ABD (agonist binding domain): the latter harbours the binding sites for the agonist glutamate and the co-agonist Gly/D-Ser (the glycine-binding site), as well as the redox and polyamine regulatory sites. The TMD (transmembrane domain) forms the ion channel that contains the site for Mg^{2+} blockade. The intracellular region is made by the CTD (C-terminal domain). Figure generated with Biorender.com.

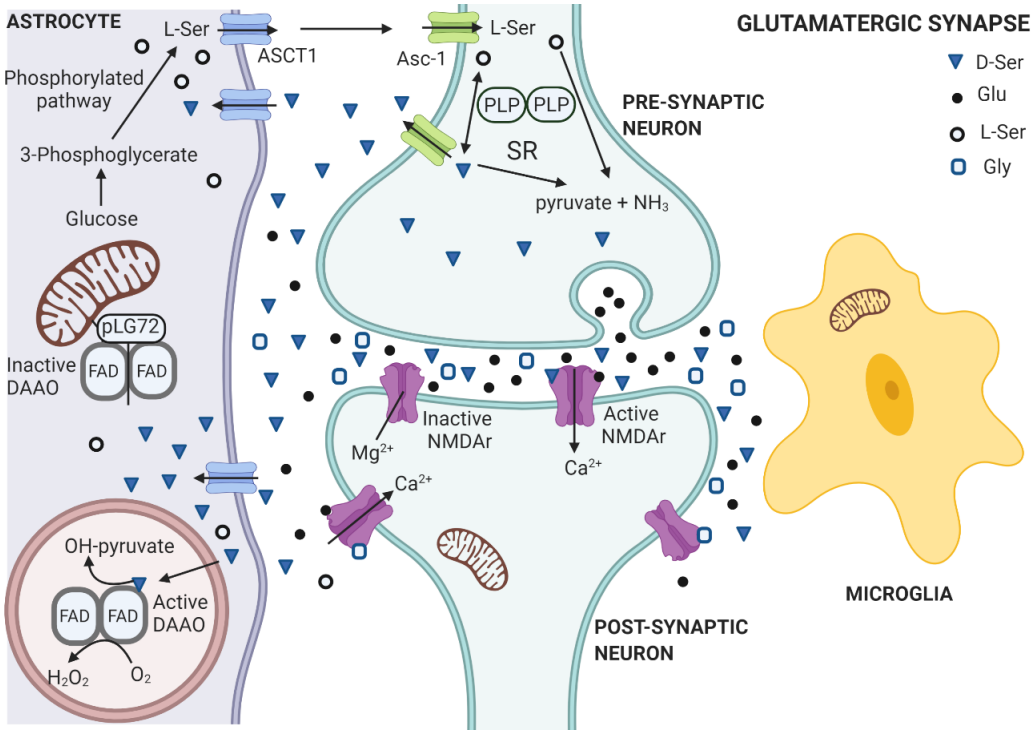

Figure 3. Schematic representation of the serine shuttle at the tripartite synapsis under physiological conditions. L-Ser is synthesized from glucose in the astrocytes through the phosphorylated pathway from the glycolytic intermediate 3-phosphoglycerate. L-Ser is released in external medium through the ASCT1 subtype of neutral amino acid transporters and then it is taken up by neurons through the Asc-1 subtype transporters. In neurons L-Ser is racemized into D-Ser by serine racemase (SR), which is delivered back to extracellular space through Asc-1 hetero-exchange with L-Ser. Extracellular D-Ser binds to NMDA receptors concomitantly with glutamate, activating the receptors at the membrane of postsynaptic neurons, thus promoting functional plasticity at synapses. Gly acts mainly on extrasynaptic NMDA receptors (NMDAr) while the synaptic ones are preferentially targeted by D-Ser as co-agonist. In healthy individuals, in absence of a presynaptic glutamatergic signal, the Mg^{2+} ion occupies the calcium channel in postsynaptic NMDA receptors. In neurons, both D- and L-Ser can be degraded by SR into pyruvate and NH_3 by the water elimination reaction. D-Ser is picked up by astrocytes from the synaptic cleft through ASCT1 hetero-exchange with the L-enantiomer, where it is degraded by the peroxisomal enzyme D-amino acid oxidase (DAAO), which activity is controlled by pLG72 (located on the cytosolic side of outer mitochondrial membrane) to prevent an excessive degradation of D-Ser. Figure generated with Biorender.com.

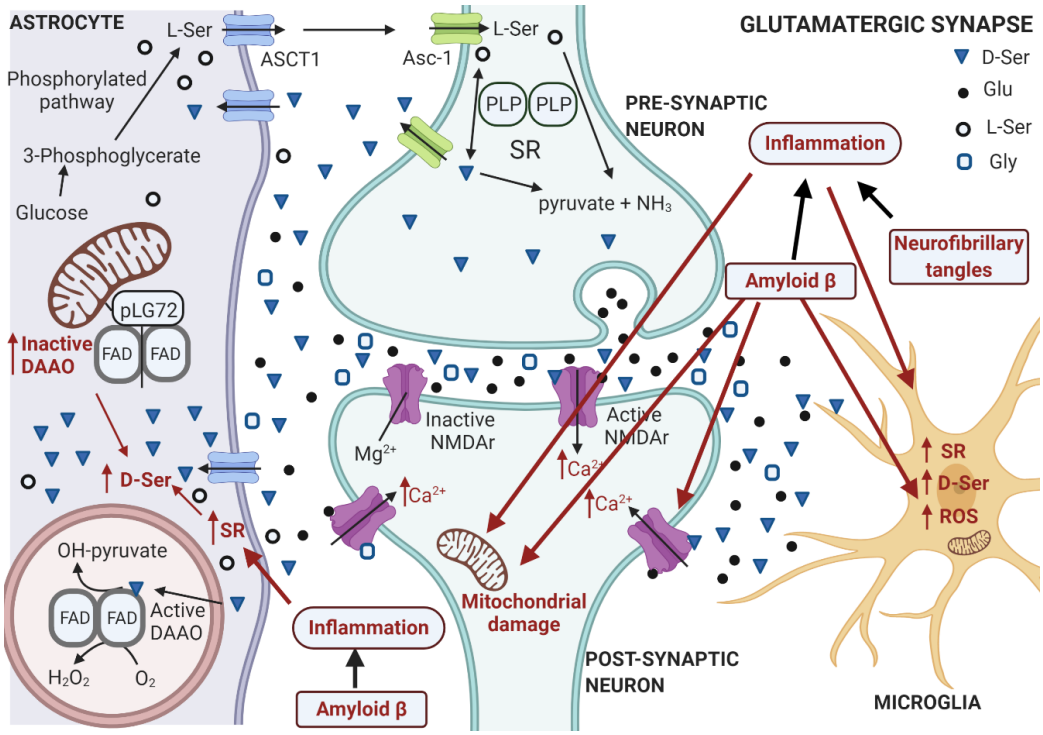

Figure 4. Schematic representation of the serine shuttle at the tripartite synapsis under AD. Aβ plaques and neurofibrillary tangles induce brain inflammation (see words and arrows depicted in red): both inflammation and Aβ damage neuronal mitochondria. Under these conditions the neuron is unable to maintain the correct resting potential: Mg^{2+} vacates the calcium channel at postsynaptic NMDA receptors allowing the influx of excessive levels of calcium ion. Aβ may further exacerbate the alteration due to excessive Ca^{2+} level by enhancing its entry interacting with postsynaptic NMDA receptors and activating D-Ser synthesis in microglia and astrocytes. The final result is a pathological neuronal overactivation. Neuronal cell survival can be also compromised by insufficient synaptic NMDA receptor signalling: the block of NMDA receptor function leads to neuronal apoptosis and degeneration. Lower glucose metabolism is associated to early stage AD since lack in ATP production affects ionic and neurotransmitter gradients. Indeed, a decrease in the astrocytic glucose metabolism could affect L-Ser production from the glycolytic intermediate 3-phosphoglycerate and, in turn, the D-Ser level. Figure generated with Biorender.com.

Table 1. Levels of D- and L-enantiomers (and of the D/total ratio) for selected amino acids in AD and HS samples.

Analytical method	Sample	Subjects (number)	Unit of measurement	Levels of analyzed amino acids (Mean ± SD)			Ref.
				[D-enantiomer]	[L-enantiomer]	D/(D+L) ratio (%)	
			Aspartate				
GC	White matter	HS (7)	N.A.	N.R.	N.R.	2.63 ± 0.37*	61
		AD (9)		N.R.	N.R.	2.77 ± 0.33*	
	Gray matter	HS (7)		N.R.	N.R.	1.51 ± 0.22*	
		AD (9)		N.R.	N.R.	1.48 ± 0.26*	
Enzymatic determination	White matter	HS (5)	nmol/g wet tissue	22.4 ± 4.6	N.R.	0.45 ± 0.18	62
		AD (4)		10.5 ± 6.6	N.R.	0.35 ± 0.20	
	Gray matter	HS (5)		18.6 ± 3.6	N.R.	0.41 ± 0.07	
		AD (4)		14.8 ± 5.9	N.R.	0.53 ± 0.49	
Derivatization with NAC/OPA followed by HPLC	Frontal cortex	HS (5)	nmol/g (probably wet) tissue	25.6 ± 4.8***	N.R.	N.R.	64**
		AD (5)		14.6 ± 3.9***	N.R.	N.R.	
	Parietal cortex	HS (5)		18.5 ± 3.5***	N.R.	N.R.	
		AD (5)		11.4 ± 2.9***	N.R.	N.R.	
	Temporal cortex	HS (5)		16.4 ± 3.4***	N.R.	N.R.	
		AD (5)		10.6 ± 2.3***	N.R.	N.R.	
	Hippocampus	HS (5)		21.4 ± 4.0***	N.R.	N.R.	
		AD (5)		11.5 ± 2.8***	N.R.	N.R.	
	Amygdala	HS (5)		13.6 ± 2.7***	N.R.	N.R.	
		AD (5)		8.17 ± 2.02***	N.R.	N.R.	
	Cerebellum	HS (5)		11.5 ± 3.9***	N.R.	N.R.	
		AD (5)		9.62 ± 2.88***	N.R.	N.R.	

Derivatization with NAC/OPA followed by HPLC	Superior frontal gyrus (frontal cortex)	HS (10)	nmol/mg total protein	0.136 ± 0.022	118 ± 16	0.494 ± 0.078	54[#]
		AD (10)		0.137 ± 0.027	140 ± 20	0.418 ± 0.068	
Derivatization with NAC/OPA followed by HPLC	Lumbar CSF	HS (8)	µM	0.036 ± 0.012	N.R.	2.55 ± 0.98	65
		AD (8)		0.054 ± 0.019	N.R.	3.52 ± 0.93	
	Ventricular CSF	HS (8)		1.23 ± 0.82	N.R.	0.61 ± 0.32	
		AD (8)		3.34 ± 2.14	N.R.	1.68 ± 0.80	
Derivatization with NAC/OPA followed by HPLC	Serum	HS (26)	µM	0.190 ± 0.137	13.4 ± 7.3	1.84 ± 1.51	60
		AD (42)		0.185 ± 0.106	16.8 ± 8.6	1.30 ± 0.89	
		Mild AD (25)		0.193 ± 0.108	16.5 ± 9.6	1.48 ± 0.55	
		Moderate AD (17)		0.174 ± 0.104	17.3 ± 7.0	1.07 ± 0.70	
Serine							
Derivatization with FDAA followed by HPLC	Frontal cortex	HS (8)	nmol/g wet tissue	66 ± 41	666 ± 222	9.9 ± 3.1*	57
		AD (7)		66 ± 40	750 ± 150	8.6 ± 4.0*	
GC-MS and HPLC derivatization with BOC/OPA followed by HPLC	Parietal cortex	HS (12)	nmol/g wet tissue	11.8 ± 5.44[##]	2453 ± 390	0.479[###]	24
		AD (17)		36.2 ± 4.43[##]	2434 ± 308	1.47[###]	
	Occipital cortex	HS (12)		1.73 ± 0.34[##]	75.0 ± 17.1	2.25[###]	
		AD (17)		1.76 ± 0.29[##]	110.5 ± 14.4	1.57[###]	
	Hippocampus	HS (12)		18.1 ± 5.1[##]	1371 ± 234	1.30[###]	
		AD (17)		33.0 ± 4.0[##]	1061 ± 175	3.02[###]	
	Lumbar CSF	HS (10)	µM	2.45 ± 0.65[##]	27.52 ± 9.28	8.17[###]	
		Probable AD (21)		12.32 ± 0.44[##]	30.86 ± 4.99	28.5[###]	
Derivatization with NPC-Phe NAC/OPA followed by UHPLC-MS	Lumbar CSF	HS (28)	µM	1.35 ± 0.29[##]	23.5 ± 4.6	5.43[###]	59
		AD (29)		1.56 ± 0.29[##]	25.2 ± 4	5.83[###]	

Derivatization with BOC/OPA followed by HPLC	Ventricular CSF	HS (5) AD (10)	µM	1.8 ± 1.2 9.0 ± 4.1	44 ± 23 76 ± 43	4.1 10.1	58
Derivatization with NBD-PZ followed by HPLC	Serum	HS (33) AD (32)	µM	2.14 ± 0.65 1.88 ± 0.51	155 ± 21 166 ± 30	1.38 ± 0.43 1.17 ± 0.44	21
Derivatization with NAC/OPA followed by HPLC	Serum	HS (26) AD (42) Mild AD (25) Moderate AD (17)	µM	1.59 ± 0.24$^{\#\#}$ 1.93 ± 0.57$^{\#\#}$ 1.84 ± 0.55$^{\#\#}$ 2.07 ± 0.60$^{\#\#}$	89.0 ± 19.1 89.9 ± 26.0 89.7 ± 26.2 90.0 ± 26.5	1.81 ± 0.37 2.17 ± 0.55 2.08 ± 0.57 2.29 ± 0.52	60
Alanine							
Enzymatic determination	White matter	HS (5) AD (4)	nmol/g wet tissue	12.3 ± 10.2 13.8 ± 7.5	N.R. N.R.	1.11 ± 0.83 0.87 ± 0.55	62
	Gray matter	HS (5) AD (4)		9.5 ± 2.9 20.8 ± 5.3	N.R. N.R.	0.84 ± 0.24 1.13 ± 0.46	
Probably derivatization with NAC/OPA followed by HPLC	Ventricular CSF	HS (8) AD (8)	µM	0.7 ± 0.3 0.8 ± 0.4	N.R. N.R.	0.70 0.80	58
Derivatization with IBC/OPA followed by HPLC	Serum	HS (116) Mild AD (128) Moderate to severe AD (76)	ng/mL	30.2 27.8 39.0	11347.0 12864.6 12325.0	0.27 0.22 0.32	67
Arginine							
Probably derivatization with FLEC followed by HPLC	Ventricular CSF	HS (5) AD (10)	µM	4.4 ± 6.5 3.9 ± 6.8	26 ± 14 33 ± 24	16.4 11.0	58

Glycine						
GC-MS and HPLC derivatization with BOC/OPA followed by HPLC	Parietal cortex	HS (12)	nmol/g wet tissue	3679 ± 57[##]	N.A.	24
		AD (17)		4058 ± 140[##]	N.A.	
	Occipital cortex	HS (12)		194 ± 43[##]	N.A.	
		AD (17)		284.5 ± 202.2[##]	N.A.	
	Hippocampus	HS (12)		1191 ± 255[##]	N.A.	
		AD (17)		1017 ± 249[##]	N.A.	
	Lumbar CSF	HS (12)	µM	291.6 ± 68.4[##]	N.A.	
		Probable AD (21)		336.9 ± 39.2[##]	N.A.	

*Values represent D/L ratio, expressed as percentage

**Values extrapolated from Figure 1 of this reference

***Mean ± SEM

#Values extrapolated from Figure 7 of this reference

##Mean ± SE

###Calculated from the data reported in the reference

SD: standard deviation; SE: standard error; SEM: standard error of the mean; N.A.: not applicable; N.R.: not reported

GC: Gas-Chromatography; BOC: N-*tert*-butyloxycarbonyl-L-cysteine; FDAA: 1-fluoro-2,4-dinitrophenyl-5-L-alanine amide; FLEC: (+)-1-(9-fluorenyl)ethyl chloroformate; IBC: N-isobutyl L-cysteine; NAC: N-acetyl-L-cysteine; NBD-PZ: 4-nitro-7-piperazino-2,1,3-benzoxadiazole; NPC-Phe: (*S*)-N-(4-nitrophenoxycarbonyl)-1-phenylalanine 2-methoxyethyl ester; OPA: *o*-phthalaldehyde

Table 2. Change in amino acid levels between AD and HS samples expressed as percentage. Δ% = 100*([AD] - [HS] / [HS]).

Sample	[D-enantiomer]	[L-enantiomer]	D/(D+L) ratio (%)	Ref.
Aspartate				
White matter	N.D.	N.D.	5.32	61
Gray matter	N.D.	N.D.	-1.99	
White matter	-53.1	N.D.	-22.2	62
Gray matter	-20.4	N.D.	29.3	
Frontal cortex	-43.0	N.D.	N.D.	64
Parietal cortex	-38.4	N.D.	N.D.	
Temporal cortex	-35.4	N.D.	N.D.	
Hippocampus	-46.3	N.D.	N.D.	
Amygdala	-39.9	N.D.	N.D.	
Cerebellum	-16.3	N.D.	N.D.	
Superior frontal gyrus (frontal cortex)	0.735	18.6	-15.4	54
Lumbar CSF	50.0	N.D.	38.0	65
Ventricular CSF	172	N.D.	175	
Serum CDR 1+2 / HS	-2.63	25.4	-29.3	60
Serum CDR 1 / HS	1.58	23.1	-19.6	
Serum CDR 2 /HS	-8.42	29.1	-41.8	
Serine				
Frontal cortex	0	12.6	-13.1	57
Parietal cortex	207	-0.775	207	24
Occipital cortex	1.73	47.3	-30.2	
Hippocampus	82.3	-22.6	132	
Lumbar CSF	403	12.1	249	
Lumbar CSF	15.6	7.23	7.4	59
Ventricular CSF	400	72.7	146	58
Serum	-12.1	7.10	-15.2	21
Serum CDR 1+2 / HS	21.4	1.01	19.9	60
Serum CDR 1 / HS	15.7	0.787	14.9	
Serum CDR 2 /HS	30.2	1.12	26.5	
Alanine				
White matter	12.2	N.D.	-21.6	62
Gray matter	119	N.D.	34.5	
Ventricular CSF	14.3	N.D.	14.3	58
Arginine				
Ventricular CSF	-11.4	26.9	-32.9	58
Glycine				
Parietal cortex		10.3		24
Occipital cortex		46.6		
Hippocampus		-14.6		
Lumbar CSF		15.5		

3.2. D-Asp levels in the serum of AD patients

In press

Serum D-serine levels are altered in early phases of Alzheimer's disease: towards a precocious biomarker

Luciano Piubelli[a*], Loredano Pollegioni[a], Valentina Rabattoni[a], Marco Mauri[a,b], Lucia Princiotta-Cariddi[c,d], Maurizio Versino[b,d], Silvia Sacchi[a]

[a]Department of Biotechnology and Life Sciences, University of Insubria, Varese, Italy
[b]Neurology Unit, Ospedale di Circolo and Fondazione Macchi, ASST Settelaghi, Varese, Italy
[c]Center of Research in Medical Pharmacology, University of Insubria, Varese, Italy
[d]Department of Medicine and Surgery, University of Insubria, Varese, Italy

[*]Corresponding author:
Luciano Piubelli, Department of Biotechnology and Life Sciences, University of Insubria, Via J. H. Dunant 3, 21100 Varese, Italy.
e-mail address: luciano.piubelli@uninsubria.it.
Tel: +39 0332 421 518. Fax: +39 0332 421 500.

Running Title: Serum D-serine and Alzheimer's Disease progression

Authors' e-mail addresses: luciano.piubelli@uninsubria.it; loredano.pollegioni@uninsubria.it, v.rabattoni@uninsubria.it; marco.mauri@uninsubria.it; l.princiottacarid@uninsubria.it; maurizio.versino@uninsubria.it; silvia.sacchi@unisubria.it

Abstract

D-Serine acts as co-agonist of N-methyl-D-aspartate receptors (NMDAR) which appear overactivated in AD, while D-aspartate is a modulatory molecule acting on NMDAR as a second agonist. The aim of this work is to clarify whether the levels of these D-amino acids in serum are deregulated in AD, with the final goal to identify novel and precocious biomarkers in AD. Serum levels of L- and D-enantiomers of serine and aspartate were determined by HPLC using a pre-column derivatization procedure and a selective enzymatic degradation. Experimental data obtained from aged-matched healthy subject (HS) and AD patients were statistically evaluated by considering age, gender and disease progression, and compared. Minor changes were apparent in serum L- and D-aspartate level in AD patients compared to HS. A positive correlation for D-serine level and age was apparent in the AD cohort. Notably, serum D-serine level and D-/total serine ratio significantly increased with the progression of the disease. Gender seems to have a minor effect on levels of all analytes tested. This work proposes serum D-serine level and D-/total serine ratio values as novel and valuable biomarkers for the progression of AD: the latter parameter allows to discriminate CDR 2 and CDR 1 patients from healthy (CDR 0) individuals.

Background

Alzheimer's disease (AD), the most common cause of late-onset dementia, is a chronic and progressive neurodegenerative disease affecting ≈6% of adults over 65 years of age [1]. The preliminary diagnosis of AD is made by a combination of clinical criteria, which includes neurological examinations, mental status tests and brain imaging. On the basis of these clinical tests only, however, diagnosis of AD becomes a difficult task. Currently, analysis of the cerebrospinal fluid (CSF) with established biomarkers [2,3] is carried out for research purposes. However, this fluid is obtained by an invasive and painful procedure: there is an extreme need for alternative, easily detectable biomarkers, which may also be sensitive and specific [4].

AD pathophysiology is characterized by the accumulation of extracellular amyloid β (Aβ) plaques and intraneuronal inclusions of the truncated and phosphorylated forms of tau

protein (neurofibrillary tangles). This appears to induce dystrophic neurites, loss of synapses, a prominent gliosis (involving changes in the morphology and function of microglia and astrocytes) and, only at later stages overt loss of neurons and associated brain atrophy [5]. Consistent with the role of the glutamatergic system in learning and memory formation, alterations in N-methyl-D-aspartate receptor (NMDAR) mediated neurotransmission have been linked with the pathological processes underlying AD [6,7]. Accordingly, Aβ induces synaptic dysfunction by perturbing synaptic Ca^{2+} handling in response to over activation of postsynaptic NMDARs [8], leading to oxidative stress, spine loss and gradual neuronal cell death, which in turn correlates with the progressive decline in memory and cognition in AD [7,9] but also by altering presynaptic functions [10].

Among the major factors affecting NMDAR-mediated neurotransmission in AD, availability of the agonist glutamate and the modulation of the receptor's functions are extremely important [11,12]: the non-competitive NMDAR antagonist memantine has been approved for treatment of moderate to advanced AD [13]. Modulatory molecules playing a role in NMDAR function may also be related to AD. In particular, D-aspartate (D-Asp) acting as a second agonist [14,15], and D-serine (D-Ser) which acts as the main endogenous co-agonist [16].

In mammals, D-Asp is abundant in the embryonic brain, while during adulthood its levels are extremely low and strictly controlled by the catabolizing enzyme D-aspartate oxidase (DASPO) [17]. The long-lasting exposure to nonphysiological, high concentration of D-Asp in DASPO knock-out mice (*Ddo*$^{-/-}$) elicited a precocious decay of synaptic plasticity and cognitive functions [18]. Moreover, severe processes related to neuroinflammation were observed in this animal model, as indicated by the appearance of dystrophic microglia and reactive astrocytes [19], distinctive features in neurodegenerative disorders [20,21]. Very recently, high D-Asp levels in *Ddo*$^{-/-}$ mice were also shown to induce changes in tau phosphorylation [22]. Notably, D-Asp content in tissues and/or biological fluids appeared altered in AD patients, despite differing results have been reported: halved D-Asp levels were detected in the white matter of AD brains compared to healthy subjects (HS) [23] whereas higher levels were measured in the CSF of AD

patients with respect to HS [24,25]. It is remarkable that all these studies were carried out on a limited number of subjects (≤10 for both for HS and AD patients).

On the other hand, brain D-Ser is synthesized starting from the corresponding L-enantiomer by the enzyme serine racemase (SR), and is degraded by both SR and D-amino acid oxidase (DAAO, mainly located in astrocytes) [26]. Notably, a strong up-regulation of SR was reported in reactive astrocytes in the hippocampus and entorhinal cortex of subjects with AD, that increased with disease progression: large part of these astrocytes were also neurotoxic [27]. Aβ aggregates induced release of D-Ser and its brain content was increased in animal models of the disease [28-30], suggesting that high D-Ser levels yield excitotoxicity, thus triggering neuronal death in AD. The DAAO inhibitor sodium benzoate improved cognitive and overall function in AD patients with early-phase disease when used at high concentration for 24 weeks [31].

Concerning the detection of D-Ser levels in AD patients, during the years contrasting results have been reported. By using traditional HPLC procedures, Nagata reported no changes in D- and L-Ser levels in frontal cortex compared to HS [32] while a decrease in D-Ser levels, coupled to a slight increase in L-Ser resulting in a significant decrease in D-/total-Ser ratio, was observed in human serum [33], albeit no details about the experimental procedure used are provided. Differently, an increase in D-Ser and SR levels was reported in post-mortem hippocampal and parietal cortex of AD patients compared to HS [30]. The same work reported higher D-Ser in the CSF of probable AD than in non-cognitively impaired subject groups by using classical HPLC procedures. These results confirmed previous observations from D'Aniello's group performed using an HPLC method coupled to enzymatic degradation [25]. Most recently, an analysis based on ultra-HPLC-tandem mass spectrometry reported tiny changes in D-Ser and D-/total-Ser level [34].

In our opinion, these confounding results are largely ascribable to the absence of standardized protocols and suitable controls. For this reason, this investigation is aimed at clarify whether D-Ser and D-Asp levels in serum are deregulated in AD using a well-established analytical procedure validated by the use of selective enzyme degradation and following the guidelines reported in [35]. This with the final goal to propose D-Ser

and/or D-Asp as novel and precocious biomarkers in AD, able of detecting the progression of the disease.

Materials and methods

Subject recruitment and sample collection

Peripheral venous blood samples were collected from patients with AD and from age- and sex-matched HS recruited from outpatients attending the Alzheimer's Assessment Unit (CDCD) at the Ospedale di Circolo and Fondazione Macchi in Varese (ASST Settelaghi), Italy. AD was diagnosed according to the NIA-AD criteria [3] and the disease stage of AD patients was assessed by using the clinical dementia rating (CDR) scale that allows to characterize five domains of cognitive and functional performance in AD dementia. Scores are defined as follows: 0: HS; 0.5: questionable or very mild dementia; 1: mild dementia; 2: moderate dementia; 3: severe dementia [36]. For this study, only AD patients presenting CDR 1 or 2 were enrolled. HS were caregivers of the recruited AD patients with Mini-Mental State Examination score ≥ 27/30 not suffering of present or past neurological and/or psychiatric pathologies influencing cognitive functions. The Ethics Committee of the Ospedale di Circolo and Fondazione Macchi of Varese approved the protocol and all participants signed a written informed consent before enrollment. Withdrawal of venous blood was performed after a fasting night, between 8:00 and 10:00 a.m., in BD Vacutainer™ SST™ II Advances Tubes (Becton Dickinson, Franklin Lakes, NJ, USA) including clot activator and gel for serum separation. Tubes were coded and serum separation was performed by centrifugation. Sera were subsequently frozen and stored at -80 °C until HPLC analyses. The AD patients recruited for this study were not affected by serious behavioral disorders, therefore they were not subjected to the administration of antipsychotic drugs.

High-performance liquid chromatography analyses

HPLC grade methanol, acetonitrile and tetrahydrofuran were from Honeywell International (Seelze, Germany). All other chemicals and reagents were from Merck Life Sciences (Darmstadt, Germany).

Serum samples were added of HPLC grade methanol (90% v/v final concentration) and vigorously vortexed for 3 min at room temperature to precipitate serum proteins, then removed by centrifugation (16,000 x *g* for 15 min at 4 °C). Supernatants were dried, suspended in 0.2 M trichloroacetic acid, neutralized with NaOH and subjected to pre-column derivatization with *o*-phthalaldehyde and N-acetyl-L-cysteine. Separation of the amino acid enantiomers was carried out by reversed-phase HPLC on a Symmetry C8 column (4.6x250 mm, bed volume 4 mL) (Waters S.p.A., Sesto San Giovanni, MI, Italy) using a HPLC PU-2089 System (Jasco Europe, Cremella, LC, Italy) equipped with a fluorescence detector, as described in [37]. Separation was carried out at 1 mL/min, under isocratic conditions in 0.1 M sodium acetate in the presence of 1% (v/v final concentration) tetrahydrofuran at pH 6.2 as mobile phase. All investigated amino acids were detected in a single run lasting 30 min. A washing step with 10 mL of 0.05 M sodium acetate buffer, 47% acetonitrile and 3% tetrahydrofuran (both v/v final concentrations), pH 6.2, was performed after each run. Identification of D- and L-amino acids was based on retention times obtained with external standards (retention times of 4.3 $\pm$ 0.2 min, 5.1 $\pm$ 0.2 min, 21.2 $\pm$ 0.6 min and 23.3 $\pm$ 0.7 min for D-Asp, L-Asp, D-Ser and L-Ser, respectively). Peaks identity was confirmed by the selective degradation of the D-enantiomers by RgDAAO M213R variant [38]: the samples were added with 10 μg of enzyme, incubated at 30 °C for 4 hours, and then subjected to derivatization and HPLC analyses. Quantification of enantiomers was based on peak areas by means of calibration curves for each enantiomer.

Distribution of the values of variables was assessed by the D'Agostino and Pearson normality test. A non normal (or suspected non normal) distribution for D-/L-Asp and D-/L-Ser was observed, both as absolute levels and as ratios: therefore, a nonparametric approach was used for all statistical analyses. Statistical significance of two-samples comparisons of continuous variables were performed using the two-tailed Mann-Whitney test. Correlations among continuous variables were assessed by Spearman nonparametric correlation analyses. Values reported represent mean ± standard deviation, unless otherwise stated. All analyses were performed using GraphPad Prism

7.0 (GraphPad Software, San Diego, CA, USA). A P-value <0.05 was considered as statistically significant.

Results

A total of 26 HS from 64 to 86 years and 42 AD patients from 64 to 87 years were enrolled for this study. The demographic and clinical characteristics of the subjects are reported in Table 1. The two groups are age-matched: the mean age was 76.7 $\pm$ 5.9 and 79.1 $\pm$ 5.4 years (mean $\pm$ SD) for HS and AD patients, respectively: statistical analyses showed no significant differences (P = 0.0834, Mann-Whitney test). Percentages of female were 53.8 and 66.7% in HS and AD patients, respectively. Mean age values of male cohorts were 76.8 ± 7.2 and 78.5 ± 5.4 years (HS and AD patients, respectively), and those of female cohorts were 76.6 ± 4.8 and 79.4 ± 5.4 years (HS and AD patients, respectively): in these cases also no statistically significant differences have been found comparing mean age values of HS and AD patients (P = 0.4687 and P = 0.0711 for male and female cohorts, respectively, Mann-Whitney test).

Levels of D- and L-aspartate and D- and L-serine in serum was assayed by pre-column derivatization procedure and confirming the identity and amount of the D-enantiomers (present at significantly lower level) by a selective enzymatic degradation. Age-related variation of the investigated amino acids was analyzed by Spearman nonparametric correlation analyses (Supplementary Figure 1): D- and L-Asp levels and D-/total-Asp ratio did not significantly vary with age, neither in samples from HS nor from AD patients (D-Asp HS: r = 0.216, P = 0.2891; D-Asp AD: r = 0.02573, P = 0.8715; L-Asp HS: r = 0.03024, P = 0.8834; L-Asp AD: r = -0.2589, P = 0.8707; D-/total-Asp ratio HS: r = 0.1133, P = 0.5814; D-/total-Asp ratio AD: r = 0.02715, P = 0.8645). The same analyses showed no correlations with age for D- and L-Ser levels and for D-/total-Ser ratio in samples from HS (D-Ser: r = 0.1002, P = 0.6264; L-Ser: r = -0.2784, P = 0.1684; D-/total-Ser ratio: r = 0.3844, P = 0.525); while a positive correlation has been found both for D-Ser (r = 0.5242, P = 0.0004) and for D-/total-Ser ratio (r = 0.3663, P = 0.0170), but not for L-Ser (r = 0.2164, P = 0.1687), in samples from AD patients.

In order to exclude any effect due to the administration of memantine on the levels of the analyzed molecules, values obtained for patients assuming and not assuming the drug were compared. In all cases, no significant difference has been observed (D-Ser: P = 0.6753; L-Ser: P = 0.4872; D-/total-Ser ratio: P = 0.7977; D-Asp: P = 0.6570; L-Asp: P = 0.0918; D-/total-Asp ratio: P = 0.3126; Mann-Whitney test). Thus, all patients were considered as a single group.[a]

Levels of D-Asp were only slightly decreased in AD patients compared to HS (-2.47%), whereas an increase (+25.3%) was observed for L-Asp: consequently, a decrease (-28.7%) was observed for D-/total-Asp ratio (Figure 1 and Supplementary Table 1). These variations resulted no statistically significant. Analyzing the data disaggregated by gender, significant variations between HS and AD patients were found only for the male cohort, in the case of L-Asp and of D-/total-Asp ratio (P = 0.0178 and 0.0464, respectively). Minor and no statistically significant differences were found for female cohort. Comparing data of male and female subjects belonging to the same group of subjects (Figure 2 and Supplementary Table 1), a statistically significant difference was apparent for HS and L-Asp only (P = 0.0178), and the relative D-/total-Asp ratio (P = 0.0464). Levels of Asp enantiomers were not affected by gender in AD patients.

D-Ser level showed a statistically significant increase in AD patients with respect to HS (+21.8%, P = 0.0060), whereas L-Ser level was unchanged (Figure 1B). Similarly to D-Ser, a statistically significant increase was observed for D-/total-Ser ratio (+20.2%, P = 0.0025) (Figure 1 and Supplementary Table 1). A similar pattern was observed comparing cohorts disaggregated by gender: in female cohorts D-Ser level increased by 28.7%, D-/total-Ser ratio increased by 31.4%, and L-Ser level was unchanged. In male cohorts, a lower increase of D-Ser and of D-/total-Ser ratio was observed (+12.3% and +11.2%, respectively) whereas the L-Ser level was unchanged. Comparison between male and female subjects of the same group (Figure 2 and Supplementary Table 1) revealed a

[a] We need to mention that the effect of other administered drugs, such as donepezil and rivastigmine, was not evaluated because of the low number of samples.

statistical significance only for D-/total-Ser ratio (P = 0.0032) of the HS subjects. Similarly to D-Asp, gender did not significantly affect level of Ser enantiomers in AD patients.

D-Serine levels increase with the progression of the disease in the early stages

Levels of aspartate and serine enantiomers have been compared between homogeneous groups regarding the stage of illness, assessed by the CDR score [39]. AD patients enrolled in this study were at initial stages of AD, corresponding to mild (CDR 1) or moderate (CDR 2) dementia.

Considering aspartate levels, comparison of mean levels of analyzed parameters observed for HS, CDR 1 and CDR 2 AD patients did not show any statistical significance (Table 2 and Figure 3A). However, a modest increase parallel to the gravity of the pathology has been observed for L-Asp, together with a parallel decrease in D-/total-Asp ratio (Table 2 and Figure 3A).

Analyses of the results obtained for serine clearly show an increase of D-Ser levels with the severity of the pathology: statistically significant differences have been found between HS and CDR 2 AD patients mean values (+30.2%, P = 0.0015) (Table 2 and Figure 3B, left). Since L-Ser levels remain unchanged (Table 2 and Figure 3B, center), an increase of the D-/total-Ser ratio was observed: statistically significant variations of this parameter have been found both between HS (CDR 0) and CDR 1 AD patients (+19.4%, P = 0.0336) and between HS and CDR 2 AD patients (+26.5%, P = 0.0016) (Table 2 and Figure 3B, right). Analysis of age distribution of HS, CDR 1 and CDR 2 AD patients, carried out using Mann-Whitney test, indicated that a statistically significant difference was observed between HS and CDR 2 AD patients only (P = 0.0105), whereas comparison between HS and CDR 1 AD patients and CDR 1 and CDR 2 AD patients was not statistically significant (P = 0.5077 and P = 0.1012, respectively, see Table 1). These results exclude that the observed increase in D-Ser serum level was due to differences in age of the cohorts analyzed.

Discussion

AD is the most common type of dementia in aged people: the pathological changes associated to AD (amyloid deposition and the resulting neuronal death) start decades before the first clinical symptoms appear. Thus, it is crucial to identify and detect parameters indicative of neuropathological changes, eventually those occurring at the synaptic level, in the very precocious stages of the disease. Diagnosis is now based on a neuropsychological evaluation and the assessment of AD biomarkers, such as Aβ oligomers and phosphorylated-tau levels in the CSF. However, CSF examinations are far from standard tests in general practice, due to the invasiveness of the procedure (a lumbar puncture), which also limits this practice for screening and clinical trials. Therefore, there is an urgent need for alternative, accessible peripheral biomarkers, such as serum biomarkers. Accordingly, we monitored the levels of D-Asp and D-Ser, two signaling molecules involved in NMDAR-mediated neurotransmission, in serum from AD patients at early stages of illness (CDR 1 or 2) and age-matched controls (CDR 0). We employed a standardized, well-validated analytical procedure based on precolumn derivatization, HPLC separation and quantification of the D-enantiomers by enzymatic degradation.

D-Asp and L-Asp serum content did not show any statistically significant variation between AD patients and HS, despite a reasonable increase of L-Asp levels (≈25%) was observed in AD patients. By analyzing data disaggregated by gender, statistically significant differences were observed for L-Asp only: in the HS male cohort L-Asp levels were significantly lower compared to the corresponding AD cohort and to female ones (independently from the diagnosis). [b] As a consequence, in the AD male cohort the D-/total-Asp ratio appeared significantly decreased compared to controls. On the other

[b] This gender difference is an interesting observation since D-Asp is involved in synthesis and release of testosterone [45,46]. Noteworthy, it has been reported that males with AD exhibit lower circulating [47,48] and brain [49] levels of testosterone than age-matched healthy males. It is possible to speculate that the alterations in testosterone levels might be due to an imparment in D-Asp synthesis that results in the observed slightly decrease in D-Asp level and L-Asp accumulation in male AD patients. This observation needs additional investigations requiring a higher number of samples.

hand, statistically significantly elevated D-Ser serum levels (≈20%) were detected in AD patients with respect of HS. Data disaggregated by gender indicate a higher increase in female (≈30%) compared to male (≈10%) cohorts, despite in this latter case the difference between AD patients and HS was not statistically significant. No significant change depending on diagnosis and/or gender is observed in L-Ser serum levels, while the D-/total-Ser ratio is higher in males compared to females HS cohorts.[c] Overall, our results point to a slight gender effect on the serum levels of both D- and L-Asp and D- and L-Ser, thus confirming previous results obtained in ventricular CSF [25] and in *post-mortem* tissues and CSF [30]. On the other hand, a significant positive correlation between serum D-serine levels and age has been observed in AD patients and not in HS, despite a negative association previously reported [39].

Separating subjects into experimental groups stratified by the CDR score showed an increasing trend for L-Asp content from cognitively HS (CDR 0) to patients with a CDR score of 2, which resulted into a specular trend in the D-/total-Asp ratio values. Lack of statistical significance for D-Asp might be ascribed to its very low concentration (0.15 - 0.2 μM), close to the limit of detection. Conversely, serum D-Ser levels paralleled the progression of the pathology: the lowest levels were detected in HS and increasing levels were observed in AD patients, being significantly higher in individuals with a CDR of 2. This positive correlation is even more evident for D-/total-Ser ratio. In this latter case, a statistically significant increase is also evident in patients with a CDR score of 1, suggesting this ratio as a more sensitive parameter of the pathology and its progression than absolute D-Ser levels.

This latter result is in line with recent observations reporting increased D-serine levels in some areas of AD brains involved in the disease progression [30], likely due to upregulation of SR expression in reactive neurotoxic astrocytes [27]. Worthy of note, converging lines of evidence indicate reduced levels of NMDAR in the same brain regions

[c] Differently from what observed for aspartate, the gender effect on serine enantiomers levels is not straightforward, in agreement with the known functions of both L- and D-Ser. For reviews see [50,51].

in AD patients [40,41]. It has been suggested that elevated levels of the coagonist D-Ser might underlie a mechanism by which Aβ oligomers trigger synapse dysfunction and the resulting memory impairment [30]: Aβ-induced D-Ser increase might represent an initial adaptive response to maintain proper neurotransmission in the early stages of the disease [42], but, since NMDARs appear overactivated in AD, they can also contribute to the excitotoxic scenario in later stages, worsening the neuropathological outcomes. D-Ser inhibits apoptosis at early phases and stimulates necrosis at later phases [43]. The development of amyloid plaques typically precedes clinically significant cognitive symptoms by at least 10-15 years: a time course comparison between plaques formation and D-Ser levels could allow to elucidate the events bringing to the dementia. Future studies should also evaluate the correlation between D-Ser levels and peripheral biomarkers of AD, i.e. blood levels of Aβ42, phosphorylated tau, etc.

As a next step in the field, analyses on subjects showing amnestic mild cognitive impairment (MCI, CDR = 0.5) and with a significantly increased probability to develop AD will allow to validate the use of serum serine levels as valuable biomarker of the disease onset. To be enrolled in this study, amnestic MCI patients need to undergo imaging analysis (*e.g.*, PET) to verify the presence of a neurodegenerative process.

Conclusions

Considerations related to the effect of Aβ on D-Ser synthesis/level, and thus on NMDAR functioning, in AD pathophysiology and our results concerning serine levels (determined by a procedure based on enzymatic selective degradation of the D-enantiomer) strengthen the idea of serum D-Ser levels and/or D-/total-Ser ratio as a valuable (and simple to assay) biological marker for AD, to evaluate the disease progression as well as the precocious stages of the illness. Accordingly, we suggest the combined use of blood-based biomarkers currently under development [44] and serine enantiomers concentration ratio as a novel and relevant strategy to increase sensitivity and specificity in the diagnosis of AD.

Acknowledgements

This work was supported by grant from Fondo di Ateneo to LuPi, SS and LoPo. VT is a Ph.D. student of the Biotechnology and Life Sciences course at the University of Insubria. LP-C is a Ph.D. student of the Clinical and Experimental Medicine and Medical Humanities course at the University of Insubria.

Competing interests

The authors declare no conflict of interest

References

[1] Qiu, C., Kivipelto, M. & von Strauss, E. Epidemiology of Alzheimer's disease: occurrence, determinants, and strategies toward intervention. *Dialogues Clin. Neurosci.* **11**:111-28 (2009).

[2] Jack, C. R. et al. Introduction to the recommendations from the National Institute on Aging-Alzheimer's Association workgroups on diagnostic guidelines for Alzheimer's disease. Alzheimers Dement. https://doi.org/10.1016/j.jalz.2011.03.004 (2011).

[3] McKhann, G. M. et al. The diagnosis of dementia due to Alzheimer's disease: Recommendations from the National Institute on Aging-Alzheimer's Association workgroups on diagnostic guidelines for Alzheimer's disease. *Alzheimers Dement.* https://doi.org/10.1016/j.jalz.2011.03.005 (2011).

[4] Humpel, C. Identifying and validating biomarkers for Alzheimer's disease. *Trends in Biotechnology* https://doi.org/10.1016/j.tibtech.2010.09.007 (2011).

[5] Danysz. W. & Parsons, C. G. Alzheimer's disease, β-amyloid, glutamate, NMDA receptors and memantine - searching for the connections. *Br. J. Pharmacol.* https://doi.org/10.1111/j.1476-5381.2012.02057.x (2012).

[6] Francis, P. T. Glutamatergic systems in Alzheimer's disease. *Int. J. Geriatr. Psychiatry* https://doi.org/10.1002/gps.934 (2003).

[7] Wenk, G. L. Neuropathologic changes in Alzheimer's disease: potential targets for treatment. *J. Clin. Psychiatry*, **67Suppl 3**:3-7 (2006).

[8] Wang, R., Reddy, P. H. Role of Glutamate and NMDA Receptors in Alzheimer's Disease. *J. Alzheimers Dis* https://doi.org/10.3233/JAD-160763 (2017).

[9] Danysz, W. & Parsons, C. G. The NMDA receptor antagonist memantine as a symptomatological and neuroprotective treatment for Alzheimer's disease: preclinical evidence. *Int. J. Geriatr. Psychiatry* https://doi.org/10.1002/gps.938 (2003).

[10] Barthet, G. & Mulle, C. Presynaptic failure in Alzheimer's disease. *Prog. Neurobiol*. https://doi.org/10.1016/j.pneurobio.2020.101801 (2020).

[11] Scott, H. A., Gebhardt, F. M., Mitrovic, A. D., Vandenberg, R. J. & Dodd, P. R. Glutamate transporter variants reduce glutamate uptake in Alzheimer's disease. *Neurobiol. Aging* https://doi.org/10.1016/j.neurobiolaging.2010.03.008 (2011).

[12] Talantova, M. et al. Aβ induces astrocytic glutamate release, extrasynaptic NMDA receptor activation, and synaptic loss. *Proc. Natl. Acad. Sci. USA* https://doi.org/10.1073/pnas.1306832110 (2013).

[13] Rudy, C. C, Hunsberger, H. C, Weitzner, D. S. & Reed, M. N. The role of the tripartite glutamatergic synapse in the pathophysiology of Alzheimer's disease. *Aging Dis.* https://doi.org/10.14336/AD.2014.0423 (2015).

[14] Errico, F., Napolitano, F., Nisticò, R. & Usiello, A. New insights on the role of free D-Asp in the mammalian brain. *Amino Acids* https://doi.org/10.1007/s00726-012-1356-1 (2012).

[15] Krashia, P. et al. Persistent elevation of D-Aspartate enhances NMDA receptor-mediated responses in mouse *substantia nigra pars compacta* dopamine neurons. *Neuropharmacology* https://doi.org/10.1016/j.neuropharm.2015.12.013 (2016).
[16] Mothet, J.-P. et al. D-Serine is an endogenous ligand for the glycine site of the N-methyl-D-aspartate receptor. *Proc. Natl. Acad. Sci. USA*. https://doi.org/10.1073/pnas.97.9.4926 (2000).
[17] Schell, M. J., Cooper, O. B. & Snyder, S. H. D-aspartate localizations imply neuronal and neuroendocrine roles. *Proc. Natl. Acad. Sci. USA.* https://doi.org/10.1073/pnas.94.5.2013 (1997).
[18] Errico, F. et al. Persistent increase of D-aspartate in D-aspartate oxidase mutant mice induces a precocious hippocampal age-dependent synaptic plasticity and spatial memory decay. *Neurobiol. Aging*. https://doi.org/10.1016/j.neurobiolaging.2009.12.007 (2011).
[19] Punzo, D. et al. Age-related changes in D-aspartate oxidase promoter methylation control extracellular D-aspartate levels and prevent precocious cell death during brain aging. *J. Neurosci.* https://doi.org/10.1523/JNEUROSCI.3881-15.2016 (2016).
[20] Liddelow, S. A. et al. Neurotoxic reactive astrocytes are induced by activated microglia. *Nature.* https://doi.org/10.1038/nature21029 (2017).
[21] Yun, S. P. et al. Block of A1 astrocyte conversion by microglia is neuroprotective in models of Parkinson's disease. *Nat. Med.* https://doi.org/10.1038/s41591-018-0051-5 (2018).
[22] Nuzzo, T. et al. Free D-aspartate triggers NMDA receptor-dependent cell death in primary cortical neurons and perturbs JNK activation, Tau phosphorylation, and protein SUMOylation in the cerebral cortex of mice lacking D-aspartate oxidase activity. *Exp. Neurol.* https://doi.org/10.1016/j.expneurol.2019.02.014 (2019).
[23] Fisher, G. H. et al. Free D-aspartate and D-alanine in normal and Alzheimer brain. *Brain Res. Bull.* https://doi.org/10.1016/0361-9230(91)90266-m (1991).
[24] Fisher, G. H. et al. Free D-amino acids in human cerebrospinal fluid of Alzheimer disease, multiple sclerosis, and healthy control subjects. *Mol. Chem. Neuropathol.* https://doi.org/10.1007/bf02815405 (1994).
[25] Fisher, G. et al. Free D- and L-amino acids in ventricular cerebrospinal fluid from Alzheimer and normal subjects. *Amino Acids.* https://doi.org/10.1007/bf01318865 (1998).
[26] Pollegioni, L. & Sacchi, S. Metabolism of the neuromodulator D-serine. *Cell. Mol. Life Sci.* https://doi.org/10.1007/s00018-010-0307-9 (2010).
[27] Balu, D. T et al. Neurotoxic astrocytes express the D-serine synthesizing enzyme, serine racemase, in Alzheimer's disease. *Neurobiol. Dis.* https://doi.org/10.1016/j.nbd.2019.104511 (2019).
[28] Wu S.-Z. et al. Induction of serine racemase expression and D-serine release from microglia by amyloid beta-peptide. J. Neuroinflammation https://doi.org/10.1186/ 1742-2094-1-2 (2004).
[29] Brito-Moreira, J. et al. Aβ oligomers induce glutamate release from hippocampal neurons. *Curr. Alzheimer Res.* https://doi.org/10.2174/156720511796391917 (2011).
[30] Madeira, C. et al. D-serine levels in Alzheimer's disease: implications for novel biomarker development. *Transl. Psychiatry* https://doi.org/10.1038/tp.2015.52 (2015).
[31] Lin, C. H. et al. Benzoate, a D-amino acid oxidase inhibitor, for the treatment of early-phase Alzheimer disease: a randomized, double-blind, placebo-controlled trial. *Biol. Psychiatry* https://doi.org/10.1016/j.biopsych.2013.08.010 (2014).
[32] Nagata, Y., Borghi, M., Fisher, G. H. & D'Aniello, A. Free D-serine concentration in normal and Alzheimer human brain. *Brain Res. Bull.* https://doi.org/10.1016/0361-9230(95)00087-u (1995).
[33] Hashimoto, K. et al. Possible role of D-serine in the pathophysiology of Alzheimer's disease. *Prog. Neuropsychopharmacol. Biol. Psychiatry* https://doi.org/10.1016/j.pnpbp.2003.11.009 (2004).
[34] Biemans, E. A. et al. CSF D-serine concentrations are similar in Alzheimer's disease, other dementias, and elderly controls. *Neurobiol. Aging.* https://doi.org/10.1016/j.neurobiolaging.2016.03.017 (2016).
[35] Mothet, J.-P., Billard, J.-M., Pollegioni, L., Coyle, J. T. & Sweedler, J. V. Investigating brain D-serine: Advocacy for good practices. *Acta Physiol. (Oxf.)* https://doi.org/10.1111/apha.13257 (2019).
[36] Hughes, C. P, Berg, L., Danziger, W. L, Coben, L. A. & Martin, L. R. A new clinical scale for the staging of dementia. *Br. J. Psychiatry* https://doi.org/10.1192/bjp.140.6.566 (1982).

[37] Nuzzo, T. et al. Decreased free D-aspartate levels are linked to enhanced D-aspartate oxidase activity in the dorsolateral prefrontal cortex of schizophrenia patients. *npj Schizophr.* https://doi.org/10.1038/s41537-017-0015-7 (2017).
[38] Sacchi, S. et al. Engineering the substrate specificity of D-amino-acid oxidase. *J. Biol. Chem.* https://doi.org/10.1074/jbc.M203946200 (2002).
[39] Calcia, M.A. et al. Plasma levels of D-serine in Brazilian individuals with schizophrenia. *Schizophr. Res.* https://doi.org/10.1016/j.schres.2012.09.014 (2012).
[40] Hynd, M. R., Scott, H. L & Dodd, P. R. Differential expression of N-methyl-D-aspartate receptor NR2 isoforms in Alzheimer's disease. *J. Neurochem.* https://doi.org/10.1111/j.1471-4159.2004.02548.x (2004).
[41] Mishizen-Eberz, A. J. et al. Biochemical and molecular studies of NMDA receptor subunits NR1/2A/2B in hippocampal subregions throughout progression of Alzheimer's disease pathology. *Neurobiol. Dis.* https://doi.org/10.1016/j.nbd.2003.09.016 (2004).
[42] Guercio, G. D. & Panizzutti, R. Potential and challenges for the clinical use of D-serine as a cognitive enhancer. *Front. Psychiatry* https://doi.org/10.3389/fpsyt.2018.00014 (2018).
[43] Esposito, S. et al. Contribution of serine racemase/D-serine pathway to neuronal apoptosis. *Aging Cell* https://doi.org/10.1111/j.1474-9726.2012.00822.x (2012).
[44] Hampel, H. et al. Blood-based biomarkers for Alzheimer disease: mapping the road to the clinic. *Nat. Rev. Neurol.* https://doi.org/10.1038/s41582-018-0079-7 (2018).

Additional references

[45] D'Aniello A. et al. Involvement of D-aspartic acid in the synthesis of testosterone in rat testes. *Life Sci.* https://doi.org/10.1016/0024-3205(96)00266-4 (1996).
[46] Topo, E., Soricelli, A., D'Aniello, A., Ronsini, S., and D'Aniello, G. The role and molecular mechanism of D-aspartic acid in the release and synthesis of LH and testosterone in humans and rats. *Reprod Biol Endocrinol*. https://doi.org/10.1186/1477-7827-7-120 (2009).
[47] Hogervorst, E. et al. Serum total testosterone is lower in men with Alzheimer's disease. *Neuro Endocrinol Lett*. **22**(3):163-168 (2001).
[48] Moffat, S. D. et al. Free testosterone and risk for Alzheimer disease in older men. *Neurology*. https://doi.org/10.1212/wnl.62.2.188 (2004).
[49] Rosario, E. R., Chang, L., Head, E. H., Stanczyk, F. Z., and Pike, C. J. Brain levels of sex steroid hormones in men and women during normal aging and in Alzheimer's disease. *Neurobiol Aging*. https://doi.org/10.1016/j.neurobiolaging.2009.04.008 (2011).
[50] Maugard, M., Vigneron, P. A., Bolaños, J. P., and Bonvento, G. L-Serine links metabolism with neurotransmission. *Prog Neurobiol*. https://doi.org/10.1016/j.pneurobio.2020.101896 (2020).
[51] Nishikawa, T. Metabolism and functional roles of endogenous D-serine in mammalian brains. *Biol Pharm Bull*. https://doi.org/10.1248/bpb.28.1561 (2005).

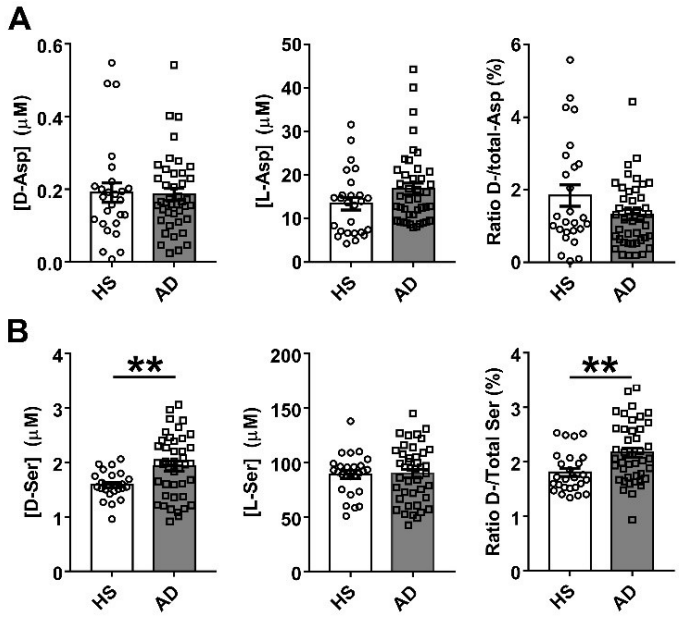

Figure 1: D- and L-Asp (A, left and center, respectively) and D- and L-Ser (B, left and center, respectively) levels and ratio between D-enantiomer and total (D+L) amino acid content (A, right, and B, right for Asp and Ser, respectively, expressed as percentage) detected in serum samples of AD patients compared to healthy subjects (HS). Dots and bars represent the single subjects' values and the standard error of the mean, respectively. **P < 0.01 (Mann-Whitney unpaired test).

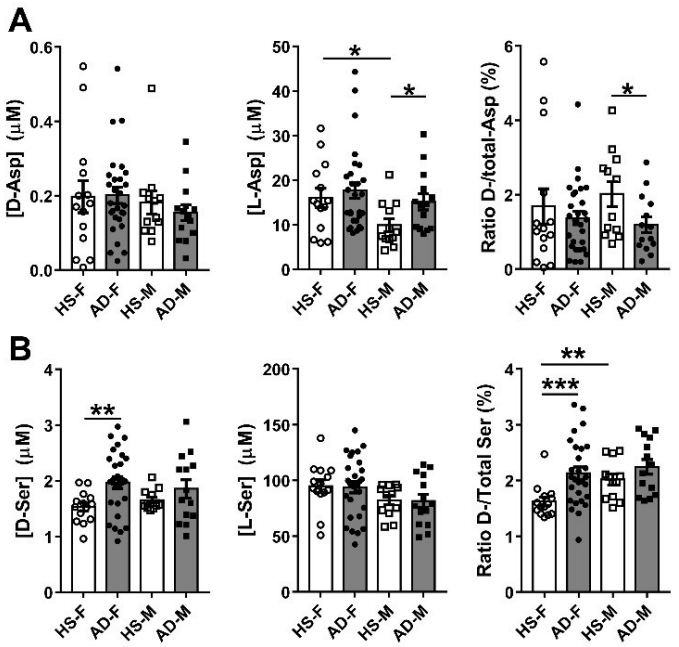

Figure 2: Gender related variations of D- and L-Asp (A, left and center, respectively) and D- and L-Ser (B, left and center, respectively) levels and ratio between D-enantiomer and total (D+L) amino acid content (A, right, and B, right for Asp and Ser, respectively, expressed as percentage) detected in serum samples of AD

patients compared to healthy subjects (HS). Dots and bars represent the single subjects' values and the standard error of the mean, respectively. *P < 0.05; **P < 0.01; ***P < 0.001 (Mann-Whitney unpaired test). F: female; M: male.

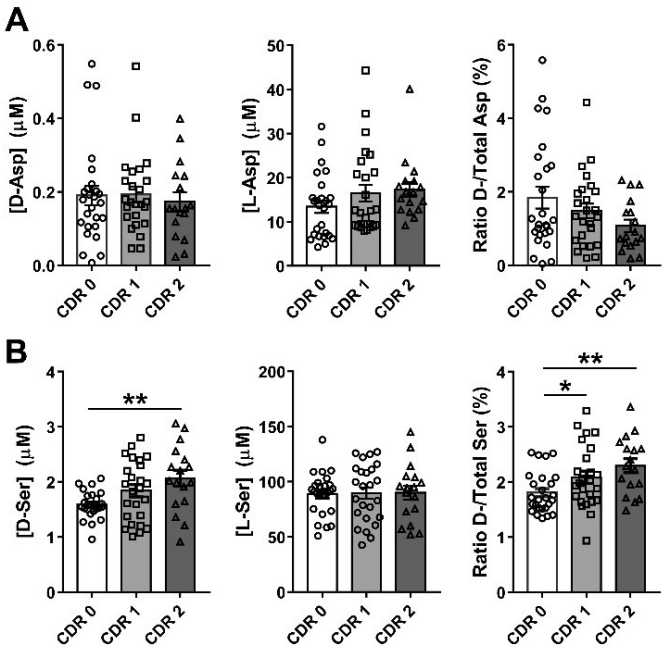

Figure 3: Modification of D- and L-Asp (A, left and center, respectively) and D- and L-Ser (B, left and center, respectively) levels and ratio between D-enantiomer and total (D+L) amino acid content (A, right, and B, right for Asp and Ser, respectively, expressed as percentage) detected in serum samples of AD patients compared to healthy subjects (CDR 0) related to the stage of the pathology. Dots and bars represent the single subjects' values and the standard error of the mean, respectively. *P < 0.05; **P < 0.01 (Mann-Whitney unpaired test). Disease stage was assessed by Clinical Dementia Rating (CDR) score (see Materials and Methods): CDR 0: healthy subjects; CDR 1: mild dementia; CDR 2: moderate dementia.

Table 1. Demographic and clinical data of the subjects enrolled for the study.

	Healthy subjects	AD patients	P-value
Demographic data			
Number	26	42	/
Male (% of total)	12 (46.2)	14 (33.3)	0.2904*
Female (% of total)	14 (53.8)	28 (66.7)	
Age, range (years)	64 – 86	64 – 87	/
Male, range (years)	64 – 86	64 – 87	/
Female, range (years)	66 – 84	68 – 86	/
Age, mean ± SD (SEM)	76.7 ± 5.9 (1.16)	79.1 ± 5.4 (0.83)	0.0834
Male, age, mean ± SD (SEM)	76.8 ± 7.2 (2.08)	78.5 ± 5.4 (1.44)	0.4687
Female, age, mean ± SD (SEM)	76.6 ± 4.8 (1.28)	79.4 ± 5.4 (1.03)	0.0711
CDR, mean ± SD (SEM)	N.A.	1.41 ± 0.50 (0.077)	/
Male, CDR, mean ± SD (SEM)	N.A.	1.43 ± 0.51 (0.14)	/
Female, CDR, mean ± SD (SEM)	N.A.	1.39 ± 0.50 (0.094)	/
CDR, number (in parentheses) and age, mean ± SD (SEM)			
CDR 1 (25)[d]	N.A.	77.9 ± 5.7 (1.15)	0.1012**
CDR 2 (17)[e]	N.A.	80.9 ± 4.4 (1.06)	
No. of subject using anti-dementia drugs (% of total)*** total)*	N.A.	38 (90.5)	
Memantine, number (% of total)	N.A.	19 (42.9)	/
Memantine, mg/die, mean ± SD (SEM)	N.A.	18.4 ± 3.8 (0.86)	/
Donepezil, number (% of total)	N.A.	14 (33.3)	/
Donepezil, mg/die, mean ± SD (SEM)	N.A.	7.5 ± 2.6 (0.69)	/
Rivastigmine, number (% of total)	N.A.	7 (16.7)	/
Rivastigmine, mg/die, mean ± SD (SEM)	N.A	6.6 ± 2.1 (0.79)	/

SD: Standard Deviation; SEM: Standard Error of the Mean; P-values refer to comparison between HS and AD patients (Mann–Whitney test). N.A.: not applicable.

*The comparison was performed using the χ^2 test.

**P-value refers to the comparison between CDR 1 and CDR 2 AD patients (Mann-Whitney test). P-values obtained from comparison between HS and AD patients disaggregated by CDR are reported in the text.

***Two AD patients were assuming both memantine and donepezil

[d] 8 male, 17 female

[e] 6 male, 11 female

Table 2. Statistical analysis of the levels of D,L-aspartate, D,L-serine, D-/total-Asp and D-/total-Ser ratios observed in serum of HS and AD patients.

Amino acid	CDR 1 vs. CDR 0		CDR 2 vs. CDR 1		CDR 2 vs. CDR 0	
	Δ%	P-value	Δ%	P-value	Δ%	P-value
D-Asp	1.58	0.6040	-9.84	0.4733	-8.42	0.9072
L-Asp	23.1	0.2431	4.85	0.2287	29.1	0.0787
Ratio D-/total-Asp	-19.6	0.7017	-27.7	0.2389	-41.8	0.0977
D-Ser	15.9	0.0873	12.5	0.2388	30.2	<u>0.0015</u>
L-Ser	0.79	0.7156	0.33	0.8443	1.12	0.9070
Ratio D-/total-Ser	19.4	<u>0.0336</u>	10.1	0.2400	26.5	<u>0.0016</u>

HS: healthy subjects; CDR 1: mild dementia; CDR 2: moderate dementia. Δ%: variation between compared groups expressed as percentage ($\Delta\% = 100*([CDR]_n-[CDR]_{n-1})/[CDR]_{n-1}$, where "n" is the CDR score, for CDR 1 vs. CDR 0 and CDR 2 vs. CDR 1, and $\Delta\% = 100*([CDR]_2-[CDR]_0)/[CDR]_0$ for CDR 2 vs. CDR 0). P-values obtained with non-parametric Mann-Whitney test are indicated for each comparison. Statistically significant P-values ($P < 0.05$) are underlined.

Supplementary Materials

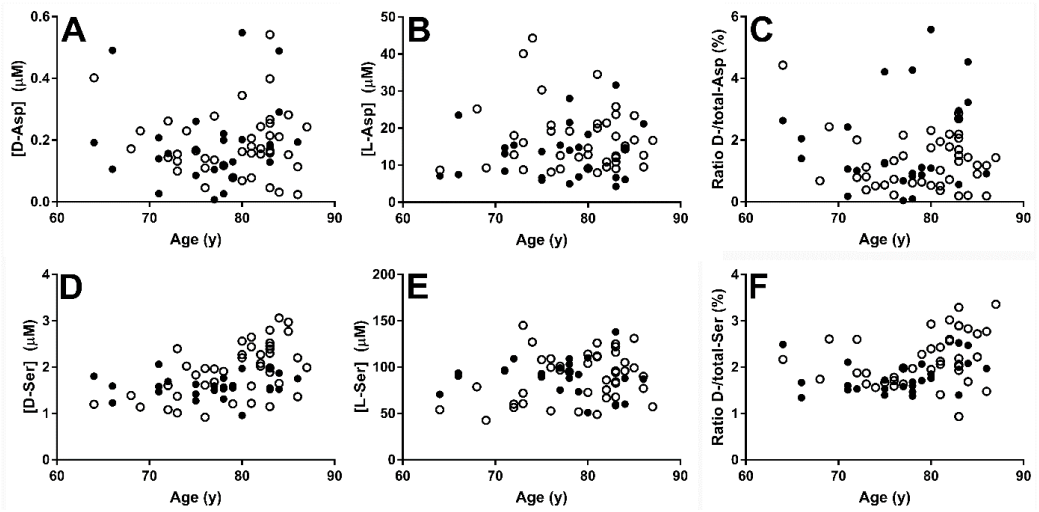

Supplementary Figure 1: Age-related distribution of D- (A) and L-Asp (B) and D- (D) and L-Ser (E) levels and of ratio between D-enantiomer and total (D+L) amino acid content (C and F for Asp and Ser, respectively; expressed as percentage) detected in serum samples of AD patients (open circles) and of healthy subjects (closed circles). Dots represent the single subjects' values.

Supplementary Table 1. Serum levels of D,L-aspartate, D,L-serine, D-/total-Asp and D-/total-Ser ratios and comparison between HS and AD patients.

Subjects		Nume-rosity	D-Asp (µM)		L-Asp (µM)		Ratio D-/total-Asp (%)	
			Mean ± SD (SEM) [RE%]	Δ% (P-value)	Mean ± SD (SEM) [RE%]	Δ% (P-value)	Mean ± SD (SEM) [RE%]	Δ% (P-value)
All	HS	26	0.190 ± 0.137 (0.0268) [71.9]	-2.47 (0.7756)	13.4 ± 7.3 (1.43) [54.3]	25.3 (0.0928)	1.84 ± 1.51 (0.295) [81.8]	-28.7 (0.2702)
	AD	42	0.185 ± 0.106 (0.0163) [56.9]		16.8 ± 8.6 (1.32) [51.0]		1.30 ± 0.89 (0.135) [68.0]	
Female	HS	14	0.197 ± 0.161 (0.0431) [81.8]	1.72 (0.6974)	16.0 ± 8.0 (2.13) [49.7]	10.4 (0.8176)	1.69 ± 1.78 (0.475) [105]	-18.6 (0.6977)
	AD	28	0.201 ± 0.114 (0.0216) [56.8]		17.7 ± 9.4 (1.77) [53.0]		1.37 ± 0.95 (0.180) [69.3]	
Male	HS	12	0.181 ± 0.107 (0.0310) [59.2]	-14.9 (0.5952)	9.90 ± 5.02 (1.449) [50.7]	52.8 (0.0178)	2.02 ± 1.16 (0.336) [57.6]	-41.0 (0.0464)
	AD	14	0.154 ± 0.081 (0.0216) [52.3]		15.1 ± 6.7 (1.79) [44.3]		1.19 ± 0.78 (0.209) [65.7]	

Supplementary Table 1. (continued)

Subjects		Nume-rosity	D-Ser (μM)		L-Ser (μM)		Ratio D-/total-Ser (%)	
			Mean ± SD (SEM) [RE%]	Δ% (P-value)	Mean ± SD (SEM) (RE%)	Δ% (P-value)	Mean ± SD (SEM) (RE%)	Δ% (P-value)
All	HS	26	1.59 ± 0.24 (0.048) [15.3]	21.8 (<u>0.0060</u>)	89.0 ± 19.1 (3.74) [21.4]	0.88 (0.7565)	1.81 ± 0.37 (0.073) [20.7]	20.2 (<u>0.0025</u>)
	AD	42	1.93 ± 0.57 (0.088) [29.6]		89.8 ± 26.0 (4.01) [28.9]		2.17 ± 0.55 (0.085) [25.5]	
Female	HS	14	1.53 ± 0.28 (0.075) [18.3]	28.7 (<u>0.0070</u>)	94.9 ± 21.2 (5.66) [22.3]	-1.0 (0.9475)	1.62 ± 0.29 (0.077) [17.8]	31.4 (<u>0.0007</u>)
	AD	28	1.97 ± 0.56 (0.106) [28.6]		93.9 ± 27.0 (5.11) [28.8]		2.13 ± 0.59 (0.111) [27.5]	
Male	HS	12	1.65 ± 0.18 (0.052) [10.9]	12.3 (0.5019)	82.2 ± 14.1 (4.08) [17.2]	-0.79 (0.9798)	2.02 ± 0.36 (0.103) [17.7]	11.2 (0.2574)
	AD	14	1.86 ± 0.60 (0.161) [32.5]		81.5 ± 22.4 (5.98) [27.4]		2.25 ± 0.49 (0.132) [22.0]	

HS: healthy subjects. D-/total-Asp and D-/total-Ser ratio are expressed as percentage. Data are Mean ± Standard Deviation (SD). The Standard Errors of the Mean (SEM) and the Relative Errors, expressed as percentage (RE% = 100x(SD/Mean)), are reported in parentheses. Δ%: variation between mean values of AD and HS expressed as percentage ($\Delta\% = (([AD]_{Mean} - [HS]_{Mean})/[HS]_{Mean})x100$). P-values obtained with non-parametric Mann-Whitney test are indicated for each comparison. Statistically significant P-values ($P < 0.05$) are underlined.

Supplementary Table 2. Serum levels of D,L-aspartate, D,L-serine, D-/total-Asp and D-/total-Ser ratios observed in HS and AD patients.

Group	CDR	Nume-rosity	Mean ± SD (SEM) (μM); [RE%]					
			D-Asp	L-Asp	Ratio D-/ total Asp	D-Ser	L-Ser	Ratio D-/ total-Ser
Healthy subjects	0	26	0.190 ± 0.137 (0.0267) [71.9]	13.4 ± 7.3 (1.43) [54.3]	1.84 ± 1.51 (0.295) [81.8]	1.59 ± 0.24 (0.048) [15.3]	89.0 ± 19.1 (3.74) [21.4]	1.81 ± 0.37 (0.073) [20.7]
Mild dementia (CDR 1)	1	25	0.193 ± 0.108 (0.0216) [56.0]	16.5 ± 9.6 (1.93) [58.5]	1.48 ± 0.98 (0.197) [66.7]	1.84 ± 0.55 (0.109) (29.7]	89.7 ± 26.2 (5.24) (29.2]	2.08 ± 0.57 (0.114) [27.2]
Moderate dementia (CDR 2)	2	17	0.174 ± 0.104 (0.0251) [59.6]	17.3 ± 7.0 (1.69) [40.2]	1.07 ± 0.70 (0.169) [65.2]	2.07 ± 0.60 (0.145) [29.0]	90.0 ± 26.5 (6.42) [29.4]	2.29 ± 0.52 (0.127) [22.8]

HS: healthy subjects. D-/total-Asp and D-/total-Ser ratio are expressed as percentage. Data are Mean ± Standard Deviation (SD). The Standard Errors of the Mean (SEM) and the Relative Errors, expressed as percentage (RE% = 100x(SD/Mean)), are reported in parentheses.

3.3. hDASPO: expression and degradation pathway of two reported isoforms

Submitted

Cellular studies of the two main isoforms of human D-aspartate oxidase

Valentina Rabattoni, Loredano Pollegioni, Silvia Sacchi*

"The Protein Factory 2.0", Dipartimento di Biotecnologie e Scienze della Vita, Università degli studi dell'Insubria, via J. H. Dunant 3, 21100 Varese, Italy

Keywords: D-aspartate, enzyme isoforms, cellular stability, protein degradation, flavoproteins

Running Title: Properties of human D-aspartate oxidase isoforms

Abbreviations

D-aspartate oxidase (DASPO), D-amino acid oxidase (DAAO), human D-aspartate oxidase (hDASPO), D-aspartate (D-Asp), D-serine (D-Ser) N-methyl-D-aspartate receptors (NMDAR), cycloheximide (CHX), chloroquine (CQ), benzyloxycarbonyl-L-leucyl-L-leucyl-L-leucinal (MG132); ubiquitin-proteasome system (UPS).

*Corresponding author: Silvia Sacchi – Dipartimento di Biotecnologie e Scienze della Vita, Università degli Studi dell'Insubria, via J.H. Dunant 3, 21100 Varese, Italy.
E-mail address: silvia.sacchi@uninsubria.it

Abstract

Human D-aspartate oxidase (hDASPO) is a peroxisomal FAD-dependent enzyme responsible for the degradation of acidic D-amino acids and in particular of D-aspartate (D-Asp). In mammalian central nervous system D-Asp behaves as a classical neurotransmitter, being able to activate presynaptic AMPA and mGluR5 receptors and acting as an agonist of N-methyl-D-aspartate receptors. This D-amino acid is thought to be involved in neural development, brain morphology and behavior and appears to be entailed in several pathological states, such as schizophrenia and Alzheimer's disease. Apparently, human *DDO* gene produces alternative transcripts encoding for three putative isoforms of the hDASPO enzyme, constituted by 341 (the "canonical" form), 369 and 282 amino acids. Despite the increasing interest in hDASPO and its physiological role, the different isoforms have only been partially characterized and little is known about the regulation of its cellular levels and activity. Here, we generated U87 human glioblastoma cell clones stably expressing hDASPO_341 and, for the first time, hDASPO_369 isoforms. They are active (showing a similar specific activity), localize to the peroxisomes, are very stable (an half-life of approximately 100 hours has been estimated) and primarily degraded through the ubiquitin-proteasome system. The overexpression of hDASPO strictly controls the D-Asp cellular level. These studies shed light on the properties of hDASPO isoforms with the final aim to clarify the mechanisms controlling the cellular level of the neuromodulator D-Asp.

Introduction

The FAD dependent flavoenzyme D-aspartate oxidase (DASPO or DDO, **EC 1.4.3.1**) was first identified in the ‘50s in rabbit kidney and liver [1] and now it is known to be widely present in eukaryotes, ranging from fungi to humans [2]. In mammals, the enzyme is primarily involved in the catabolism of acidic D-amino acids, the best substrate is D-aspartate (D-Asp). DASPO catalyzes their oxidative deamination into the corresponding α-ketoacids, along with the production of hydrogen peroxide and ammonia [3]. Neutral and basic D-AAs are similarly deaminated by the homologous flavoenzyme, D-amino acid oxidase (DAAO, **EC 1.4.3.3**) [4].

In mammals, free D-Asp has been reported to play different roles: in the endocrine system it modulates steroidogenesis, and the synthesis and release of several hormones [5-8] while in the central nervous system it stimulates mGlu5 and presynaptic AMPA receptors [9, 10], as well as N-methyl-D-aspartate receptors (NMDAR), acting as agonist [11]. In the brain D-Asp is abundant during embryonic and perinatal phases and drastically decreases later on [7, 12]. This peculiar temporal distribution pattern is due to the concomitant onset of DASPO expression and activity, mainly observed in neurons [12, 13]. D-Asp has been proposed as a signaling molecule involved in neural development, brain morphology and behavior, and the postulated role of DASPO in strictly regulating its levels has been strengthened [11, 14, 15].

On this regard, several studies performed in animal models demonstrated that the persistent deregulation of D-Asp levels causes age-dependent effects: an improvement of spatial memory and cognitive abilities in young individuals is followed by a rapid deterioration of learning and memory, leading to precocious brain aging [16, 17]. A protective role of DASPO has been proposed: the enzyme would prevent NMDAR hyper-stimulation through the strict regulation of postnatal brain levels of D-Asp.

Despite the increasing interest in hDASPO properties and physiological role, little is known about the processes involved in the regulation of its activity at the cellular level. Notably, the UniProtKB database reports three different isoforms of hDASPO (identifier Q99489, Fig.1) encoded by alternative transcripts of the human *DDO* gene: i) isoform 1 (hDASPO_341, 341 amino acids), referred to as the "canonical isoform", is homologous to the single protein form in rodents; ii) isoform 2 (hDASPO_282), apparently originated by alternative splicing of the transcript, whose sequence is identical to the hDASPO_341 one but lacks of 59 residues in the central region (95-153 in the canonical isoform); iii) isoform 3 (hDASPO_369), which appears highly conserved in primates, is characterized by the presence of 28 additional N-terminal residues, probably due to the recognition of an upstream alternative start codon. The shorter protein isoforms were produced in *E. coli* [18, 19], while the longer one has never been expressed. Notably, the recombinant deleted hDASPO_282 form was fully produced as inclusion bodies in *E. coli* [19]. The three-dimensional structure of human DASPO_341 (hDASPO, PDB entry code 6RKF), and

an extensive characterization of its biochemical properties, have been recently published [18].

In order to deep inside the role of the two main hDASPO isoforms, here we investigated the functional properties, the degradation kinetic and the mechanisms involved in protein turnover by ectopically expressing hDASPO_341 and hDASPO_369 isoforms in the U87 human glioblastoma cell line. This study demonstrated that both hDASPO isoforms are active (thus, able to control D-Asp cellular level), are highly stable and mainly degraded through the ubiquitin-proteasome system.

Results

Expression of hDASPO isoforms in U87 cells

Expression plasmids were generated by subcloning the sequences encoding the hDASPO_341 and hDASPO_369 isoforms in the pcDNA3 vector. The corresponding DNA fragments were produced by PCR amplification of hDASPO cDNA using different 5'-primers designed to anneal to the alternative ATG sites and to insert, beside two unique restriction sites, a 5'-sequence coding for 3 copies of the FLAG epitope (N-terminal 3XFLAG). The generated pcDNA3_3XFLAG-hDASPO_341 and pcDNA3_3XFLAG-hDASPO_369 expression constructs were used to transfect human glioblastoma U87 cells and cell clones stably expressing the long or the short hDASPO isoform were selected.

Western blot analysis on selected cell clones confirmed the expression of both hDASPO_341 and hDASPO_369 isoforms (Fig. 2A), although the longer one at a 4-fold lower level (Fig. 2B). The Western blot analysis of U87 3XFLAG-hDASPO_341 cell lysates with the anti-hDASPO antibody recognized a band at the expected molecular mass (≈ 42.0 kDa, corresponding to 3XFLAG-hDASPO_341) and a band at ≈ 37.0 kDa. On the other hand, the same analysis performed on U87 3XFLAG-hDASPO_369 cell lysates revealed the presence of three bands: in addition to the 37 kDa band, signals at ≈ 40.5 and 44.0 kDa were also apparent (Fig. 2A). In both cell clones, the band at the lowest molecular mass, ≈ 37.0 kDa, should correspond to an aspecific signal since it was also present in control samples (U87 untransfected cells) and since recombinant hDASPO, when added

to control U87 cell lysates, shows a lower mobility rate, yielding a band at ≈39 kDa (Fig. 2A). Based on the molecular mass, the bands at ≈ 40.5 and 44 kDa correspond to untagged hDASPO_341 and 3XFLAG-hDASPO_369 isoforms, respectively: both bands were recognized by the anti-hDASPO antibody, while only the latter one was detected by the anti-FLAG antibody (not shown). Therefore, U87 cells transfected with the pcDNA3_3XFLAG-hDASPO_369 construct expressed both protein isoforms at comparable levels (Fig. 2B).

The identity of the expressed protein isoforms in the U87 3XFLAG-hDASPO_369 cells was determined using immunoprecipitation (IP) experiments. In details, two consecutive IP rounds were carried out: the first one using the whole cell extract and the anti-FLAG M2 affinity resin; the second using the obtained post-IP sample and the anti-hDASPO antibody crosslinked to Dynabeads Protein G. Western blot analyses of the immunoprecipitated samples confirmed that both 3XFLAG-hDASPO_369 and the untagged hDASPO_341 isoforms were present in the cell extract (Fig. 2C,D), and that the 37.0 kDa band was an aspecific signal, since it was not immunoprecipitated by the anti-hDASPO antibody (Fig.2D, post-IP II lane). The untagged hDASPO_341 originates by the translation of the hDASPO_369 encoding transcript at an alternative, down-stream starting codon.

hDASPO isoforms are active

A sensitive fluorimetric assay using the Amplex UltraRed reagent and based on the detection of hydrogen peroxide produced by hDASPO in the presence of a saturating concentration of the substrate D-Asp (16.7 mM) [20], was used to assess the enzymatic activity of the two protein isoforms. 3XFLAG-hDASPO_369 and 3XFLAG-hDASPO_341 were immunoprecipitated from the corresponding cell lysates using an anti-FLAG M2 affinity resin, and the activity assays were performed on the purified protein form. The specific activity of the two hDASPO isoforms, calculated by normalization for the amount of the immunoprecipitated protein in each well, as assessed by Western blot analysis, were very similar (34.4 ± 7.6 and 38.7 ± 6.9 U/mg for the 3XFLAG-hDASPO_369 and

3XFLAG-hDASPO_341 isoform, respectively) and close to the value determined for the recombinant purified hDASPO (55.1 ± 3.9 U/mg).

hDASPO expression controls cellular levels of D-aspartate

HPLC analysis of amino acid enantiomers showed that the ectopical expression of both hDASPO isoforms deeply affect D-Asp cellular content: basal D-Asp levels (0.044 ± 0.006 nmol/mg proteins in control cells transfected with the pcDNA3 empty vector) were fully depleted in 3XFLAG-hDASPO_341 and 3XFLAG-hDASPO_369 expressing cells (Fig. 3A, left panel), whereas the L-enantiomer content was unaffected (6.67 ± 1.14, 5.97 ± 1.25 and 6.60 ± 0.96 nmol/mg proteins in control, hDASPO_341 and hDASPO_369 expressing cells, respectively). Accordingly, a dramatic decrease of the D-Asp/total Asp ratio in the cells expressing both hDASPO isoforms was also evident (Fig. 3A, right panel). On the other hand, serine (Ser) enantiomers levels appeared only marginally altered by the expression of both hDASPO isoforms: L-Ser content slightly increased (12.74 ± 5.16, 10.79 ±2.99 and 8.16 ± 0.93 nmol/mg proteins in hDASPO_341 and hDASPO_369 expressing cells compared to controls, respectively) and the D-Ser/total Ser ratio remained unchanged (Fig. 3B).

hDASPO isoforms are peroxisomal enzymes

The peroxisomal targeting of hDASPO should be determined by the non-canonical C-terminal PTS1 sequence (-SNL). The subcellular localization of hDASPO_369 and hDASPO_341 isoforms was verified by immunostaining and confocal analysis performed on the stable clones expressing the two protein isoforms and on U87 untransfected cells as a control. The ectopically expressed 3XFLAG-hDASPO_369 and 3XFLAG-hDASPO_341 were specifically detected using either the anti-FLAG or the anti-hDASPO antibody (no immunorecognition was observed in control cells, Fig. 4A,D). Both protein isoforms showed a punctuate distribution within the cells (Fig. 4B,C and E,F) consistent with their targeting to the peroxisomal compartment, as demonstrated by the large overlapping of FLAG immunofluorescence signals to PMP70 ones (red and green channel, respectively; Fig. 4B,C, merge panels). Conversely, no signal overlapping was apparent when the

protein isoforms were co-stained with the protein marker recognized by the anti-mitochondria antibody (green and red channel, respectively; Fig. 4E,F, merge panels). In this case we used the anti-hDASPO antibody, which allowed to detect both the 3XFLAG-hDASPO_369 and the untagged hDASPO_341 isoforms expressed by U87 3XFLAG-hDASPO_369 cells: the same punctuate distribution pattern was evident. Notably, both protein isoforms were not detected in the cytosol, at least at significant levels.

hDASPO isoforms are long-lived proteins

The cellular stability of 3XFLAG-hDASPO_369 and 3XFLAG-hDASPO_341 was investigated by treatment with cycloheximide (CHX), an inhibitor of protein synthesis that prevents translational elongation. Western blot analysis showed only a slight decrease in both the FLAG-tagged hDASPO isoforms abundance during time: about 80% of the initially observed protein isoform was still detectable at 32 hours after the treatment (Fig. 5). Thus, for both proteins, an half-life of approximately 100 hours was estimated. Furthermore, the N-terminal 3XFLAG additional sequence did not appear to influence the kinetics of protein degradation, since the same half-life value was also determined for the untagged hDASPO_341 expressed in the U87 cell clones transfected with the pcDNA3_3XFLAG-hDASPO_369 construct (Fig. 5). These results indicated that hDASPO is a long-lived protein, as it was previously reported for hDAAO [21].

hDASPO isoforms are degraded by the ubiquitin-proteasome system

The mechanisms involved in hDASPO degradation were investigated by treating U87 cell clones expressing 3XFLAG-hDASPO_369 or 3XFLAG-hDASPO_341 isoforms with inhibitors of autophagy or of the ubiquitin-proteasome system (blocking the preferential degradation pathway should lead to the accumulation of the protein), upon incubating the cells overnight under starvation conditions (i.e. in culture media containing 1% FBS). Starvation is a physiological stimulus inducing numerous changes within the cell: two out of the major effects are a decreased protein synthesis and the activation of proteolytic pathways [22]; accordingly, under starvation conditions the effect of the inhibitors of protein degradation pathways should be enhanced.

Since autophagy is responsible for cytoplasmic bulk degradation and is thought to be important for the turnover of whole organelles and long-lived proteins [23, 24], we investigated the effect of the two autophagy inhibitors, namely chloroquine (CQ, 75 μM) and ammonium chloride (NH_4Cl, 10 mM), on the cellular levels of hDASPO variants. The chosen inhibitors act by different mechanism: CQ inhibits autophagy mainly by impairing autophagosome fusion with lysosomes, whereas NH_4Cl acts on the proton gradient affecting lysosomal pH and thus the degradative activity of hydrolytic enzymes within this organelle [25, 26]. No difference in the relative abundance of 3XFLAG-hDASPO_369 and 3XFLAG-hDASPO_341 was detected in treated cells compared to controls (Fig. 6A), despite CQ and NH_4Cl treatments were prolonged up to 10 hours, suggesting that they do not affect the turnover of these protein variants. This result was unexpected since hDAAO, which is also targeted to peroxisomes and shares a high degree of sequence identity and enzymatic functionality with hDASPO, was reported to be primarily degraded by the lysosome/endosome system [21].

The effect of MG132 on hDASPO cellular level was also investigated. This compound acts as a proteasomal inhibitor interacting with the 'chymotrypsin-like' component and blocking one or more peptidases within the 20S proteasome core, without affecting protein-ubiquitinating and -deubiquitinating enzymes [27]. The treatment of stably transfected cells with 25 μM MG132 lead to the gradual and moderate accumulation of both 3XFLAG-hDASPO_369 and 3XFLAG-hDASPO_341 proteins (Fig. 6B): a 1.6-fold increase at 6-10 hours after treatment was detected for both hDASPO isoforms. This resembles what previously observed for hDAAO (i.e. a 1.5-fold increase) [21], and eventually suggests a slow synthesis of both flavoproteins under starvation conditions. hDASPO_369 and hDASPO_341 behaved again exactly in the same way, indicating that the N-terminal sequence (absent in the shorter isoform) did not affect the degradation mechanism as well as the targeting to, and the recognition by, the ubiquitin-proteasome system (UPS).

Ubiquitination of hDASPO isoforms

hDAAO was demonstrated to form ubiquitin conjugates by *in vitro* and cellular studies, and it was proposed that this signal drives its targeting to the UPS during the protein degradation [21]. *In vitro* ubiquitination experiments were carried out by mixing 5 μg of purified recombinant hDASPO (i.e. hDASPO_341 isoform), 0.6 mg/mL ubiquitin, 5 mM ATP, 1 mM dithiothreitol, 2 mM $MgCl_2$, 1 μM ubiquitin aldehyde (to inhibit deubiquitinating enzymes), 25 μM MG132 (to block the proteasome degradation activity) and 4 mg/mL U87 cell extract (to provide the components of the UPS). Upon incubation for 60 min at 37 °C, aliquots of the reaction mixtures were analyzed by Western blot. Distinct bands at high molecular mass, corresponding in size to mono- (44.5 kDa), multi- or polyubiquitinated (57.2 – 102 kDa) hDASPO species, were observed, see Fig. 7A: the same bands were absent in control samples (i.e. reaction mixtures prepared by omitting the recombinant hDASPO or ubiquitin).

The assay of the enzymatic activity on the same samples (using saturating concentration of substrate and cofactor, i.e. at 15 mM D-Asp and 40 μM FAD) showed no change in hDASPO enzymatic activity (Fig. 7B).

The ubiquitination state of hDASPO isoforms at the cellular level was investigated by immunoprecipitation experiments on the U87 cell clones stably overexpressing the hDASPO isoforms and transiently transfected with a FLAG-tagged ubiquitin expression construct. The highest expression level of FLAG-ubiquitin was observed 48 h after transfection with the pCMV-FLAG-ubiquitin vector (data not shown). Accordingly, cells were treated with 25 μM MG132 48 hours after transfection, collected 6 hours after treatment and cell lysates were immunoprecipitated with the anti-FLAG M2 affinity resin. Western blot analysis indicated that both hDASPO isoforms have been modified by ubiquitin: an intense anti-hDASPO signal was detected at high molecular mass in the immunoprecipitated protein samples from both 3xFLAG-hDASPO_341 and 3XFLAG-hDASPO_369 expressing cells (Fig. 8, lanes 1 and 4, respectively). The detected signal is specific for the ubiquitin conjugated protein isoforms since it is absent in U87 control cells transiently transfected with the FLAG-ubiquitin expression vector and treated with MG132 (Fig. 8, lane 7). Notably, an anti-hDASPO immunorecognition signal was also

evident in 3xFLAG-hDASPO_341 and 3XFLAG-hDASPO_369 U87 cell clones not treated with the proteasome inhibitor or not overexpressing FLAG-ubiquitin and subjected to MG132 treatment (Fig. 8, lanes 2-3 and 5-6), although the intensity was lower than for treated samples (lanes 1 and 4, Fig.8). This observation supports the assumption that hDASPO isoforms are polyubiquitinated in the model cellular system.

Discussion

In the brain of mammals, D-Ser is critical for neurotransmission since it modulates the activation state of NMDAR by acting as the main endogenous co-agonist of this receptor. For this reason its synthesis, transport and degradation processes have been characterized in depth [28-30]. A second D-amino acid, D-Asp, is also involved in neurotransmission, due to its relatively high affinity for the glutamate binding site of NMDAR. D-Asp shows a peculiar temporal occurrence in the brain, with its levels peaking during early embryonic development and drastically falling after birth [6, 7, 15]: the regulation of D-Asp levels is mainly exerted by the catabolic activity of hDASPO. This peroxisomal flavoenzyme, together with hDAAO (which is responsible for the selective degradation of D-Ser) [31], belongs to the amino acid oxidase family of flavoproteins. Despite the two orthologue flavoproteins share an high sequence identity and a similar overall tertiary structure, hDASPO and hDAAO profoundly differ in their quaternary structure, cofactor binding affinity, kinetic properties and mechanisms [18]. These findings indicate that they should regulate the brain levels of D-Asp and D-Ser differently. Interestingly, three different isoforms of hDASPO can be identified in the UniProtKB database: hDASPO_341 (37,5 kDa, the “canonical” protein isoform), hDASPO_282 (30 kDa), and hDASPO_369 (41 kDa). We focused on the hDASPO_341 and hDASPO_369 isoforms. Both protein isoforms were expressed in U87 cells after transfection: the 3XFLAG-hDASPO_369 isoform was expressed at a significantly lower level (Fig. 2). Notably, the cells transfected with the pcDNA3_3XFLAG-hDASPO_369 construct produced both the long and the untagged short protein isoforms at similar levels (Fig. 2B), suggesting that the translation of hDASPO_369 encoding transcript can occur from the alternative starting codon at a similar frequency. Notably, both hDASPO_369 and

hDASPO_341 isoforms were active and efficiently targeted to the peroxisomes. Furthermore, both the ectopically expressed isoforms fully depleted D-Asp cellular pool while not significantly affected the levels of D-Ser and the corresponding L-enantiomers (Fig. 3). On this side, we need to mention that the cells expressing the 3XFLAG-hDASPO_369 protein also generated the wild-type (341 amino acids long) enzyme form. Similarly to the homologous hDAAO protein [21], both hDASPO isoforms were highly stable proteins and likely characterized by a slow cellular turnover: their estimated half-life was ≈100 hours (Fig. 5), even higher than that for catalase (≈30 hours) [32]. This value is in line with the peroxisomal localization of hDASPO isoforms, since most data indicate a peroxisomal half-life of around 2 days [33]: peroxisomes are thought to be mainly degraded by autophagy, with a process mediated by p62 and LC3-II named pexophagy [33], that can be upregulated in response to different stresses, such as nutrient starvation. Accordingly, ectopically expressed hDAAO accumulated in U87 cells in this condition upon blocking the lysosome/endosome pathway [21]. On the contrary hDASPO_341 and hDASPO_369 isoforms were degraded by the UPS.

Actually, *in vitro* and cellular studies revealed that hDASPO isoforms can be ubiquitinated (Fig. 7A and 8), a modification that did not affect the enzymatic activity (Fig. 7B). This observation suggests that (poly)ubiquitin conjugation represents the cellular signal that triggers the targeting of hDASPO to the UPS and thus, that the modified flavoenzyme should be retrotraslocated to the cytoplasm for degradation. It is known that excessive peroxisomal matrix proteins may be exported to the cytosol where they are degraded by cytosolic proteases or the proteasome [34]. In this context, it is noteworthy that peroxisomal membrane receptors involved in the import apparatus (e.g. Pex5p, Pex7p, and Pex20p) can also be degraded by the UPS [34] and that the ubiquitination pattern controls their targeting: when the export is impaired, they are polyubiquitinated and extracted from the peroxisomal membrane for degradation by the UPS, a process called RADAR (Receptor Accumulation and Degradation in the Absence of Recycling) [35]. Since the RADAR quality control pathway is most likely conserved in mammals, it is tempting to speculate that this mechanism is involved in the regulation of hDASPO cellular levels.

We can conclude that the additional N-terminal sequence in the long hDASPO isoform does not affect the enzyme functionality, subcellular localization, half-life and degradation pathway. However, due to the presence of this additional sequence, hDASPO_369 may interact with different effector molecules, inhibitors or regulatory proteins compared to hDASPO_341. In order to clarify how the cellular levels of D-Asp are controlled, further studies will focus on the effects due to post-translational modifications and ligand interactions on hDASPO isoforms.

Materials and Methods

Expression vectors

The cDNA encoding hDASPO was purchased as a full ORF clone from the PlasmID Repository at Harvard Medical School (HsCD00335325 pCMV-SPORT6) and amplified with primers, reported in Supplementary Table 1, specifically designed to obtain the two different isoforms with three copies of the FLAG (DYKDDDDK) epitope fused to the N-terminal end. These cDNAs were then subcloned into pcDNA3 vector, and the resulting constructs were confirmed by automated sequencing. The pCMV-FLAG-ubiquitin vector for the expression of N-terminal FLAG tagged human ubiquitin, was kindly provided by Professor Herman Wolosker (Technion – Israel Institute of Technology, Haifa, Israel).

Cell culture and transfection

The U87 human glioblastoma cells (ATCC) were maintained in Dulbecco's Modified Eagle Medium (DMEM) supplemented with 10% fetal bovine serum (FBS), 1 mM sodium pyruvate, 2 mM L-glutamine, 2.5 µg/mL amphotericin B and 1% penicillin/streptomycin (all from Euroclone) at 37 °C in a 5% CO_2 incubator and transfected using the FuGENE HD transfection reagent (6 µL; Roche) and 2 µg of pcDNA3_3XFLAG-hDASPO_341 or -hDASPO_369 constructs. Stable clones were selected adding 0.4 mg/mL G418 to the growth medium. To perform ubiquitination studies, U87 3XFLAG-hDASPO_341 or -hDASPO_369 cells were transiently transfected with 2 µg of the pCMV-FLAG-ubiquitin vector. For immunolocalization studies, 10^4 U87 3XFLAG-hDASPO_341, 3XFLAG-hDASPO_369 cells and U87 control cells were seeded onto previously gelatinised

coverslips (diameter 12 mm, Thermo Scientific). At 24 h after seeding, cells were extensively washed with PBS (10 mM dibasic sodium phosphate, 2 mM monobasic potassium phosphate, 137 mM NaCl, 2.7 mM KCl, pH 7.4) and fixed with 4% p-formaldehyde for 10 min at room temperature.

To evaluate the stability of hDASPO_341 and _369 isoforms and assess their rate of degradation, U87 3XFLAG-hDASPO_341 and -hDASPO_369 cells were seeded in 6-well plates ($2.7x10^5$ cells/well) and treated up to 32 hours with cycloheximide (CHX, 100 μg/mL; Sigma), a potent inhibitor of protein synthesis, and collected at different times for Western blot analysis [21]. Changes in hDASPO isoforms cellular levels were determined by densitometric analysis upon acquisition with an Odyssey Fc Imaging System (LI-COR Biosciences). Data were fit to a single exponential decay equation to estimate the half-life.

Processes involved in hDASPO degradation were investigated by treating the cell clones expressing the two protein isoforms with specific inhibitors of autophagy/lysosomal pathway or the ubiquitin-proteasomal system (UPS) [21]. After seeding, the cells were grown overnight under starvation conditions (DMEM supplemented with 1% FBS) and then the lysosomal hydrolase inhibitors chloroquine (CQ, 75 μM; Sigma) or NH_4Cl (10 mM; Sigma) or the proteasomal inhibitor benzyloxycarbonyl-L-leucyl-L-leucyl-L-leucinal (MG132, 25 μM; Sigma) were added. At different time points (up to 10 hours), cells were collected by trypsinization and the protein levels analyzed by Western blot. Starvation conditions have been used to maximize the effect of inhibition of the degradation pathways, as previously reported [21,36].

Immunoblot

For Western blot analysis, stably transfected or control cells were resuspended in sample buffer (12.5 mM Tris-HCl, pH 6.7, 3% SDS, 5% glycerol and 62.5 mM dithiothreitol) to have 5000 cells/μL and 10 μL of each sample was subjected to SDS-PAGE. Proteins were then transferred to polyvinylidene difluoride membranes (Immobilon-P, Millipore) and saturation of aspecific sites was performed by incubation (2 h at room temperature or overnight at 4 °C) in a blocking solution containing 4% dried milk in Tris-buffered saline

(TBS; 10 mM Tris–HCl pH 8.0, 0.5 M NaCl) with the addition of 0.1% Tween-20 (TBST). Membranes were then incubated with primary antibodies at room temperature for 1.5 h, extensively washed in TBST and then incubated for 1 h at room temperature with specific peroxidase-conjugated immunoglobulins. The immunoreactivity signals were detected by enhanced chemiluminescence (WESTAR ETA C Ultra 2.0 reagents; Cyanagen) using the Odyssey Fc Imaging System (LI-COR Biosciences).

The primary antibodies used were: rabbit polyclonal anti-hDASPO (1:1000, Davids Biotechnologie); rabbit polyclonal anti-FLAG (1:500, Sigma); mouse monoclonal anti-β-tubulin (1:2000, Thermo Scientific).

The different immunorecognition signals in cell lysates were measured using the Image Studio Lite Software (LI-COR Biosciences). The intensity values of the bands detected by the anti-hDASPO antibody were normalized to the values of the anti-β-tubulin ones. After normalization, the ratio of the intensity signals corresponding to treated and control cells, collected at the same incubation time, was calculated.

Immunostaining and confocal analysis

In order to analyze the subcellular localization of the hDASPO isoforms, p-formaldehyde fixed U87 3XFLAG-hDASPO_341, 3XFLAG-hDASPO_369 and U87 control cells were permeabilized and the unspecific binding sites were blocked by incubation in PBS supplemented with 0.2% Triton X-100 and 4% horse serum. DASPO isoforms were subsequently stained using rabbit polyclonal anti-hDASPO (1:500, Davids Biotechnologie) and mouse monoclonal anti-FLAG antibody (1:500, Invitrogen); peroxisomes and mitochondria were stained by rabbit polyclonal anti-PMP70 (peroxisomal membrane protein 70, 1:500, Sigma) and mouse monoclonal anti-mitochondria antibody (1:500, Millipore). Cells were incubated with primary antibodies overnight at 4 °C and, after extensive washing in PBS supplemented with 1% horse serum, with anti-rabbit Alexa 488 and anti-mouse Alexa 546 antibodies (1:1000, Molecular Probes) diluted in PBS, 0.1% Triton X-100, and 1.5% horse serum.

Immunostained coverslips were imaged using an inverted laser scanning confocal microscope (TCS SP5, Leica Microsystems), equipped with a 63.0 × 1.25 NA plan

apochromatic oil immersion objective. Confocal image stacks (5 sections with optimized thickness) were acquired using the Leica TCS software with a sequential mode to avoid interference between each channel due to spectral overlap and without saturating any pixel.

Immunoprecipitation

To determine the specific activity of 3XFLAG-hDASPO_341 and 3XFLAG-hDASPO_369, the enzymes were purified from cell extracts by immunoprecipitation (IP) using anti-FLAG M2 Affinity resin (Sigma). Briefly, U87 cell clones stably expressing the two isoforms were suspended in ice-cold lysis buffer (50 mM sodium phosphate pH 8.0, 0.7 µg/mL pepstatin, 1 µg/mL leupeptin, 5 µM FAD, 0.1% ethanol, 1 mg/mL DNAse) and sonicated. The cell lysates were then centrifuged at 13000 g for 30 min at 4 °C; the protein concentration of the supernatant (Pre-IP sample) was quantified using the Bradford reagent (Sigma). A volume of sample corresponding to 0.5 mg (or 2 mg for U87 3XFLAG-hDASPO_369 cells) of total protein was subjected to IP using 40 µL of anti-FLAG M2 Affinity resin and incubated overnight at 4 °C under constant rotation. The sample was then centrifuged at 8000 g for 1 minute and the supernatant (Post-IP sample) was stored for Western blot analysis. The pelleted resin and the bound flagged protein were resuspended in 50 µL of lysis buffer for the subsequent activity measurements (IP sample).

To confirm the identity of the protein forms expressed in cells transfected with the pcDNA3_3XFLAG-hDASPO_369 vector, after a first IP using the whole cell extract and the anti-FLAG M2 Affinity resin, a second IP was performed using the anti-hDASPO antibody. In details, after the removal of flagged proteins, the obtained post-IP sample was incubated with 50 µL of Dynabeads Protein G (Invitrogen) previously cross-linked to 10 µg of rabbit anti-hDASPO antibody (Davids Biotechnologie) using dimethyl pimelimidate (DMP), and the procedure previously reported [21]. After an overnight incubation at 4 °C with rotation, the supernatant (post-IP sample) was collected by separating the beads on the magnet; beads were extensively washed with lysis buffer, suspended in 50 µL of non-reducing SDS-PAGE sample buffer (IP sample) and boiled. SDS-PAGE and Western

blot analyses were performed using an amount of pre-IP and post-IP samples corresponding to 20 μg of total protein and 10 μL of the IP samples.

DASPO activity assay

hDASPO activity was assayed on total cell lysates and on hDASPO isoforms purified by IP using the Amplex UltraRed assay kit (Invitrogen) based on the detection of H_2O_2 by the peroxidase-mediated oxidation of the fluorogenic Amplex UltraRed Dye [20]. Cells were suspended in ice-cold 50 mM sodium phosphate buffer, pH 8.0, containing 0.7 μg/mL pepstatin, 1 μg/mL leupeptin, 5 μM FAD, 0.1% ethanol, and 1 mg/mL DNAse, sonicated, and centrifuged at 13000 g for 30 min at 4 °C. The protein concentration in the supernatant was quantified using the Bradford assay (Sigma)**.** The IP samples were obtained as reported above. A volume of cell extract corresponding to 2.5 and 5 μg of total protein content or to 2 and 3 μL of the resuspended IP samples were aliquoted in black 96-well plates and added of lysis buffer to a final volume of 100 μL. Then 50 μL of the activity assay solution (55 μM Amplex UltraRed, 0.15 U/mL horseradish peroxidase, 7.5 mM NaN_3, 50 mM D-Asp and 15 μM FAD in 50 mM sodium phosphate buffer, pH 8.0) were added to each well. The fluorescence measurements (excitation at 535 nm and emission at 590 nm) were recorded at 25 °C every 5 minutes for a total of 30 minutes and values were corrected for controls wells (without the samples) to subtract background signal. As a positive control, different amounts of the recombinant purified enzyme (0.0025-0.1 milliunit range) were assayed in parallel. The assay specificity was assessed using lysates of control U87 cells stably transfected with the empty pcDNA3 vector, as a negative control, and adding 2 mM 5-aminonicotinic acid (an inhibitor of hDASPO, K_i = 3.8 μM) [37] to hDASPO expressing cells.

The concentration of H_2O_2 in the wells was calculated using a calibration curve (0.25–7.5 μM H_2O_2). hDASPO specific activity (μmol/min/mg) was then calculated dividing the nanomoles of H_2O_2 produced in a minute by the milligrams of enzyme present in the samples, determined in turn by Western blot and densitometric analysis, using a calibration curve prepared analyzing known amounts of the recombinant purified hDASPO.

In vitro ubiquitination

Recombinant hDASPO was expressed in *E. coli* BL21(DE3) LOBSTR host cells (Novagen) and purified as reported in [18]. *In vitro* ubiquitination experiments were carried out using 2 and 5 μg of hDASPO, incubated with 0.6 mg/mL ubiquitin, 1 μM ubiquitin aldehyde, 5 mM ATP, 25 μM MG132, 1 mM dithiothreitol, 2 mM $MgCl_2$ and 4 mg/mL U87 cell extract in 20 mM Tris-HCl (pH 8.0), in a total volume of 60 μL, at 37 °C for 60 min. Controls were performed by omitting ubiquitin or hDASPO in the mixture. The ubiquitin-hDASPO conjugates were resolved by SDS-PAGE and analyzed by Western blot using rabbit anti-hDASPO antibody. For preparation of U87 cell extract, the cells were collected, resuspended (10^7 cells/mL) in lysis buffer (20 mM Tris-HCl pH 8.0, 1 mM dithiothreitol, 5 mM KCl, 2 mM $MgCl_2$, 2 μM leupeptin, 1 μM pepstatin, 50 μM phenylmethanesulfonyl fluoride, 25 μM MG132) and subjected to sonication (three cycles of 10 s each). The cell lysate was cleared by centrifugation (see above).

Before and after *in vitro* modification, recombinant hDASPO activity was assayed in 100 mM disodium pyrophosphate buffer (pH 8.3), 40 μM FAD using 15 mM D-Asp as substrate, at 25 °C and air saturation, measuring oxygen consumption by the Clark electrode [18].

In vivo ubiquitination

To evaluate whether hDASPO undergoes ubiquitination in the selected cell line, U87 3XFLAG-hDASPO_341 or -hDASPO_369 cells were transiently transfected with FLAG-ubiquitin and, 48 hours after transfection, the cells were treated for 6 hours with 25 μM MG132. Cells were subsequently collected by trypsinization, resuspended in denaturing lysis buffer (20 mM Tris-HCl, pH 8.0, 150 mM NaCl, 1% SDS and 1 mM EDTA, supplemented with proteases inhibitors as above), boiled for 7 min and sonicated. The cell lysate was then centrifuged at 13000 g for 30 min at 4 °C and the supernatant was diluted 1:10 in IP buffer (20 mM Tris-HCl, pH 8.0, 150 mM NaCl, 0.5% NP-40, 0.5% Triton X-100 and 1 mM EDTA, supplemented with proteases inhibitors). The FLAG-tagged hDASPO isoforms and ubiquitin where co-immunoprecipitated using ANTI-FLAG M2 Affinity Gel (Sigma). A volume of sample corresponding to 0.5 mg or 1 mg of total

proteins for U87 3XFLAG-hDASPO_341 and -hDASPO_369 cells, respectively, was added to 50 µL of the ANTI-FLAG agarose resin and immunoprecipitation was performed as detailed above. The resin was resuspended in 50 µL of a non-reducing SDS-PAGE sample buffer (IP sample) and boiled. 20 µL of the IP samples were subjected to SDS-PAGE on an 8–15% polyacrylamide gel and the ubiquitin-hDASPO conjugates revealed by Western blot analysis using the anti-hDASPO antibody (Davids Biotechnologie).

HPLC analysis

To determine cellular D- and L-Asp levels, as well as D- and L-Ser, the cells stably expressing the 3XFLAG-hDASPO_341 variant were analyzed using the procedure reported in [15] with minor modifications. Cell pellets were homogenized in 1:5 (w/v) 0.2 M TCA, sonicated (three cycles, 10 s each) and the resulting cell extracts were clarified by centrifugation at 13,000 g for 20 min. The precipitated protein pellets were stored at −80 °C for quantification, while 10 µL of the supernatants were neutralized with NaOH and subjected to precolumn derivatization with 20 uL of 74.5 mM o-phthaldialdehyde (OPA) and 30.5 mM N-acetyl L-cysteine (NAC) in 50% methanol. Diastereoisomer derivatives were resolved on a Symmetry C8 reversed-phase column (5 µm, 4.6 × 250 mm, Waters) under isocratic conditions (0.1 M sodium acetate buffer, pH 6.2, 1% tetrahydrofuran, and 1 mL/min flow rate). A washing step in 0.1 M sodium acetate buffer, 3% tetrahydrofuran, and 47% acetonitrile was performed after each run. Identification of peaks was based on retention times and confirmed by: i) adding known amounts of external standards to the samples, ii) by the selective degradation catalyzed by the M213R or wild-type RgDAAO for D-Asp and D-Ser, respectively: 10 µg of the enzymes were added to the samples, which were incubated at 30 °C for 60 min and then derivatized. The peak area for D-Asp or D-Ser corresponded to the one decreased following the enzymatic treatment. Total protein content of homogenates was determined using the Bradford assay method after resolubilization of the TCA precipitated protein pellets in 1% SDS. The total amount of D- and L-amino acids detected in cell extracts was normalized by the total protein content.

Acknowledgements

This research was supported by Università degli studi dell'Insubria, grant "Fondo di Ateneo per la Ricerca" to SS and LP. VR is a Ph.D. student of the Biotechnology and Life Sciences course at the University of Insubria.

Conflict of interest

The authors declare no conflict of interest.

Author contributions

VR conceived, designed and performed the experiments under the supervision of SS. LP conceived the work, contributed to the analysis and discussion of the results and critically revised the manuscript. All authors have read and agreed to the published version of the manuscript.

References

1. Still JL, Buell MV, Knox WE and Green DE (1949) Studies on the cyclophorase system; D-aspartic oxidase. J Biol Chem 179, 831-837.
2. Takahashi S (2020) D-Aspartate oxidase: distribution, functions, properties, and biotechnological applications. Appl Microbiol Biotechnol 104, 2883-2895.
3. Negri A, Massey V and Williams CH Jr (1987) D-aspartate oxidase from beef kidney. Purification and properties. J Biol Chem 262, 10026-10034.
4. Pollegioni L, Piubelli L, Sacchi S, Pilone MS and Molla G (2007) Physiological functions of D-amino acid oxidases: from yeast to humans. Cell Mol Life Sci 64, 1373-1394.
5. Di Fiore MM, Santillo A and Chieffi Baccari G (2014) Current knowledge of D-aspartate in glandular tissues. Amino Acids 46, 1805-1818.
6. Dunlop DS, Neidle A, McHale D, Dunlop DM and Lajtha A (1986) The presence of free D-aspartic acid in rodents and man. Biochem Biophys Res Commun 141, 27-32.
7. Hashimoto A, Kumashiro S, Nishikawa T, Oka T, Takahashi K, Mito T, Takashima S, Doi N, Mizutani Y, Yamazaki T, Kaneko T and Ootomo E (1993) Embryonic development and postnatal changes in free D-aspartate and D-serine in the human prefrontal cortex. J Neurochem 61, 348-351.
8. Ota N, Shi T and Sweedler JV (2012) D-Aspartate acts as a signaling molecule in nervous and neuroendocrine systems. Amino Acids 43, 1873-1886.
9. Cristino L, Luongo L, Squillace M, Paolone G, Mango D, Piccinin S, Zianni E, Imperatore R, Iannotta M, Longo F, Errico F, Vescovi AL, Morari M, Maione S, Gardoni F, Nisticò R and Usiello A (2015) D-Aspartate oxidase influences glutamatergic system homeostasis in mammalian brain. Neurobiol Aging 36, 1890-1902.
10. Molinaro G, Pietracupa S, Di Menna L, Pescatori L, Usiello A, Battaglia G, Nicoletti F and Bruno V (2010) D-aspartate activates mGlu receptors coupled to polyphosphoinositide hydrolysis in neonate rat brain slices. Neurosci Lett 478, 128-130.
11. Errico F, Nisticò R, Napolitano F, Mazzola C, Astone D, Pisapia T, Giustizieri M, D'Aniello A, Mercuri NB and Usiello A (2011) Increased D-aspartate brain content rescues hippocampal age-related synaptic plasticity deterioration of mice. Neurobiol Aging 32, 2229-2243.

12. Schell MJ, Cooper OB and Snyder SH (1997) D-aspartate localizations imply neuronal and neuroendocrine roles. Proc Natl Acad Sci U S A 94, 2013-2018.
13. Errico F, Napolitano F, Nisticò R, Centonze D and Usiello A (2009) D-aspartate: an atypical amino acid with neuromodulatory activity in mammals. Rev Neurosci 20, 429-440.
14. Errico F, Napolitano F, Nisticò R and Usiello A (2012) New insights on the role of free D-aspartate in the mammalian brain. Amino Acids 43, 1861-1871.
15. Punzo D, Errico F, Cristino L, Sacchi S, Keller S, Belardo C, Luongo L, Nuzzo T, Imperatore R, Florio E, De Novellis V, Affinito O, Migliarini S, Maddaloni G, Sisalli MJ, Pasqualetti M, Pollegioni L, Maione S, Chiariotti L and Usiello A (2016) Age-related changes in D-aspartate oxidase promoter methylation control extracellular D-aspartate levels and prevent precocious cell death during brain aging. J Neurosci 36, 3064-3078.
16. Errico F, Nisticò R, Napolitano F, Oliva AB, Romano R, Barbieri F, Florio T, Russo C, Mercuri NB and Usiello A (2011) Persistent increase of D-aspartate in D-aspartate oxidase mutant mice induces a precocious hippocampal age-dependent synaptic plasticity and spatial memory decay. Neurobiol Aging 32, 2061-2074.
17. Errico F, Nisticò R, Palma G, Federici M, Affuso A, Brilli E, Topo E, Centonze D, Bernardi G, Bozzi Y, D'Aniello A, Di Lauro R, Mercuri NB and Usiello A (2008) Increased levels of D-aspartate in the hippocampus enhance LTP but do not facilitate cognitive flexibility. Mol Cell Neurosci 37, 236-246.
18. Molla G, Chaves-Sanjuan A, Savinelli A, Nardini M and Pollegioni L (2020) Structure and kinetic properties of human D-aspartate oxidase, the enzyme-controlling D-aspartate levels in brain. FASEB J 34, 1182-1197.
19. Setoyama C and Miura R (1997) Structural and functional characterization of the human brain D-aspartate oxidase. J Biochem 121, 798-803.
20. Sacchi S, Novellis V, Paolone G, Nuzzo T, Iannotta M, Belardo C, Squillace M, Bolognesi P, Rosini E, Motta Z, Frassineti M, Bertolino A, Pollegioni L, Morari M, Maione S, Errico F and Usiello A (2017) Olanzapine, but not clozapine, increases glutamate release in the prefrontal cortex of freely moving mice by inhibiting D-aspartate oxidase activity. Sci Rep 7, 46288.
21. Cappelletti P, Campomenosi P, Pollegioni L and Sacchi S (2014) The degradation (by distinct pathways) of human D-amino acid oxidase and its interacting partner pLG72--two key proteins in D-serine catabolism in the brain. FEBS J 281, 708-723.
22. Zhao J, Zhai B, Gygi SP and Goldberg AL (2015) mTOR inhibition activates overall protein degradation by the ubiquitin proteasome system as well as by autophagy. Proc Natl Acad Sci U S A 112, 15790-15797.
23. Ciechanover A (2005) Proteolysis: from the lysosome to ubiquitin and the proteasome. Nat Rev Mol Cell Biol 6, 79-87.
24. Zhang T, Shen S, Qu J and Ghaemmaghami S (2016) Global Analysis of Cellular Protein Flux Quantifies the Selectivity of Basal Autophagy. Cell Rep 14, 2426-2439.
25. Amenta JS, Hlivko TJ, McBee AG, Shinozuka H and Brocher S (1978) Specific inhibition by NH4CL of autophagy-associated proteloysis in cultured fibroblasts. Exp Cell Res 115, 357-366.
26. Mauthe M, Orhon I, Rocchi C, Zhou X, Luhr M, Hijlkema KJ, Coppes RP, Engedal N, Mari M and Reggiori F (2018) Chloroquine inhibits autophagic flux by decreasing autophagosome-lysosome fusion. Autophagy 14, 1435-1455.
27. Groll M and Huber R (2004) Inhibitors of the eukaryotic 20S proteasome core particle: a structural approach. Biochim Biophys Acta 1695, 33-44.
28. Le Bail M, Martineau M, Sacchi S, Yatsenko N, Radzishevsky I, Conrod S, Ait Ouares K, Wolosker H, Pollegioni L, Billard JM and Mothet JP (2015) Identity of the NMDA receptor coagonist is synapse specific and developmentally regulated in the hippocampus. Proc Natl Acad Sci U S A 112, E204-E213.
29. Pollegioni L and Sacchi S (2010) Metabolism of the neuromodulator D-serine. Cell Mol Life Sci 67, 2387-2404.
30. Wolosker H (2011) Serine racemase and the serine shuttle between neurons and astrocytes. Biochim Biophys Acta 1814, 1558-1566.
31. Sacchi S, Caldinelli L, Cappelletti P, Pollegioni L and Molla G (2012) Structure-function relationships in human D-amino acid oxidase. Amino Acids 43, 1833-1850.
32. Mellman WJ, Schimke RT and Hayflick L (1972) Catalase turnover in human diploid cell cultures. Exp Cell Res 73, 399-409.

33. Huybrechts SJ, Van Veldhoven PP, Brees C, Mannaerts GP, Los GV and Fransen M (2009) Peroxisome dynamics in cultured mammalian cells. Traffic 10, 1722-1733.
34. Nordgren M, Wang B, Apanasets O and Fransen M (2013) Peroxisome degradation in mammals: mechanisms of action, recent advances, and perspectives. Front Physiol 4, 145.
35. Léon S, Goodman JM and Subramani S (2006) Uniqueness of the mechanism of protein import into the peroxisome matrix: transport of folded, co-factor-bound and oligomeric proteins by shuttling receptors. Biochim Biophys Acta 1763, 1552-1564.
36. Leithe E and Rivedal E (2004) Epidermal growth factor regulates ubiquitination, internalization and proteasome-dependent degradation of connexin43. J Cell Sci 117, 1211-1220.
37. Katane M, Yamada S, Kawaguchi G, Chinen M, Matsumura M, Ando T, Doi I, Nakayama K, Kaneko Y, Matsuda S, Saitoh Y, Miyamoto T, Sekine M, Yamaotsu N, Hirono S and Homma H (2015) Identification of novel D-Aspartate oxidase inhibitors by in silico screening and their functional and structural characterization in vitro. J Med Chem 58, 7328-7340.

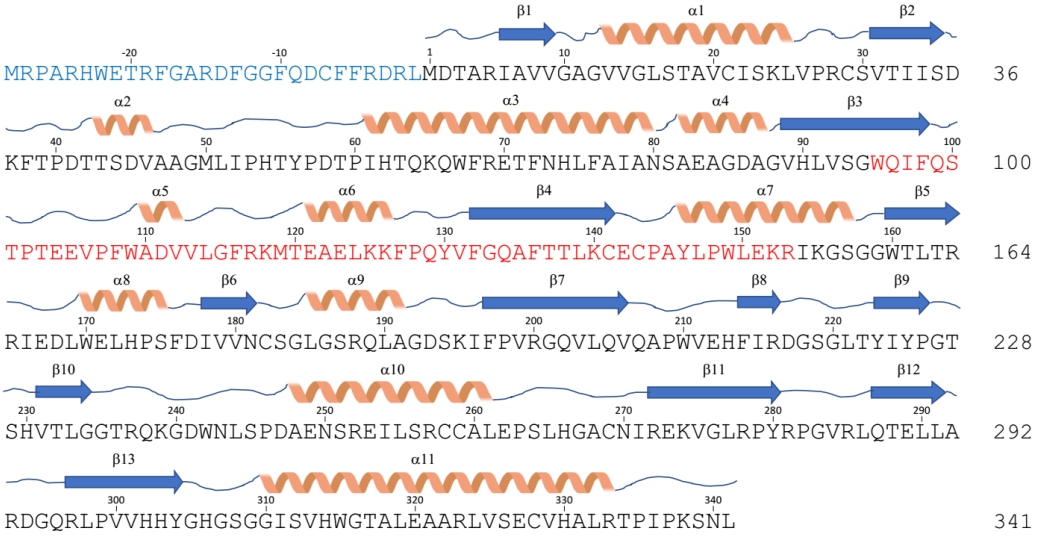

Fig. 1: Schematic representation of the amino acid sequence of the three known hDASPO isoforms. The lacking sequence of hDASPO_282 is shown in red while the N-terminal 28 additional residues of hDASPO_369 are shown in blue. The secondary structure scheme of hDASPO_341 is reported above.

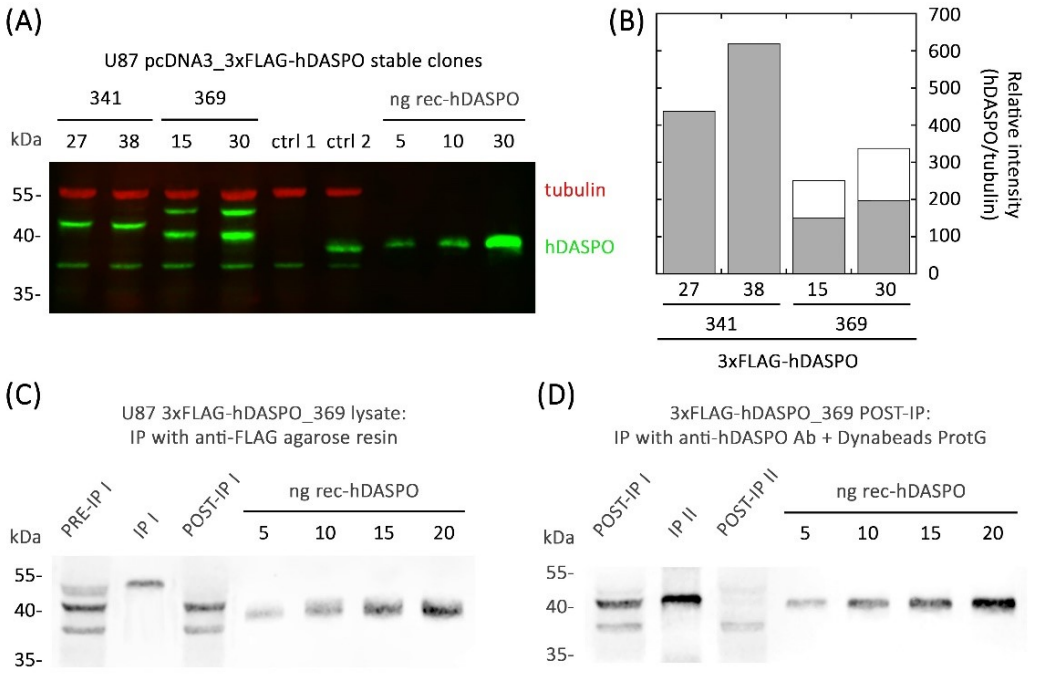

Fig. 2: Expression of hDASPO isoforms in U87 glioblastoma cells. (A, B) Relative expression levels of the protein isoforms in U87 cell clones stably transfected with pcDNA3 3XFLAG-hDASPO_341 (clones 27 and 38) or pcDNA3 3XFLAG-hDASPO_369 (clones 15 and 30) detected by dual fluorescent Western blot analysis using rabbit anti-hDASPO and mouse anti-tubulin antibodies (A) and corresponding densitometric analysis (panel B; grey bars: hDASPO_341; white bars: hDASPO_369). Amounts of sample corresponding to 5×10^4 cells were loaded. Ctrl1: untrasfected cells; Ctrl2: untrasfected cells to which 10 ng of recombinant hDASPO

were added. Recombinant hDASPO (38.6 kDa) was used as a positive control. (C, D) IP studies aimed to confirm the identity of the hDASPO forms detected in lysates of U87 cells transfected with pcDNA3 3XFLAG-hDASPO_369. The presence of hDASPO was revealed by Western blot analysis using anti-hDASPO antibody: (C) 3XFLAG-hDASPO_369 (44 kDa) was immunoprecipitated from the whole cell lysate using an anti-FLAG agarose resin and (D) the ensuing post-IP sample (showing bands at 37 and 40.5 kDa) was further immunoprecipitated using anti-hDASPO antibodies conjugated to Dynabeads Protein G. Bands corresponding to 3XFLAG-hDASPO_369 (44 kDa) and hDASPO_341 (40.5 kDa) were observed in the IP I and IP II samples, respectively.

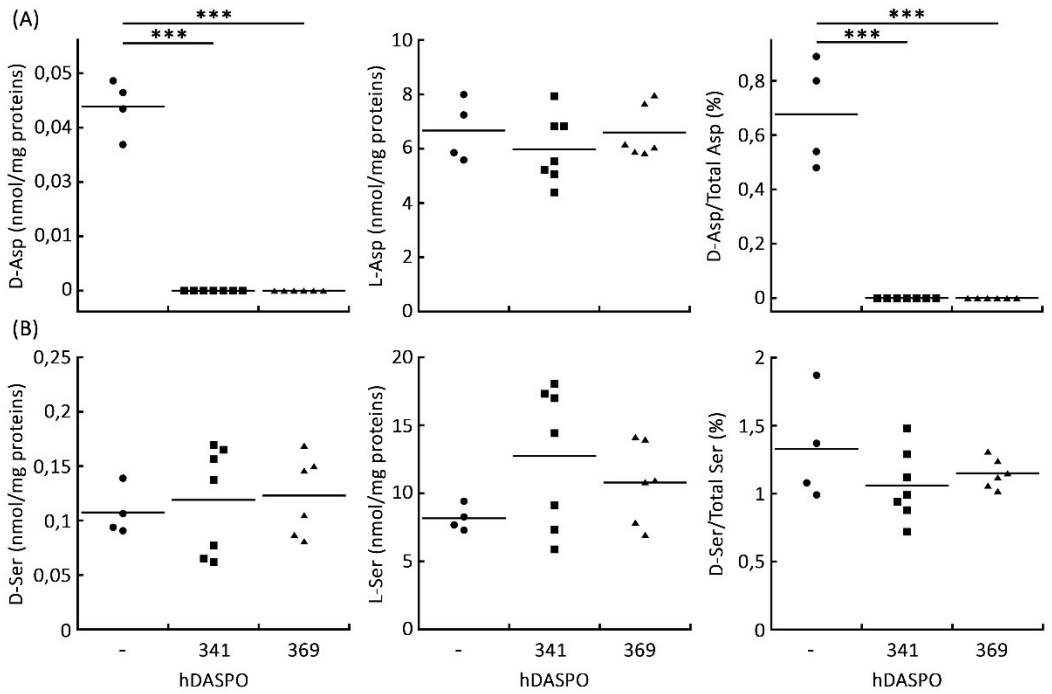

Fig. 3: HPLC analysis of the cellular content of Asp and Ser enantiomers. The amount of D- and L-Asp (A) and of D- and L-Ser (B) in U87 cells stably transfected with pcDNA3_3xFLAG-hDASPO_341, pcDNA3_3xFLAG-hDASPO_369 and in control cells transfected with the empty vector, was measured and normalized for the total protein content in each sample. The D-enantiomer/total stereoisomers ratio is also reported (right panels). ***$p < 0.0001$. Data were analyzed by unpaired parametric t-test. Graphs report single data point as well as mean values.

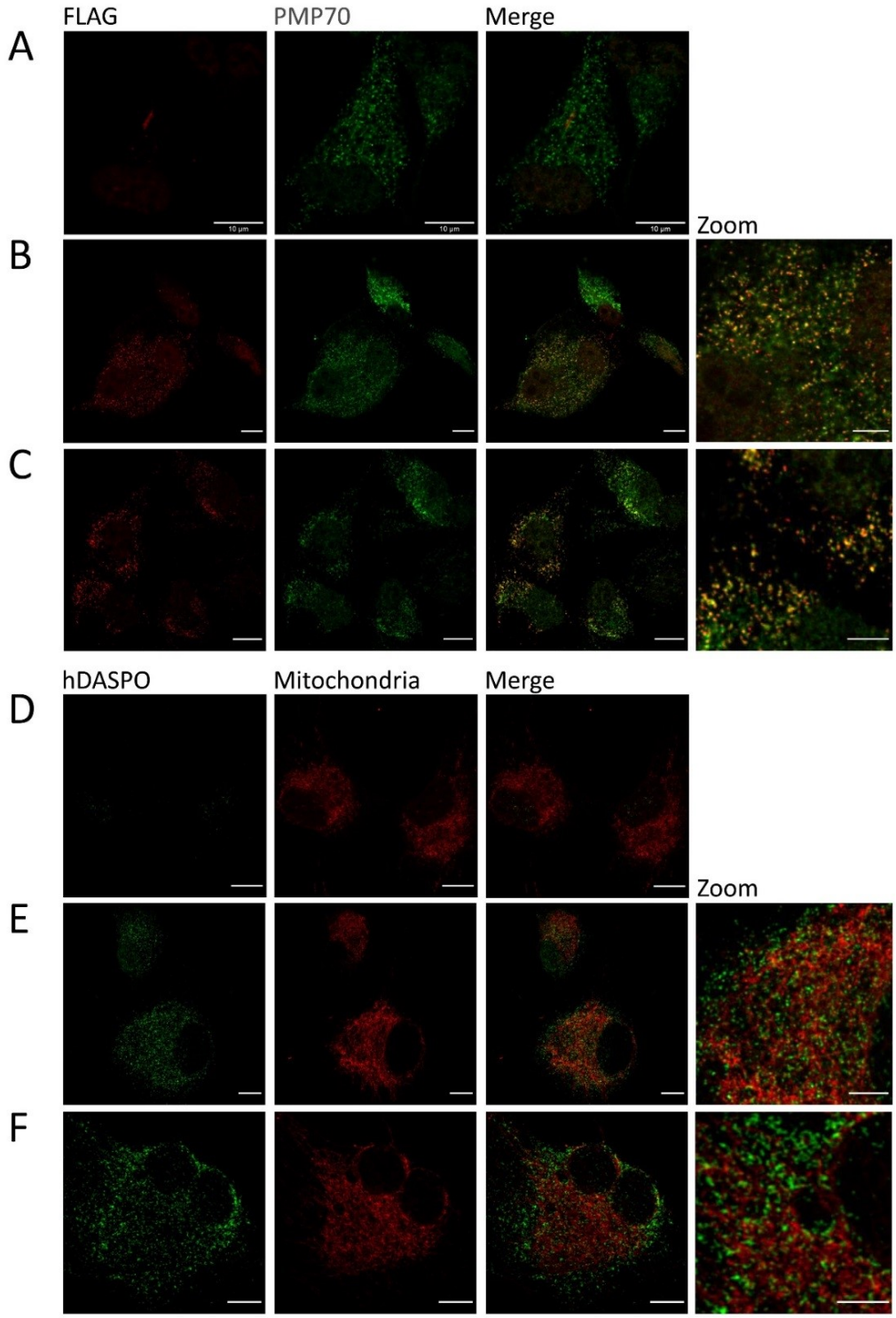

Fig. 4: Confocal analysis of U87 stable clones expressing 3XFLAG-hDASPO protein isoforms and control cells. U87 untransfected cells, as well as 3XFLAG-hDASPO_369 (B, E) and 3XFLAG-hDASPO_341 (C, F) expressing

cells were double-stained with the anti-FLAG and the anti-PMP70 (A-C) or the anti-hDASPO and the anti-mitochondria antibodies (D-F). (A, D) Control cells showed no (aspecific) signals either with the red (A) or the green (D) channel, respectively. (B, C) 3XFLAG-hDASPO_369 (B) and 3XFLAG-hDASPO_341 (C) signals (red channel) largely overlapped with PMP70 ones (green channel), strongly indicating a peroxisomal localization for both protein isoforms. (E, F) No signal overlapping with the mitochondria is instead observed for both the 3XFLAG-hDASPO_369 (E) and _341 (F) hDASPO isoforms (compare the signal distribution in the merge panels).

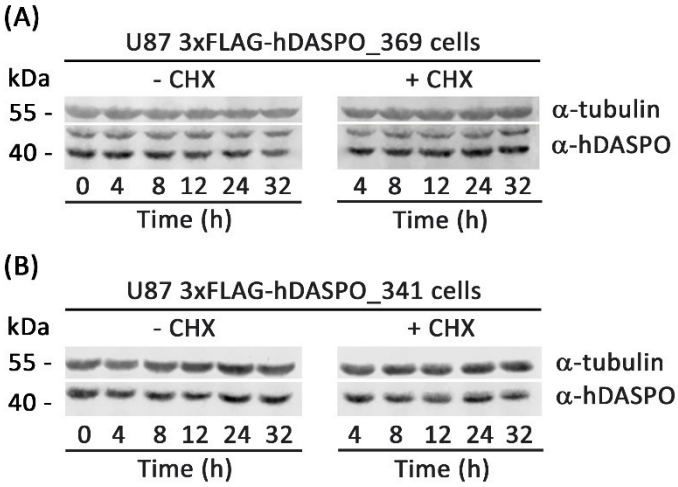

Fig. 5: Analysis of hDASPO degradation rate. U87 cells stably expressing 3XFLAG-hDASPO_369 or 3XFLAG-hDASPO_341 isoforms were treated with 100 µg/mL CHX. (A) In U87 3XFLAG-hDASPO_369 CHX-treated cells, only a small decrease (~20% at 32 h) in the signal detected at 39 kDa (untagged hDASPO_341) and 44 kDa (3XFLAG-hDASPO_369) by anti-hDASPO antibodies was apparent compared to the control. (B) Similarly, a small change in the intensity of the 42 kDa band corresponding to 3XFLAG-hDASPO_341 was observed following CHX addition, thus indicating that both the protein isoforms are highly stable. Values are the mean ± SD (n = 4-8), normalized to tubulin and expressed relatively to the control without CHX (i.e. cells collected at the same time after the addition of PBS).

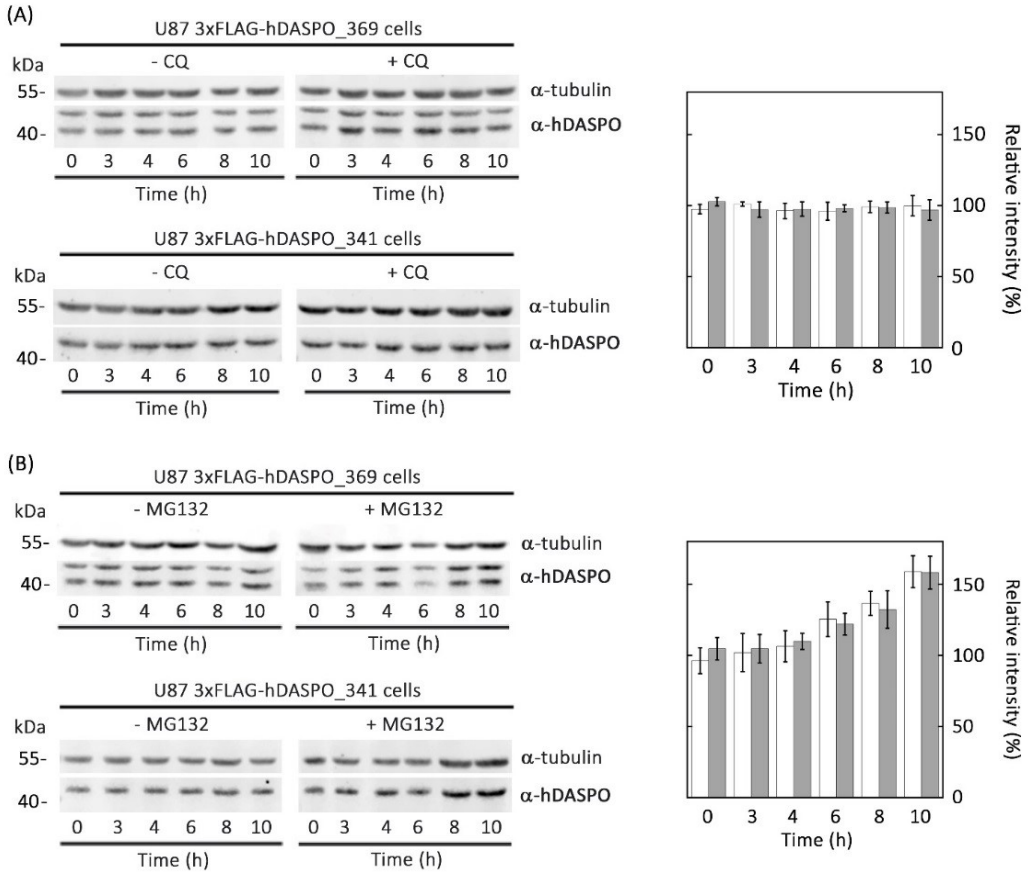

Fig. 6: Effect of inhibitors of the degradation pathways on 3XFLAG-hDASPO_369 and 3XFLAG-hDASPO_341 cellular levels. (A) The cell clones were incubated under starvation conditions and treated with 75 µM CQ or PBS as a control, for up to 10 h. Western blot and quantification analysis showed no variation in the amount of 3XFLAG-hDASPO_369 (white bars) or 3XFLAG-hDASPO_341 (grey bars) in treated cells compared to controls. (B) U87 cells stably expressing 3XFLAG-hDASPO_369 or 3XFLAG-hDASPO_341 under starvation were treated with 25 µM MG132 or 0.1% DMSO for up to 10 h. Western blot analysis using anti-hDASPO antibody and quantitative analysis demonstrated that both 3XFLAG-hDASPO_369 and 3XFLAG-hDASPO_341 significantly accumulated after adding the inhibitor. For each time point, the value is expressed as the mean ± SD (n = 4), normalized to tubulin, and expressed relative to the control (i.e. cells collected at the same time after adding PBS or DMSO, see left lanes in Western blot panels).

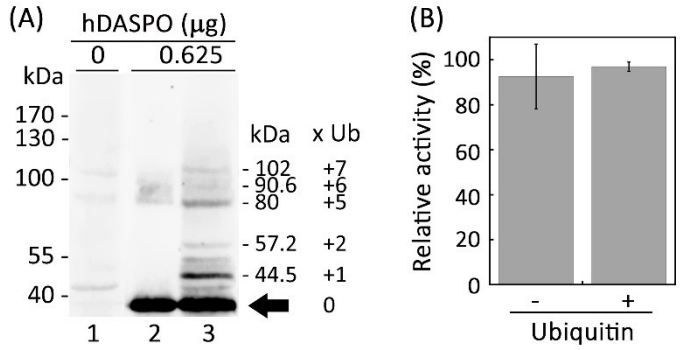

Fig. 7: *In vitro* ubiquitination assay of recombinant hDASPO. The purified recombinant hDASPO (5 µg) was incubated with U87 cell extracts (4 mg/mL), ubiquitin, ATP, MG132 and ubiquitin aldehyde (in a final volume of 60 µL) and incubated at 37 °C for 60 minutes. To detect the formation of hDASPO-ubiquitin conjugates, an aliquot of the reaction mixture (corresponding to 0.625 µg of recombinant protein) was analyzed by Western blotting using anti-hDASPO antibody. (A) Distinct bands, corresponding to distinct hDASPO modified forms (mono- or polyubiquitinated) were evident in the reaction mixture only (lane 3) and absent in control samples (prepared by omitting ubiquitin, lane 2, or using the same volume of the reaction mixture without adding the recombinant protein, lane 1). The arrow indicates the unmodified protein. (B) Activity assays performed on the in vitro ubiquitination and control mixtures revealed that recombinant hDASPO activity is not affected by the modification. Activity measurements are reported as relative activity after the incubation at 37 °C compared to the starting value. Data represent mean values ± standard deviation (n=3).

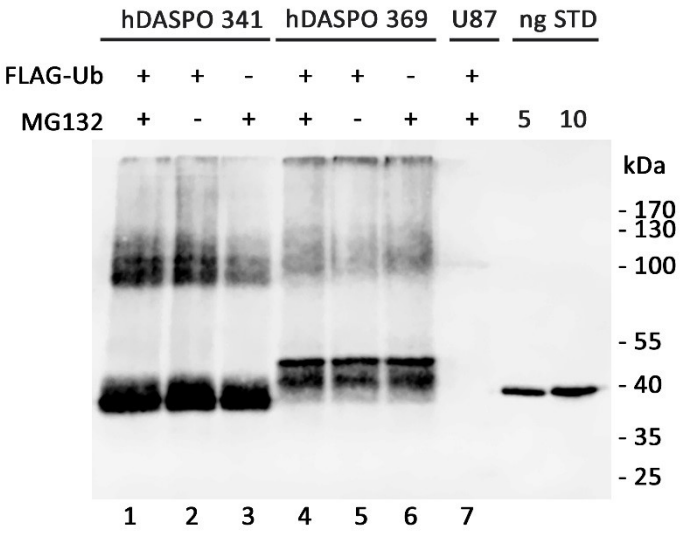

Fig. 8: Ubiquitination analysis in U87 cells stably expressing hDASPO isoforms and transiently transfected with FLAG-ubiquitin. Forty-eight hours after transfection with pCMV-FLAG-ubiquitin, U87 control cells (lane 7) and cells stably expressing the 3XFLAG-hDASPO_341 (lanes 1-3) and -hDASPO_369 (lanes 4-6) isoforms were treated with 25 µM MG132 for 6 hours and then proteins were immunoprecipitated under denaturing conditions using anti-FLAG M2 Affinity resin. Cells transfected but not treated with the proteasome inhibitor or not transfected and added with MG132 were processed as controls. The presence of ubiquitinated-hDASPO was revealed by Western blot analysis using anti-hDASPO antibody.

Supplementary Table 1. Primers used for cloning human hDASPO_341 and hDASPO_369 cDNA in the pcDNA3 mammalian expression vector. Sequences recognized by the indicated endonucleases are underlined. In bold is reported the sequence encoding for the 3XFLAG peptide.

Oligo	**Sequence**	**Cloning site**
3XFLAG hDASPO 341_for	5'-ACAGCGGGATCCCACC**ATGGATTACAAGGATGACGACGATAAGGACTATAAGGACGATGATGACAAGGACTACAAAGATGATGACGATAAAC**TCGACACAGCACGGATTGCAGTTGTCG-3'	BamHI
3XFLAG hDASPO 369_for	5'-ACAGCGGGTACCCACC**ATGGATTACAAGGATGACGACGATAAGGACTATAAGGACGATGATGACAAGGACTACAAAGATGATGACGATAAAC**TCAGACCAGCCAGGCACTGGGAAACAAG-3'	KpnI
3XFLAG hDASPO 341/369_rev	5'-ACAGCGGCGGCCGCCTACAGGTTTGACTTGGGAATGGGGG-3'	NotI

3.4. Investigating the post-translational modifications of the human flavoenzyme D-aspartate oxidase

Material and Methods

Recombinant protein

The cDNA coding for hDASPO was cloned in the pET11a vector under the control of the T7 promoter. The His-tagged recombinant protein was expressed in *E. coli* BL21(DE3) LOBSTR host cells (Novagen) upon induction with IPTG during the exponential phase of growth and purified by HiTrap chelating chromatography (GE Healthcare) as reported in (Molla et al., 2020). The final protein preparation was equilibrated in 20 mM Tris–HCl buffer, pH 8.0, 10% glycerol, 5 mM 2-mercaptoethanol, for long term storage at -80 °C. The concentration of the purified enzyme was determined spectrophotometrically using the extinction coefficient at 455 nm (12.18 mM^{-1} cm^{-1}). The apoprotein form of hDASPO was prepared by several steps of extensive dialysis against solutions containing increasing concentrations of KBr (from 1.5 to 3 M), following the previously reported procedure (Molla et al., 2020).

Cell cultures

hDASPO coding sequence was cloned in the pcDNA3 vector for the high-level, constitutive expression in mammalian cell lines. Cloning was performed by PCR amplification using HsCD00335325 pCMV-SPORT6 (purchased by the PlasmID Repository at Harvard Medical School) as the donor plasmid and the following primers: 5'-ACAGCGGGATCCCACC**ATGGATTACAAGGATGACGACGATAAGGACTATAAGGACGATGATGACAAGGACTACAAAGATGATGACGATAAAC**TCGACACAGCACGGATTGCAGTTGTCG-3' (forward) and 5'-ACAGCGGCGGCCGCCTACAGGTTTGACTTGGGAATGGGGG-3' (reverse), which allow the insertion of a sequence coding for a 3xFLAG peptide at the N-terminal end of the protein (reported in bold) and subcloning into *BamHI* and *NotI* restriction sites (underlined) of the expression vector. The resulting construct, namely pcDNA3-3xFLAG-hDASPO, was confirmed by automated sequencing.

Human U87 glioblastoma cells (ATCC) were maintained in DMEM supplemented with 10% fetal bovine serum (FBS), 1 mM sodium pyruvate, 2 mM L-glutamine, 1% penicillin/streptomycin, and 2.5 µg/mL amphotericin B (all from Euroclone) at 37 °C in a 5% CO_2 incubator. Transfection mixtures were set up using 6 µL of FuGENE HD transfection reagent (Promega) and 2 µg of pcDNA.3-3xFLAG-hDASPO vector. Stable clones were selected adding 0.4 mg/mL G418 to the growth medium. On the selected cell clones, hDASPO expression level was monitored by Western blot analysis.

Determination of disulfide bonds

To evaluate the number of accessible cysteines in hDASPO, the holo- and apoprotein forms were reacted with 0.1 mM 5,5'-dithiobis(2-nitrobenzoic acid) (DTNB), in 0.45 M sodium phosphate buffer pH 8.0, 0.45 mM EDTA, either under native and denaturing conditions (in the presence of 4 M urea) (Pollegioni et al., 1997). Upon reaction with DTNB, samples were incubated for 15 min at 25 °C and absorbance was recorded at 412 nm. Quantification of free sulfhydryl groups was performed both using the molar extinction coefficient of the product TNB (ε =14.15 and 14.29 $mM^{-1}cm^{-1}$ in sodium phosphate buffer and 4 M urea, respectively) and a calibration curve obtained by titrating DTNB with different concentrations of L-cysteine (0-200 µM).

In vitro S-nitrosylation and detection of S-nitroso cysteines

In order to perform *in vitro* modification studies, the reducing agent 2-mercaptoethanol (added to the storage buffer to ensure long storage stability of the enzyme) was removed. Thus, aliquots of the hDASPO preparation were 10-fold diluted in 20 mM Tris–HCl buffer, pH 8.0, 10% glycerol and concentrated to the starting volume using an Amicon centrifugal filter device (Ultracel – 30K, Merck Millipore). The procedure was repeated twice and the protein concentration was determined as stated above.

In vitro nitrosylation of recombinant hDASPO was performed by incubation with S-nitrosoglutathione (GSNO) as the NO donor (Wang et al., 2011). Reaction mixtures were prepared by diluting the proteins in HEN buffer (25 mM HEPES pH 7.7, 1 mM EDTA, 0.1 mM neucoproine) to a final concentration of 1 mg/mL (25 µM) and adding 500 µM GSNO

(200 µl final volume). Mixtures containing the recombinant protein added with 500 µM reduced (GSH) or oxidized (GSSG) glutathione were prepared as controls. Reaction mixtures were incubated 1 hour in the dark, at 25 °C, under constant rotation. S-Nitrosylation was verified by fluorescence detection, following a fluorescence switch assay and gel electrophoresis analysis. The fluorescence switch assay was set up by using the fluorescent probe Alexa Fluor 350 C_5 Maleimide (Molecular Probes/ThermoFisher Scientific; excitation and emission wavelengths of 345 and 444 nm, respectively) and a procedure modified from (Han et al., 2008). The excess of GSNO (or GSH, or GSSG) was removed from the reaction mixtures by 3 steps of concentration/dilution in HEN buffer using Amicon Ultra 30K 0.5 mL Centrifugal Filters (Merck Millipore), see above. Unmodified free thiols in hDASPO were saturated by reacting the protein with 20 mM methyl methanethiosulfonate (MMTS), in the presence of 2.5% SDS, for 30 min at 50 °C. The excess of MMTS was removed by 4 concentration/dilution steps in HEN buffer, as above. Nitrosylated thiols were reduced by incubating the mixtures for 1 h at room temperature upon the addition of 5 mM sodium ascorbate and finally labeled with 50 µM Alexa Fluor 350 C_5 Maleimide for 16 hours at 4 °C. Labeled samples were analyzed by SDS-PAGE under non-reducing conditions: the gel was rinsed with MilliQ water and imaged on transilluminator by a Gel Doc 2000 (Biorad). Each step of the procedure was performed protecting reaction mixtures and samples from light, in order to avoid the dissociation of the modified thiols.

In vitro sulfhydration and detection of S-sulfhydrated cysteines

The modification by H_2S of cysteine residues in hDASPO was investigated by incubation with NaHS as a sulfur donor. Recombinant hDASPO, prepared as reported above, was diluted in storage buffer (20 mM Tris-HCl, pH 8.0, 10% glycerol) to a concentration of 1 mg/mL, added with 1 mM NaHS and incubated at 37 °C for 1 h. The presence of modified cysteines was analyzed by performing the fluorescence switch assay and non-reducing SDS-PAGE, as detailed above.

In vitro phosphorylation

In vitro phosphorylation experiments were performed by incubating 7 µg of recombinant hDASPO with 12 mU of PRKACA (the catalytic subunit of protein kinase A - Invitrogen) in 50 mM Tris-HCl pH 7.5, 10 mM $MgCl_2$, 1 mM DTT and 50 µM ATP, in a total volume of 50 µL, at 30 °C for 60 minutes. Mixtures prepared with 4 µg of CREB1 (CAMP responsive element binding protein 1, which is phosphorylated by PKA) (Gonzalez and Montminy, 1989) instead of hDASPO or by omitting hDASPO were prepared as controls. At different time points, aliquots of the reactions were withdrawn and blocked by adding the SDS-PAGE sample buffer and boiling. Proteins were resolved by SDS-PAGE in reducing conditions. The gel was subsequently fixed for 30 minutes in 50% methanol, 10% acetic acid (repeated twice), rinsed with MilliQ water and then stained upon incubation with the Pro-Q Diamond Phosphoprotein Stain (ThermoFisher Scientific) for 7 minutes (step repeated twice). After destaining with 20% acetonitrile in 50 mM sodium acetate, pH 4.0 for 30 minutes, the gel was imaged upon acquisition with an Odyssey Fc Imaging System (LI-COR Biosciences).

Activity assays

hDASPO activity following *in vitro* nitrosylation or sulfhydration reactions was determined by the O_2 consumption assay (Rosini et al., 2018; Molla et al., 2020). Recombinant hDASPO was added with 500 µM GSNO or 1 mM NaHS; control measurements were performed in the absence of the NO or H_2S donors. Aliquots of the reaction mixtures were diluted 1:20 in storage buffer and immediately assayed for residual activity by an oxygen electrode at pH 8.5, air saturation and 25 °C, using 15 mM D-Asp in the presence of 40 µM FAD. The enzyme's residual activity was calculated by comparing the values measured before and after the *in vitro* modification reactions.

Cellular studies were also performed to investigate the effect of nitrosylation or sulfhydration on hDASPO functionality. The enzyme's modifications were induced by treating U87 cells stably expressing hDASPO with the NO donors (±)-(E)-4-ethyl-2-[(E)-hydroxyimino]-5-nitro-3-hexenamide (NOR-3, 50 µM, Santa Cruz Biotechnology) and 3-(2-hydroxy-1-methyl-2-nitrosohydrazino)-N-methyl-1-propanamine (NOC-7, 50 µM, Santa Cruz Biotechnology) for 2 hours, as reported in (Shoji et al., 2006), or with the H_2S

precursor NaHS (50 and 100 µM, Santa Cruz Biotechnology) for 30 minutes: the activity was assayed on cell lysates by using the Amplex UltraRed reagent (Invitrogen) and 15 mM D-Asp as substrate. The assay is based on the detection of H_2O_2 by peroxidase-mediated oxidation of the fluorogenic Amplex UltraRed Dye (Sacchi et al., 2008). Controls were set up by treating these cell clones with an equal amount of DMSO or by treating U87 cells transfected with the pcDNA3 empty vector with the NO or H_2S donors or DMSO.

Results

Bioinformatic analyses predict several sites of post-translational modification in hDASPO

hDASPO primary structure harbors nine Cys residues, among which five appear to be highly conserved since are present in all mammalian DASPOs (Fig. 1).

Fig. 1: Frequency of sequence conservation among mammalian DASPOs. Weblogo representation of conserved residues identified by the alignment of selected regions of DASPO sequences from *Homo sapiens,*

Mus musculus, Rattus norvegicus, Sus scrofa, Bos taurus, Cavia porcellus, Macaca fascicularis and *Pongo abelii*. The x-axis identifies the amino acid positions (the annotated numbering refers to the human enzyme) and the height of symbols is proportional to the degree of conservation of single residues. Panels represent sequence stretches of 20 positions each, containing cysteine residues (reported in red). Figure prepared using WebLogo (https://weblogo.berkeley.edu/logo.cgi).

Notably, among these strictly conserved cysteines, four are also present in the homologous flavoenzyme hDAAO (corresponding to Cys21, 182, 258, 259 in hDASPO). All cysteine residues of hDASPO should be present in the free reduced form, since no disulfide bonds were identified by the disulfide bonding state predictors DISULFIND (at http://disulfind.dsi.unifi.it/) (Ceroni et al., 2006) and CYSPRED (at http://gpcr.biocomp.unibo.it/cgi/predictors/cyspred/pred_cyspredcgi.cgi) (Fariselli et al., 1999) that resulted in very high confidence values of disulfide bonding state prediction for all cysteine residues.

Putative nitrosylated residues were predicted using different web-based tools (see Table I). With the exception of Cys182, which was indicated as unmodified by all the prediction softwares, the analyses yielded divergent results. It is noteworthy that the SNO site (Lee et al., 2012), which applies the maximal dependence decomposition approach to explore conserved nitrosylation motifs, identified the vast majority of hDASPO cysteines as potential nitrosylation sites (Table I). Protein S-sulfhydration is a newly discovered post-translational modification of cysteine residues. The related underlying mechanism is still largely unknown and a prediction of putative modification sites is currently unfeasible, although accumulated evidence suggest that this modification may share similar chemical features with protein S-nitrosylation.

Phosphorylation sites were also predicted by means of free computational tools on the web (Table II). Despite several residues in hDASPO were identified as modified by the different predictors, the estimated levels of serine, threonine and tyrosine phosphorylation are heterogeneous. Moreover, in the case of DIPHOSPH 1.3, no phosphorylation site was identified when the group predictor for human was selected instead of the default one. However, when single kinases are specified as the putative modifying enzyme, hDASPO appeared to be mainly subjected to phosphorylation by

cAMP-dependent protein kinase (PKA), protein kinase C (PKC), and protein kinase involved in the cell cycle regulation (cdk5 and CKII).

Table I: Prediction of nitrosylation sites by web-based tools. Cysteine residues indicated in bold are strictly conserved in hDASPO and hDAAO. In the last column, underscored residues are those present in the consensus sequence of identified putative nitrosylation motifs by SNO site.

hDASPO

Cys position	GPS SNO 1.0	iSNO PseAAC	iSNO AAPair	Deep Nitro	SNO Site	Sequence -10 +10
21	●	●			●	AGVVGLSTAV**C**ISKLVPRCSV
29		●			●	AVCISKLVPR**C**SVTIISDKFT
141		●			●	VFGQAFTTLK**C**ECPAYLPWLE
143			●		●	GQAFTTLKCE**C**PAYLPWLEKR
182						
258					●	AENSREILSR**C**CALEPSLHGA
259	●				●	ENSREILSRC**C**ALEPSLHGAC
269		●			●	CALEPSLHGA**C**NIREKVGLRP
328			●		●	ALEAARLVSE**C**VHALRTPIPK

GPS SNO 1.0 at http://sno.biocuckoo.org (Xue et al., 2010); iSNO PseAAC at http://app.aporc.org/iSNO-PseAAC/ (Xu et al., 2013a); iSNO AAPair at http://app.aporc.org/iSNO-AAPair/ (Xu et al., 2013b); DeepNitro at http://deepnitro.renlab.org/webserver.html (Xie et al., 2018); SNOSite at http://csb.cse.yzu.edu.tw/SNOSite/Prediction.html (Lee et al., 2011).

Table II: Prediction of phosphorylation sites in hDASPO by web-based tools. For NetPhos 3.0 prediction the score value was set above 0.75.

hDASPO

residues	NetPhos 3.0	DIPHOSPH 1.3	PHOSPHONET	GPS 5.0
Ser (23)	5 (22%)	1 (4%)	7 (30%)	0
Thr (24)	9 (37%)	4 (17%)	10 (41%)	0
Tyr (7)	1 (14%)	0	7 (100%)	0

NetPhos 3.0 at http://www.cbs.dtu.dk/services/NetPhos/ (Blom et al., 1999); DIPHOSPH 1.3 at http://www.dabi.temple.edu/disphos/; PHOSPHONET at http://www.phosphonet.ca; and GPS 5.0 at http://gps.biocuckoo.cn (Wang et al., 2020).

Structural and modification analyses suggest the identity of the "editable" cysteine residues

Cysteine residues exposure to modification was assessed by performing a solvent accessible surface analysis on the protein structure (Fig. 2). With the only exception of Cys182, which is completely buried in the protein structure, all hDASPO cysteine residues are relatively close to the protein surface: Cys269 and Cys259 result largely exposed, while Cys141 and Cys 144, although close to the surface, are oriented with their side chains facing the protein core (Fig. 2A). Worthy of note, in hDASPO cysteines are grouped in small clusters, with the only exception of Cys182 (Fig. 2A): Cys21 and Cys29 are located at 10.3 and 9.0 Å from Lys24, respectively, which is part of the identified nitrosylation motif consensus sequence (Table I). Moreover, two flanking charged residues (Arg28 at 11.7 Å from Cys29, and Arg323 at 8.8 Å from Cys21) are also present (Fig. 2B): this has been proposed as one feature distinguishing S-nitrosylation sites (Gould et al., 2013). It is noteworthy that the conserved cysteines 21 and 29 are located within the Rossmann fold for the cofactor binding; thus the modification of one or both of these residues might strongly affect the enzyme's properties. A putative acid-base motif is observed close to Cys258: Arg257 at 6.6 Å and Glu253 at 10 Å; Cys269 appears completely exposed and far from charged residues; whereas Cys328 is located at 9.0 Å from Glu327 (Fig. 2B). All the aforementioned residues are surrounded by a hydrophobic environment that might account for further stabilization of SNO-Cys.

The solvent accessibility of cysteine residues was experimentally investigated by reacting hDASPO with DTNB under non-reducing conditions, in the presence or absence of a denaturing agent. Consistent with structural information, the reaction of the native protein with DTNB yielded a number of free Cys residues of 4.0±0.4, while in the presence of 4 M urea the same assay yielded a number of 9.3±0.7 Cys, indicating that 5 Cys are not solvent-accessible in the native conformation of hDASPO. Notably, under native conditions hDASPO apoprotein exposed two additional Cys (6.3±0.3).

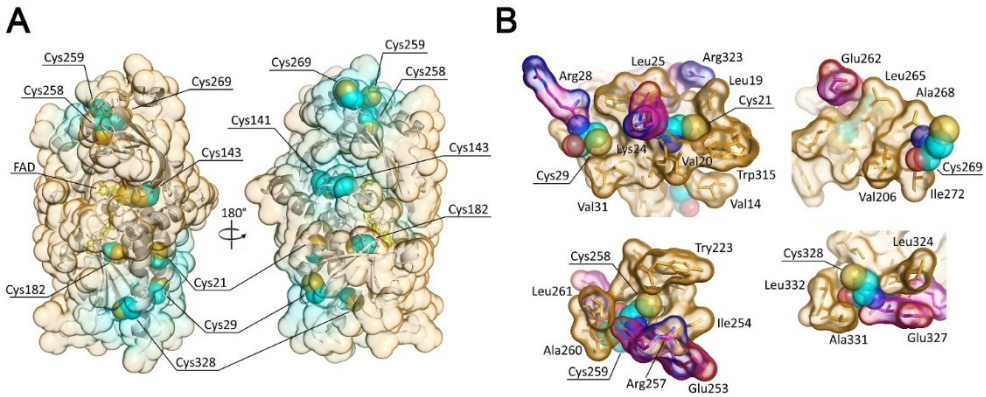

Fig.2: Analysis of the position, exposure to the solvent and amino acidic environment of hDASPO cysteine residues. A) Solvent accessible surface (SAS) as calculated for the hDASPO monomer (pdb code 6RKF). Cysteine residues in the structure are represented as sphere (carbon atoms in cyan, sulphur atoms in yellow); the FAD cofactor is represented as sticks (yellow). The backbone is shown as cartoon. Protein surface is colored by proximity of cysteine residues (cyan = cysteine residues located within 5 Å from the surface; orange = cysteine residues located at a distance higher than 15 Å from the surface). SAS has been calculated based on a solvent radius of 1.4 Å. B) Analysis of the environment of selected cysteine residues, represented as sphere (carbon atoms in cyan, sulphur atoms in yellow, nitrogen atoms in blue, oxygen atoms in red): the surrounding residues are depicted as sticks and the van der Waals surface is shown. Hydrophobic residues are colored in orange, while charged residues are colored by element (carbon atoms in magenta, nitrogen atoms in blue and oxygen atoms in red).

Recombinant hDASPO is modified by the NO donor GSNO

25 µM recombinant hDASPO in HEN buffer (i.e. a preparation from which the reducing agent 2-mercaptoethanol was previously removed) was incubated with 500 µM GSNO as a NO donor (or with the same concentration of GSH or GSSG as negative controls), 1 hour in the dark, at 25 °C, under constant rotation. S-nitrosylated cysteine residues (SNO-Cys) were detected by a fluorescent switch assay. In details, after the removal of the

excess of GSNO, free sulfhydryls were blocked with MMTS under strong denaturing conditions (2.5% SDS in HEN buffer) to ensure the complete blockade of buried cysteines. The excess of MMTS was removed and SNO-CHS were selectively reduced to free thiols by sodium ascorbate, and immediately labeled with Alexa Fluor 350 C_5 Maleimide. Positive controls were prepared by omitting the MMTS blocking step, so that all cysteine residues were reduced during the incubation in sodium ascorbate.

SDS-PAGE analysis, performed under non-reducing conditions, clearly indicated that recombinant hDASPO was modified by GSNO (Fig. 3). No aspecific labeling was observed in negative control samples.

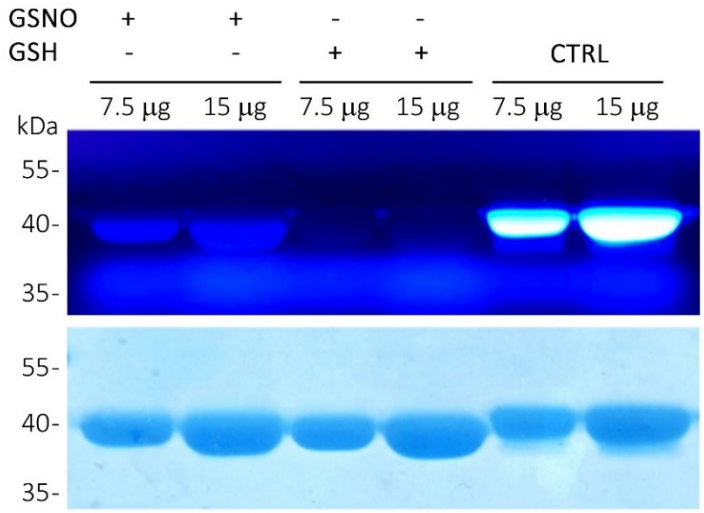

Fig. 3: Non-reducing SDS-PAGE analysis of recombinant hDASPO following in vitro S-nitrosylation. Different amounts of protein (7.5 and 15 µg) were loaded. Mixtures in which the NO donor GSNO was replaced with GSH were analyzed as a negative control; whereas positive controls (CTRL) were represented by protein samples in which all cysteine residues were labelled by Alexa Fluor 350 C5 Maleimide (by omitting the MMTS blocking step during the fluorescence switch assay). Image acquisition was performed upon excitation of the fluorescent probe (top) and by Coomassie staining (bottom).

Recombinant hDASPO is modified by NaHS to a minor extent

In vitro sulfhydration reaction mixtures were set up by diluting the recombinant protein, after the removal of 2-mercaptoethanol, in non-reducing storage buffer to a final concentration of 1 mg/mL (25 µM). Mixtures were then added with the sulfide donor NaHS (1 mM) and incubated at 37 °C for 1 h. The presence of modified cysteine residues

was detected by the fluorescent switch assay, as above. In this case, faint fluorescent bands were detected for hDASPO samples treated with NaHS. The intensity of these bands was only slightly higher compared to those observed in control samples in which NaHS was omitted (Fig. 4), suggesting that the recombinant protein might eventually be sulfhydrated, even though to low extent.

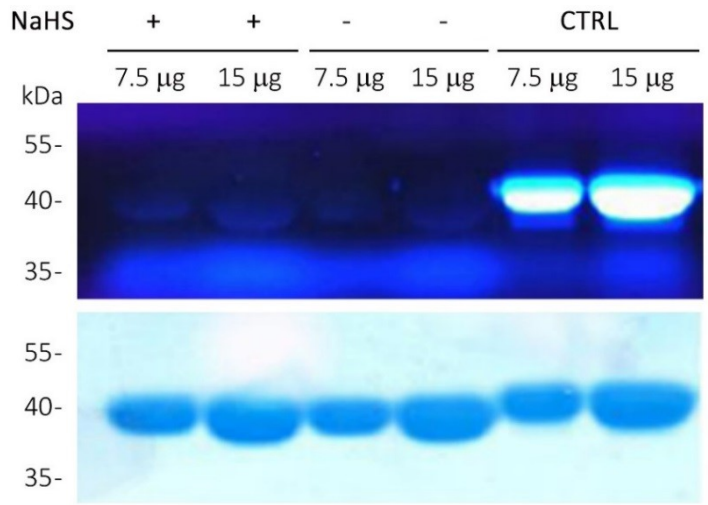

Fig. 4: Non-reducing SDS-PAGE analysis of recombinant hDASPO following in vitro S-sulfhydration. Different amounts of protein (7.5 and 15 µg) were loaded. Mixtures in which the sulfide donor NaHS was omitted were analyzed as a negative control; whereas positive controls (CTRL) were represented by protein samples in which all cysteine residues were labelled by Alexa Fluor 350 C5 Maleimide (by omitting the MMTS blocking step during the fluorescence switch assay). Image acquisition was performed upon excitation of the fluorescent probe (top) and by Coomassie staining (bottom).

Recombinant hDASPO is not modified by protein kinase A

7 µg of purified recombinant hDASPO were incubated with 12 mU of the catalytic subunit of protein kinase A (PRKACA) in the presence of 50 µM ATP, 10 mM $MgCl_2$, 1 mM DTT in 50 mM Tris-HCl pH 7.5. Positive controls were performed replacing hDASPO with the CAMP responsive element binding protein 1 (CREB1), which is known to be phosphorylated by PRKACA (Gonzalez and Montminy, 1989). Negative controls were instead prepared by omitting PRKACA or hDASPO in the mixtures (the latter to verify the absence of aspecific signals). Upon incubation at 30 °C, at different time points, aliquots of the reaction mixtures were withdrawn, blocked and resolved by SDS-PAGE. The protein modification was assessed by staining the gel with Pro-Q Diamond

Phosphoprotein Stain, which selectively binds to the phosphate moiety of phosphoproteins (Agrawal and Thelen, 2009). No difference in the intensity of the bands corresponding to hDASPO was detected between samples and the negative control lacking PRKACA (Fig. 5). Since in the same conditions the kinase was able to modify CREB1, as assessed by the intense signal obtained after 1 hour of incubation, we can conclude that hDASPO cannot be phosphorylated by protein kinase A.

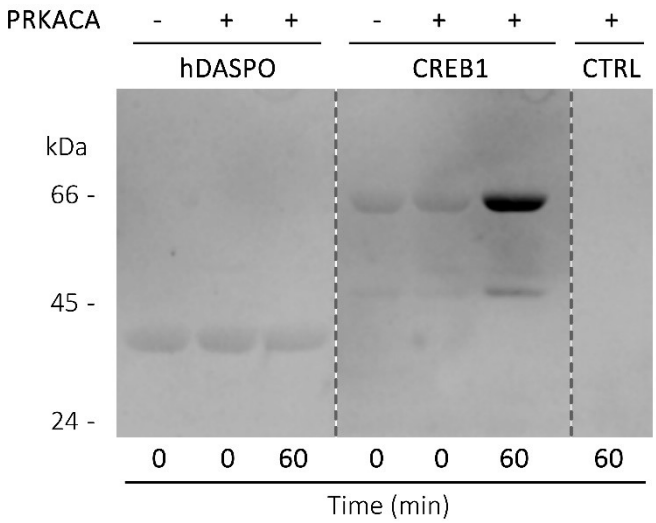

Fig. 5: SDS-PAGE analysis of recombinant hDASPO following in vitro phosphorylation. At different time points (0 and 60 minutes) after the addition of PRKACA, aliquots of the reaction mixture corresponding to 2 µg of hDASPO were withdrawn, blocked with SDS-PAGE sample buffer and loaded on a 12% acrylamide gel. Mixtures in which PRKACA or hDASPO (CTRL) were omitted were analyzed as negative controls, whereas for positive controls hDASPO was replaced with CREB1 (1.2 µg/lane). Dashed lines represent non continuous lanes. Image acquisition was performed upon excitation of the fluorescent dye.

Effect of nitrosylation and sulfhydration on recombinant hDASPO properties

Following *in vitro* nitrosylation and sulfhydration with 500 µM GSNO or 1 mM NaHS, the activity of hDASPO was assayed using saturating concentrations of D-Asp (15 mM) and FAD (40 µM), and compared to control measurements (without NO or H_2S donors in the reaction mixture). The results showed no significant difference in the enzymatic activity following the incubation with GSNO or NaHS compared to control mixtures, thus indicating that both secondary modifications have no effect on its functionality (Fig. 6).

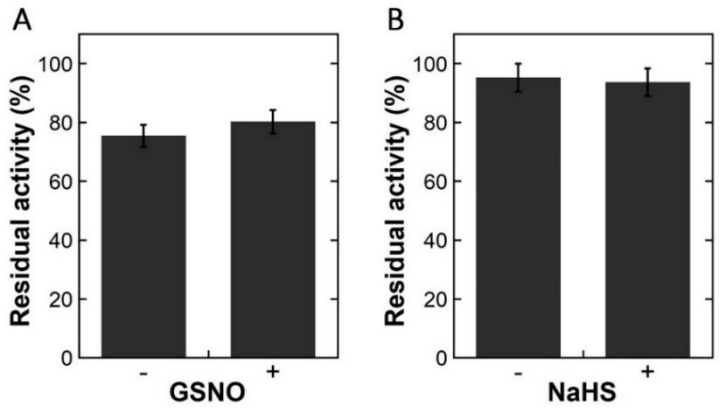

Fig. 6: Residual activity (%) of hDASPO after one hour of incubation in the presence or absence of 500 µM GSNO (A) or in the presence or absence of 1 mM NaHS (B). Data are the mean ± SD (n = 5) and expressed relatively to the activity recorded before the incubation.

The effect of sulfhydration by 1 mM NaHS unchanged the activity of hDASPO, even at longer incubation times (Fig. 7A). On the other hand, NaHS exerted a concentration-dependent effect on hDASPO activity: ≈ 35% of its activity was lost in the presence of 20 mM NaHS (Fig. 7B).

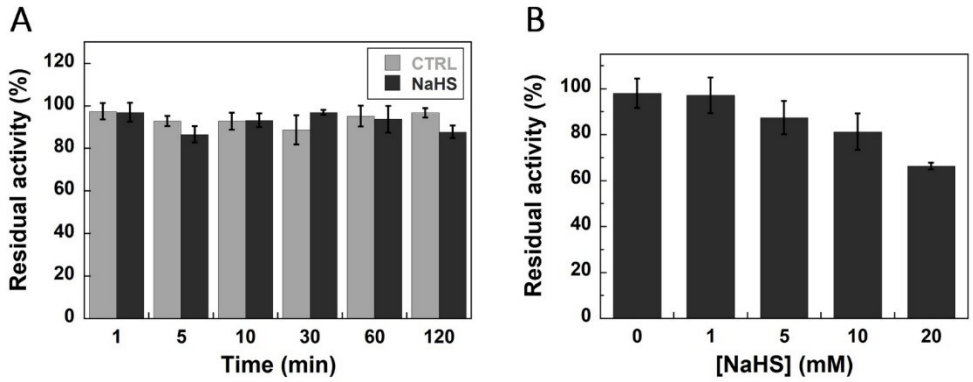

Fig. 7: Effect of sulfhydration on hDASPO activity: (A) at different times of incubation with 1 mM NaHS; (B) after 1 h of incubation with different concentrations of NaHS. Data are the mean ± SD (n = 3-6) and expressed relative to the activity measured without NaHS.

Effect of hDASPO nitrosylation and sulfhydration in a model cellular system

The human U87 glioblastoma cell line was selected in this study to investigate the effect of post-translational modifications on hDASPO functionality, since it has been previously used to express the homologous flavoenzyme hDAAO and to investigate the processes involved in the regulation of this enzyme, including the effect exerted by NO on its

activity (Shoji et al., 2006; Cappelletti et al., 2014), and since the endogenous hDASPO expression level is below detection.

U87 cells were transfected with pcDNA3_3XFLAG-hDASPO expression construct, encoding for the N-terminal FLAG-tagged enzyme and clones stably expressing the enzyme were selected in DMEM added with 0.4 mg/mL G418. hDASPO nitrosylation was induced by treating the selected cell clones for 2 hours with the NO donors NOR-3 or NOC-7 (50 µM) or DMSO (as a control); similarly, sulfhydration was performed by treating the cells for 30 minutes with different concentrations of the H_2S precursor NaHS (50 and 100 µM). The activity of the enzyme was then assayed on equal amounts of cell lysates by using the Amplex UltraRed assay and 15 mM D-Asp as substrate. As shown in Fig. 8, the results confirmed *in vitro* experiments: the treatments with both the NO and H_2S donors did not lead to any relevant effect on the fluorescence signal corresponding to hDASPO activity compared to controls.

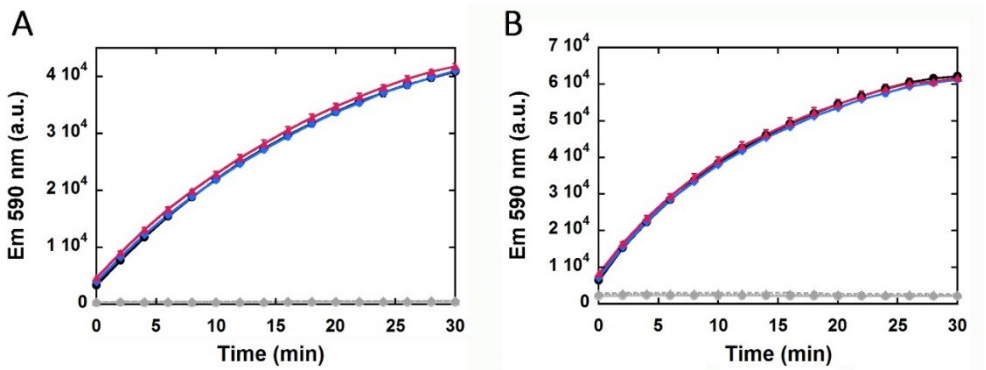

Fig. 8: Effect of nitrosylation and sulfhydration on hDASPO activity in the model cellular system. (A) U87 cells stably expressing the enzyme were treated with 50 µM NOR-3 (blue line), 50 µM NOC-7 (red line), or with an equal amount of DMSO (black line) for 2 hours. No significant variation in hDASPO activity was evident between the treatments and control samples. No activity was measured in U87 cells transfected with the empty vector and added with NOR-3 (dotted grey line), NOC-7 (dashed grey line) or DMSO (solid grey line). (B) The same cell clones were treated with 50 µM NaHS (blue line), 100 µM NaHS (red line), or with an equal amount of DMSO (black line) for 30 minutes. Control U87 cells were added with 50 µM NaHS (dotted grey line), 100 µM NaHS (dashed grey line) or DMSO (solid grey line). Also in this case no difference between controls and treatments was observed. The activity of the enzyme was determined by the Amplex UltraRed assay; data were expressed as fluorescence change at 590 nm over time. Data are the mean ± SD (n = 4).

Conclusions

The studies on post-translational modifications of human DASPO are still ongoing. The discussion of the results obtained so far are reported in the final conclusions of this thesis (paragraph 4).

In the future, I plan to evaluate whether other protein kinases can phosphorylate the enzyme *in vitro*. In addition, further analyses will be performed to verify whether longer incubation times or higher concentrations of nitric oxide donors could lead to changes in the enzymatic activity. Further cellular analyses will allow to assess whether other signals, such as high substrate concentration, can induce post-translational modifications and activity modulation on the ectopically expressed hDASPO.

References

Agrawal, G. K., and Thelen, J. J. (2009). A high-resolution two dimensional Gel- and Pro-Q DPS-based proteomics workflow for phosphoprotein identification and quantitative profiling. *Methods in Molecular Biology*, *527*, 3–19.

Blom, N., Gammeltoft, S., and Brunak, S. (1999). Sequence and structure-based prediction of eukaryotic protein phosphorylation sites. *Journal of molecular biology*, *294*(5), 1351–1362.

Cappelletti, P., Campomenosi, P., Pollegioni, L., and Sacchi, S. (2014). The degradation (by distinct pathways) of human D-amino acid oxidase and its interacting partner pLG72--two key proteins in D-serine catabolism in the brain. *The FEBS journal*, *281*(3), 708–723.

Ceroni, A., Passerini, A., Vullo, A., and Frasconi, P. (2006). DISULFIND: a disulfide bonding state and cysteine connectivity prediction server. *Nucleic acids research*, *34* (Web Server issue), W177–W181.

Fariselli, P., Riccobelli, P., and Casadio, R. (1999). Role of evolutionary information in predicting the disulfide-bonding state of cysteine in proteins. *Proteins*, *36*(3), 340–346.

Gonzalez, G. A., and Montminy, M. R. (1989). Cyclic AMP stimulates somatostatin gene transcription by phosphorylation of CREB at serine 133. *Cell*, *59*(4), 675–680.

Gould, N., Doulias, P. T., Tenopoulou, M., Raju, K., and Ischiropoulos, H. (2013). Regulation of protein function and signaling by reversible cysteine S-nitrosylation. *The Journal of biological chemistry*, *288*(37), 26473–26479.

Han, P., Zhou, X., Huang, B., Zhang, X., and Chen, C. (2008). On-gel fluorescent visualization and the site identification of S-nitrosylated proteins. *Analytical biochemistry*, *377*(2), 150–155.

Lee, T. Y., Chen, Y. J., Lu, T. C., Huang, H. D., and Chen, Y. J. (2011). SNOSite: exploiting maximal dependence decomposition to identify cysteine S-nitrosylation with substrate site specificity. *PloS one*, *6*(7), e21849.

Molla, G., Chaves-Sanjuan, A., Savinelli, A., Nardini, M., and Pollegioni, L. (2020). Structure and kinetic properties of human d-aspartate oxidase, the enzyme-controlling d-aspartate levels in brain. *FASEB journal*, *34*(1), 1182–1197.

Pollegioni, L., Campaner, S., Raibekas, A. A., and Pilone, M. S. (1997). Identification of a reactive cysteine in the flavin-binding domain of Rhodotorula gracilis D-amino acid oxidase. *Archives of biochemistry and biophysics*, *343*(1), 1–5.

Rosini, E., Caldinelli, L., and Piubelli, L. (2018). Assays of D-Amino Acid Oxidase Activity. *Frontiers in molecular biosciences*, *4*, 102.

Sacchi, S., Bernasconi, M., Martineau, M., Mothet, J. P., Ruzzene, M., Pilone, M. S., Pollegioni, L., and Molla, G. (2008). pLG72 modulates intracellular D-serine levels through its interaction with D-amino acid oxidase: effect on schizophrenia susceptibility. *The Journal of biological chemistry*, *283*(32), 22244–

22256.
Shoji, K., Mariotto, S., Ciampa, A. R., and Suzuki, H. (2006). Mutual regulation between serine and nitric oxide metabolism in human glioblastoma cells. *Neuroscience letters*, *394*(3), 163–167.
Wang, S., Circu, M. L., Zhou, H., Figeys, D., Aw, T. Y., and Feng, J. (2011). Highly sensitive detection of S-nitrosylated proteins by capillary gel electrophoresis with laser induced fluorescence. *Journal of chromatography. A*, *1218*(38), 6756–6762.
Wang, C., Xu, H., Lin, S., Deng, W., Zhou, J., Zhang, Y., Shi, Y., Peng, D., and Xue, Y. (2020). GPS 5.0: An Update on the Prediction of Kinase-specific Phosphorylation Sites in Proteins. *Genomics, proteomics and bioinformatics*, *18*(1), 72–80.
Xie, Y., Luo, X., Li, Y., Chen, L., Ma, W., Huang, J., Cui, J., Zhao, Y., Xue, Y., Zuo, Z., and Ren, J. (2018). DeepNitro: Prediction of Protein Nitration and Nitrosylation Sites by Deep Learning. *Genomics, proteomics and bioinformatics*, *16*(4), 294–306.
Xu, Y., Ding, J., Wu, L. Y., and Chou, K. C. (2013). iSNO-PseAAC: predict cysteine S-nitrosylation sites in proteins by incorporating position specific amino acid propensity into pseudo amino acid composition. *PloS one*, *8*(2), e55844.
Xu, Y., Shao, X. J., Wu, L. Y., Deng, N. Y., and Chou, K. C. (2013). iSNO-AAPair: incorporating amino acid pairwise coupling into PseAAC for predicting cysteine S-nitrosylation sites in proteins. *PeerJ*, *1*, e171.
Xue, Y., Liu, Z., Gao, X., Jin, C., Wen, L., Yao, X., and Ren, J. (2010). GPS-SNO: computational prediction of protein S-nitrosylation sites with a modified GPS algorithm. *PloS one*, *5*(6), e11290.

4. Conclusions

D-AAs had been long believed to be unnatural compounds not having a physiological role in mammals. However, in the 1990s, the discovery of unexpectedly high concentrations of free, endogenous D-Ser in mammalian brain opened a new avenue in D-AAs research field (Hashimoto et al., 1992). Indeed, other D-AAs, among which in particular D-Asp were detected in the same tissues (Hashimoto et al., 1993). In the following years, D-Ser and D-Asp have been discovered to bear fundamental roles in important physiological functions in mammals, and to be related to several pathological states (Ota et al., 2012; Sasabe et al., 2016; Genchi, 2017; Guercio and Panizzutti, 2018). In the CNS in particular, D-Ser modulates the activation of NMDAr by acting as the main co-agonist of the receptor, and is thus involved in pivotal brain functions such as memory, learning and behavior (Mothet et al., 2000; Panatier et al., 2006; Kakegawa et al., 2011; Filali and Lalonde, 2013). On the other hand, by acting as an alternative endogenous agonist of the receptor, D-Asp affects NMDAr-dependent processes: it is considered a signaling molecule involved in synaptic plasticity, establishing dendritic morphology, nervous system development and cognition (Errico et al., 2012; Punzo et al., 2016). Accordingly, it is not surprising that altered concentrations of both D-Ser and D-Asp have been reported in several pathologies and neurological disorders such as schizophrenia, bipolar disorder, and AD (Hashimoto et al., 2003; Hashimoto et al., 2005; Errico et al., 2015b; Madeira et al., 2015; Balu et al., 2019).

AD is a chronic and progressive neurodegenerative disease whose etiology appears to be complex and multifactorial. Its pathophysiology involves the accumulation of extracellular amyloid β (Aβ) plaques and the formation of hyperphosphorylated tau protein aggregates (neurofibrillary tangles) (Danysz and Parsons, 2012), but alterations in other processes relevant to neurotransmission have also been reported. Notably, several evidences indicate that, although NMDAr hypofunction is commonly observed in nonpathological brain aging (Billard, 2008), an excessive activation of the receptor may contribute to the pathological processes underlying this disease: the hyperstimulation of glutamate signaling causes excitotoxicity and leads to a gradual loss of synaptic functions, ultimately followed by neuronal cell death, which correlates with the

progressive decline in memory and cognition seen in AD patients (Danysz and Parsons, 2012; Wenk, 2006).

Given the role exerted by D-Ser and D-Asp on NMDAr functionality, several studies in the last 20 years aimed at investigating their levels in tissues and/or biological fluids of AD patients, to verify whether there is an actual correlation between their presence/concentration and the onset and/or the progression of the disease; nevertheless no consistent and conclusive results have been obtained (Nagata et al., 1995; D'Aniello et al., 1998; Fisher et al., 1998; Madeira et al., 2015). Several of these works present some issues: the limited number of subjects enrolled, the different analytical methods used (differing in detection sensitivity) and the absence of standardized protocols and appropriate controls. The issues affecting D-amino acids detection were recently discussed (Mothet et al., 2019).

For these reasons, the first part of this PhD project was aimed at clarifying whether the levels of these two D-AAs are deregulated in AD patients and exploring their potential as novel and precocious biomarkers for the diagnosis, through the analysis of patients' sera. Therefore, in collaboration with the Alzheimer's Assessment Unit at the Ospedale di Circolo, and Fondazione Macchi, ASST Settelaghi in Varese, we collected venus blood samples from 42 AD diagnosed individuals (at early stages of illness) and 26 age-matched healthy subjects (HS). The serum levels of Asp and Ser enantiomers were determined by HPLC using a standardized, sensitive, well-established analytical procedure based on pre-column derivatization and fluorescence detection. The analysis were performed following the guidelines reported in (Mothet et al., 2019) to avoid misinterpretation of experimental data: external controls and the selective enzymatic degradation of D-Asp and D-Ser peaks allowed their identification and accurate quantification. The obtained results were statistically evaluated and compared considering age, gender and the progression stage of the disease, assessed by the clinical dementia rating (CDR) scale which allows to evaluate the cognitive and functional performance of patients. In this case, only a minor and not statistically significant decrease in D-Asp levels was apparent between controls and AD patients, whereas a moderate but still not significant increase

in L-Asp levels (+25.3%) was observed in AD patients only. Notably, by analyzing data disaggregated by gender this increase was statistically significant in male. Consequently, in the AD male subjects the D-/total-Asp ratio appeared significantly decreased with respect to controls. Moreover, data disaggregated by the severity of the disease, as assessed by the CDR score, showed a positive (although not significant) correlation between L-Asp content and the stage of dementia, which resulted into an opposite trend in the D-/total-Asp ratio. On the contrary, significantly higher D-Ser serum levels (+21.8%) were detected in AD patients compared to HS and a significant positive correlation between D-Ser levels and age was observed in the AD cohort (and not in HS), despite a negative association previously reported (Calcia et al., 2012). Furthermore, both serum D-Ser level and D-/total-Ser ratio significantly increased with the progression of the disease.

This latter result is consistent with a recent clinical study reporting a positive correlation between D-Ser blood levels and a decline of cognitive processes in AD patients (Lin et al., 2019). Moreover, an increase in D-Ser levels was observed both in animal models of AD and in brain regions of AD patients involved in the disease progression (Madeira et al., 2015) and Aβ aggregates were reported to induce D-Ser release in cultured microglia (Wu et al., 2004). Based on these findings, it has been suggested that elevated D-Ser levels might represent a mechanism through which Aβ oligomers trigger synapse dysfunction and the resulting cognitive decline in AD (Madeira et al., 2015): D-Ser increase might represent an initial adaptive response to maintain proper neurotransmission in the early phases of the disease (Guercio and Panizzutti, 2018), but subsequently it causes NMDAr hyperactivation, thus contributing to excitotoxicity.

Our work contributes to strengthen the hypothesis of serum D-Ser levels and/or D-/total-Ser ratio as valuable and easily affordable biomarkers for AD, able to evaluate both the progression and the precocious stages of the disease, on its own or in combination with other AD biomarkers. Further studies, investigating an higher number of samples and eventually employing protocol of analysis improved in sensitivity (for D-Asp), are needed to understand whether D-Asp can also fulfill the same purpose.

Owing to its critical role in the mammalian brain, the molecular and cellular processes involved in D-Ser synthesis, transport, and degradation have been widely investigated (Pollegioni and Sacchi, 2010; Wolosker, 2011; Le Bail et al., 2015). In the central nervous system, the regulation of D-Ser levels is exerted by the PLP-dependent enzyme serine racemase (SR) and the FAD-containing enzyme D-amino acid oxidase (DAAO).

Conversely, despite the relevant role played by D-Asp in the development of endocrine functions and in neurotransmission, little is known about its metabolism in mammals including humans. Indeed, the synthetic pathway of this D-AA is still unclear and its levels are mainly regulated by the catabolic activity of D-aspartate oxidase (DASPO). Human DASPO and DAAO (hDASPO and hDAAO) are orthologue flavoproteins which share a high sequence identity and a similar tertiary structure, while greatly differ in their quaternary structure, cofactor binding affinity, kinetic properties and mechanisms (Molla et al., 2020). Thus, it has been suggested that they differently regulate D-Asp and D-Ser brain levels.

Differently from hDAAO, human *DDO* gene apparently produces alternative transcripts encoding for three putative isoforms of hDASPO, constituted by 341 (the "canonical" form), 369 and 282 amino acids. Interestingly, the 28 N-terminal residues longer hDASPO_369 appears highly conserved in primates, including humans (sequence identity > 95% by BLAST) and in 23 different species it is the only isoform reported or predicted; nonetheless, it has never been expressed or studied. On the other hand, hDASPO_282, lacking a large portion in the central region in the canonical isoform, is unique to human: the deletion was reported to largely affect the isoform solubility, likely due to incorrect folding (Setoyama and Miura, 1997).

For this reason, in the second part of my PhD program, I focused on hDASPO_341 and hDASPO_369: I investigated the ectopical expression of these two isoforms (fused to an N-terminal 3XFLAG-tag) in the U87 human glioblastoma cell line, previously used to express and study the regulation of hDAAO cellular levels and activity (Sacchi et al., 2008; Sacchi et al., 2011; Cappelletti et al., 2014).

I demonstrated that both hDASPO isoforms were expressed in the cellular system (even though the longer one at significantly lower levels). Intriguingly, the cells transfected

with the construct encoding for the FLAG-tagged hDASPO_369 also produced the untagged hDASPO_341 at similar levels, suggesting that the translation can occur from the alternative starting codon with a similar frequency. Both hDASPO isoforms were active and efficiently targeted to the peroxisomes.

Concerning the cellular processes involved in the degradation, both hDASPO isoforms were highly stable and likely characterized by a slow cellular turnover, similarly to the orthologous hDAAO (Cappelletti et al., 2014). An half-life of approximately 100 hours was estimated for both hDASPO isoforms, which is consistent with their peroxisomal localization.

Peroxisomes are thought to be mainly degraded by autophagy, with a process named pexophagy (Huybrechts et al., 2009). Accordingly, our group has previously demonstrated that hDAAO accumulated in U87 cells upon blocking the lysosome/endosome pathway (Cappelletti et al., 2014). On the contrary, under the same conditions the cellular levels of hDASPO_341 and hDASPO_369 were unaffected. Since peroxisomes constantly produce ROS (Fransen et al., 2012), they contain a highly sophisticated system to ensure protein quality: the peroxisomal matrix harbors several proteases (e.g., LONP2, IDE, and Tysnd1) that function as regulators of intra-peroxisomal proteostasis. In addition, excessive peroxisomal matrix proteins may be exported to the cytosol where they are degraded by cytosolic proteases or the proteasome (Nordgren et al., 2013). Apparently, this is the case for hDASPO isoforms: they both accumulated following MG132 treatment, indicating that their degradation occurs through the UPS.

Moreover, both *in vitro* and cellular studies revealed that hDASPO isoforms can be ubiquitinated. This post-translational modification could represent the cellular signal that triggers the targeting of hDASPO to the UPS and thus, that the modified flavoenzyme should be retrotraslocated to the cytoplasm for degradation. Worthy of note, several peroxisomal membrane receptors which are involved in the import apparatus (e.g., Pex5p, Pex7p, and Pex20p) can also be degraded by the UPS (Nordgren et al., 2013) and their targeting depends on the ubiquitination pattern:

when export is impaired, they are polyubiquitinated and extracted from the peroxisomal membrane for degradation by the UPS through a process named RADAR (Receptor

Accumulation and Degradation in the Absence of Recycling) (Léon et al., 2006). Since this quality control process is likely conserved in mammalian cells, it is tempting to speculate that it is involved in the regulation of hDASPO cellular levels too.
From these studies I concluded that the additional N-terminal sequence in the longer hDASPO isoform does not affect the enzyme functionality, subcellular localization as well as half-life and degradation pathway.

A recent publication reported a substantial decrease in D-Asp content in *post-mortem* brain samples of schizophrenic patients that was associated to a significant increase in hDASPO activity, with no variations in the levels of its encoding transcript (Nuzzo et al., 2017). These findings suggest that the interaction with effector molecules, inhibitors, regulatory proteins or other processes, such as post-translational modifications, might control the enzyme's activity during schizophrenia onset. To further deep inside the mechanisms that might modulate the functionality of hDASPO in physiological or pathological conditions, I decided to evaluate whether its activity is affected by S-nitrosylation, S-sulfhydration and phosphorylation.
S-nitrosylation is a reversible, non-enzymatic reaction wherein nitric oxide (NO) is covalently attached to a thiol group of a protein Cys residue to form an S-nitrosothiol. To date, about 1000 proteins have been demonstrated to undergo this secondary modification (Stamler and Hess, 2010). Noteworthy, it has been reported that in U87 cells nitrosylation regulates the activity of both SR and hDAAO (Shoji et al., 2006): NO was shown to inhibit SR while enhancing hDAAO activity, thus it was suggested to tightly control D-Ser cellular content. Due to the high sequence identity between hDAAO and hDASPO, I investigated whether this transient post-translational modification could also regulate the activity of hDASPO.
The analyses were performed only on the canonical hDASPO_341 isoform, since it is the only one currently available in a recombinant purified form. hDASPO_341 contains nine cysteines, of which four are highly conserved in all mammalian DASPOs and DAAOs. All these cysteines are likely present in the free reduced form, since no disulfide bond was identified by two different disulfide bonding state predictors with a very high confidence

value. Moreover, analysis of the solvent accessible surface on the protein structure showed that with the only exception of Cys182 which is deeply buried in the protein core, Cys residues are positioned relatively close to the protein surface, although the side chains of Cys141 and Cys144 are oriented towards the protein inner structure. Consistent with structural information, experimental data indicate that 4 Cys residues were easily accessible in the native hDASPO, thus potentially exposed to modifications, and that two additional residues appeared exposed in the apoprotein form of hDASPO. The analysis of hDASPO structure (Molla et al., 2020) revealed that two cysteine residues (Cys21 and Cys29) are close to two charged residues (Arg28 and Arg323) a feature that has been proposed to distinguish S-nitrosylation sites (Gould et al., 2013). Considering that these two Cys are within the Rossman fold (involved in flavin binding), their modification might deeply affect the enzyme's properties. However, despite *in vitro* experiments confirmed that recombinant hDASPO can be nitrosylated, activity assays suggested that the enzyme's properties are not affected by the modification. This result was also confirmed at the cellular level: no difference in the enzyme's activity was observed after U87 cells stably expressing hDASPO_341 were treated with different NO donors.

Hydrogen sulfide (H_2S) has recently emerged as an important gasotransmitter and signaling molecule (Paul and Snyder, 2015): the corresponding modification, i.e. sulfhydration, occurs on reactive Cys residues, like nitrosylation. Moreover, it has been reported that nitrosylation and sulfhydration might occur on the same Cys residues, often exerting opposite effects on the functionality of enzymes (Mustafa et al., 2009). Sulfhydration mechanism is still largely unknown and a prediction of putative modification sites is currently unfeasible. The effect of this secondary modification on hDASPO was investigated by incubating the recombinant enzyme with a sulfide precursor (NaHS). In this case, only barely detectable levels of S-sulfhydration were observed and the modified recombinant enzyme was partially inactivated (66% residual activity) although only at NaHS concentrations in the millimolar range (20 mM). Since in the brain H_2S physiological levels are reported in the nM range (Furne et al., 2008), it is not conceivable that this modification regulates the enzyme's activity at the cellular

level. Accordingly, our cellular studies confirmed the negligible effect of H_2S on ectopically expressed hDASPO. Further cellular analyses will allow to assess whether other signals, such as high substrate concentration, can induce post-translational modification and activity modulation.

Bioinformatic analyses performed with several computational tools on hDASPO primary structure assigned a high prediction score for phosphorylation to several residues; in particular, using DIPHOSPH 1.3, hDASPO appeared to be mainly subjected to phosphorylation by protein kinase A (PKA), protein kinase C (PKC), and other protein kinases involved in the cell cycle regulation (cdk5 and CKII). Our results showed that the recombinant enzyme was not modified *in vitro* by PKA.

Further analyses will be performed to evaluate whether other protein kinases could modify the recombinant enzyme.

In conclusion, these studies highlighted a main role of D-amino acids on relevant human physiological processes and pathological conditions. A significant correlation between serum D-Ser level and AD was apparent, further confirming its usefulness as a precocious biomarker for AD diagnosis. Concerning D-Asp, these studies shed light on the properties of two isoforms of human DASPO, as well as on the mechanisms involved in modulating their cellular level and activity. On this side, the definition of the mechanisms that regulate the cellular levels of D-Asp by acting on the catabolic enzyme hDASPO might allow the identification of new molecular targets for the treatment of pathologies in which the NMDAr mediated neurotransmission is likely to be affected.

5. Bibliography

Amery, L., Brees, C., Baes, M., Setoyama, C., Miura, R., Mannaerts, G. P., and Van Veldhoven, P. P. (1998). C-terminal tripeptide Ser-Asn-Leu (SNL) of human D-aspartate oxidase is a functional peroxisome-targeting signal. *Biochemical Journal*, 336(2), 367–371.

Ariyoshi, M., Katane, M., Hamase, K., Miyoshi, Y., Nakane, M., Hoshino, A., Okawa, Y., Mita, Y., Kaimoto, S., Uchihashi, M., Fukai, K., Ono, K., Tateishi, S., Hato, D., Yamanaka, R., Honda, S., Fushimura, Y., Iwai-Kanai, E., Ishihara, N., … Matoba, S. (2017). D-Glutamate is metabolized in the heart mitochondria. *Scientific Reports*, 7(August 2016), 1–9.

Armstrong, D. W., Gasper, M., Lee, S. H., Zukowski, J., and Ercal, N. (1993). D-amino acid levels in human physiological fluids. *Chirality*, 5(5), 375–378.

Balu, D.T. (2016). The NMDA receptor and schizophrenia: from pathophysiology to treatment. *Advances in pharmacology*, 76, 351–382.

Balu, D. T., Pantazopoulos, H., Huang, C. C. Y., Muszynski, K., Harvey, T. L., Uno, Y., Rorabaugh, J. M., Galloway, C. R., Botz-Zapp, C., Berretta, S., Weinshenker, D., and Coyle, J. T. (2019). Neurotoxic astrocytes express the D-serine synthesizing enzyme, serine racemase, in Alzheimer's disease. *Neurobiology of Disease*, 130(June), 104511.

Bastings, J. J. A. J., van Eijk, H. M., Damink, S. W. O., and Rensen, S. S. (2019). D-amino acids in health and disease: a focus on cancer. *Nutrients*, 11(9), 1–18.

Beard, M. E. (1990). D-Aspartate oxidation by rat and bovine renal peroxisomes: an electron microscopic cytochemical study. *Journal of Histochemistry and Cytochemistry*, 38(9), 1377–1381.

Billard, J. M. (2008). D-Serine signalling as a prominent determinant of neuronal-glial dialogue in the healthy and diseased brain. *Journal of Cellular and Molecular Medicine*, 12(5B), 1872–1884.

Blennow, K. (2017). A review of fluid biomarkers for Alzheimer's disease: moving from CSF to blood. *Neurology and Therapy*, 6(s1), 15–24.

Blennow, K., Hampel, H., Weiner, M., and Zetterberg, H. (2010). Cerebrospinal fluid and plasma biomarkers in Alzheimer disease. *Nature Reviews Neurology*, 6(3), 131–144.

Buerger, K., Ewers, M., Pirttilä, T., Zinkowski, R., Alafuzoff, I., Teipel, S. J., DeBernardis, J., Kerkman, D., McCulloch, C., Soininen, H., and Hampel, H. (2006). CSF phosphorylated tau protein correlates with neocortical neurofibrillary pathology in Alzheimer's disease. *Brain*, 129(11), 3035–3041.

Calcia, M. A., Madeira, C., Alheira, F. V., Silva, T. C. S., Tannos, F. M., Vargas-Lopes, C., Goldenstein, N., Brasil, M. A., Ferreira, S. T., and Panizzutti, R. (2012). Plasma levels of D-serine in Brazilian individuals with schizophrenia. *Schizophrenia Research*, 142(1–3), 83–87.

Caldinelli, L., Molla, G., Bracci, L., Lelli, B., Pileri, S., Cappelletti, P., Sacchi, S., and Pollegioni, L. (2010). Effect of ligand binding on human D-amino acid oxidase: Implications for the development of new drugs for schizophrenia treatment. *Protein Science*, 19(8), 1500–1512.

Cappelletti, P., Campomenosi, P., Pollegioni, L., and Sacchi, S. (2014). The degradation (by distinct pathways) of human D-amino acid oxidase and its interacting partner pLG72 - two key proteins in D-serine catabolism in the brain. *FEBS Journal*, 281(3), 708–723.

Carvajal, F. J., Mattison, H. A., and Cerpa, W. (2016). Role of NMDA receptor-mediated glutamatergic signaling in chronic and acute neuropathologies. *Neural Plasticity*, 2016.

Castañé, A., Santana, N., and Artigas, F. (2015). PCP-based mice models of schizophrenia: differential behavioral, neurochemical and cellular effects of acute and subchronic treatments. *Psychopharmacology*, 232(21–22), 4085–4097.

Cho, S. E., Na, K. S., Cho, S. J., and Kang, S. G. (2016). Low D-serine levels in schizophrenia: a systematic review and meta-analysis. *Neuroscience Letters*, 634, 42–51.

Coyle, J. T., and Tsai, G. (2004). The NMDA receptor glycine modulatory site: A therapeutic target for improving cognition and reducing negative symptoms in schizophrenia. *Psychopharmacology*, 174(1), 32–38.

Cristino, L., Luongo, L., Squillace, M., Paolone, G., Mango, D., Piccinin, S., Zianni, E., Imperatore, R., Iannotta, M., Longo, F., Errico, F., Vescovi, A. L., Morari, M., Maione, S., Gardoni, F., Nisticò, R., and Usiello, A. (2015). D-Aspartate oxidase influences glutamatergic system homeostasis in mammalian brain. *Neurobiology of Aging*, 36(5), 1890–1902.

Csapó, J., Albert, C., and Csapóné Kiss, Z. (2009). The D-amino acid content of foodstuffs (A Review). *Acta Univ Sapientiae, Aliment* 1, 5–30.

D'Aniello, A., D'Onofrio, G., Pischetola, M., D'Aniello, G., Vetere, A., Petrucelli, L., and Fisher, G. H. (1993). Biological role of D-amino acid oxidase and D-aspartate oxidase. Effects of D-amino acids. *Journal of Biological Chemistry*, 268(36), 26941–26949.

D'Aniello, A., Palescandolo, R., and Scardi, V. (1975). The distribution of the D-aspartate oxidase activity in cephalopoda. *Comparative Biochemistry and Physiology*, 50(1), 209–210.

D'Aniello, A. (2007). D-aspartic acid: an endogenous amino acid with an important neuroendocrine role. *Brain Research Reviews*, 53(2), 215–234.

D'Aniello, A., Di Cosmo, A., Di Cristo, C., Annunziato, L., Petrucelli, L., and Fisher, G. (1996). Involvement of D-aspartic acid in the synthesis of testosterone in rat testes. *Life Sciences*, 59(2), 97–104.

D'Aniello, A., Di Fiore, M. M., Fisher, G. H., Milone, A., Seleni, A., D'Aniello, S., Perna, A. F., and Ingrosso, D. (2000b). Occurrence of D-aspartic acid and N-methyl-D-aspartic acid in rat neuroendocrine tissues and their role in the modulation of luteinizing hormone and growth hormone release. *The FASEB Journal*, 14(5), 699–714.

D'Aniello, A., Lee, J. M., Petrucelli, L., and Di Fiore, M. M. (1998). Regional decreases of free D-aspartate levels in Alzheimer's disease. *Neuroscience Letters*, 250(2), 131–134.

D'Aniello, A., Luongo, L., Romano, R., Iannotta, M., Marabese, I., Boccella, S., Belardo, C., de Novellis, V., Arra, C., Barbieri, A., D'Aniello, B., Scandurra, A., Migliozzi, L., Fisher, G., Guida, F., and Maione, S. (2017). D-Aspartic acid ameliorates painful and neuropsychiatric changes and reduces β-amyloid Aβ1-42 peptide in a long lasting model of neuropathic pain. *Neuroscience Letters*, 651, 151–158.

D'Aniello, G., Tolino, A., D'Aniello, A., Errico, F., Fisher, G. H., and Di Fiore, M. M. (2000a). The role of D-aspartic acid and N-methyl-D-aspartic acid in the regulation of prolactin release. *Endocrinology*, 141(10), 3862–3870.

D'Aniello, S., Somorjai, I., Garcia-Fernàndez, J., Topo, E., and D'Aniello, A. (2011). D-Aspartic acid is a novel endogenous neurotransmitter. *The FASEB Journal*, 25(3), 1014–1027.

Danysz, W., and Parsons, C. G. (2012). Alzheimer's disease, β-amyloid, glutamate, NMDA receptors and memantine - Searching for the connections. *British Journal of Pharmacology*, 167(2), 324–352.

Daves, L. P., and Johnston, G. A. R. (1975). D-aspartate oxidase activity in extracts of mammalian central nervous tissue. *Journal of Neurochemistry*, 25(3), 299–304.

Davies, B. M., and Beech, H. R. (1960). The effect of 1-arylcylohexylamine (sernyl) on twelve normal volunteers. *The British Journal of Psychiatry*, 106, 912–924.

de Bartolomeis, A., Errico, F., Aceto, G., Tomasetti, C., Usiello, A., and Iasevoli, F. (2015). D-Aspartate dysregulation in Ddo-/- mice modulates phencyclidine-induced gene expression changes of postsynaptic density molecules in cortex and striatum. *Progress in Neuro-Psychopharmacology and Biological Psychiatry*, 62, 35–43.

de Souza, L. C., Chupin, M., Lamari, F., Jardel, C., Leclercq, D., Colliot, O., Lehéricy, S., Dubois, B., and Sarazin, M. (2012). CSF tau markers are correlated with hippocampal volume in Alzheimer's disease. *Neurobiology of Aging*, 33(7), 1253–1257.

Di Giorgi-Gerevini, V., Melchiorri, D., Battaglia, G., Ricci-Vitiani, L., Ciceroni, C., Busceti, C. L., Biagioni, F., Iacovelli, L., Canudas, A. M., Parati, E., De Maria, R., and Nicoletti, F. (2005). Endogenous activation of metabotropic glutamate receptors supports the proliferation and survival of neural progenitor cells. *Cell Death and Differentiation*, 12(8), 1124–1133.

Dunlop, D. S., Neidle, A., McHale, D., Dunlop, D. M., and Lajtha, A. (1986). The presence of free D-aspartic acid in rodents and man. *Biochemical and Biophysical Research Communications*, 141(1), 27–32.

Dym, O., and Eisenberg, D. (2001). Sequence-structure analysis of FAD-containing proteins. *Protein science*, 10(9):1712-1728.

Errico, F., D'Argenio, V., Sforazzini, F., Iasevoli, F., Squillace, M., Guerri, G., Napolitano, F., Angrisano, T., Di Maio, A., Keller, S., Vitucci, D., Galbusera, A., Chiariotti, L., Bertolino, A., De Bartolomeis, A., Salvatore, F., Gozzi, A., and Usiello, A. (2015b). A role for D-aspartate oxidase in schizophrenia and in schizophrenia-related symptoms induced by phencyclidine in mice. *Translational Psychiatry*, 5(2).

Errico, F., Nisticò, R., Di Giorgio, A., Squillace, M., Vitucci, D., Galbusera, A., Piccinin, S., Mango, D., Fazio, L., Middei, S., Trizio, S., Mercuri, N. B., Teule, M. A., Centonze, D., Gozzi, A., Blasi, G., Bertolino, A., and Usiello, A. (2014). Free D-aspartate regulates neuronal dendritic morphology, synaptic plasticity, gray matter volume and brain activity in mammals. *Translational Psychiatry*, 4(April).

Errico, F., Bonito-Oliva, A., Bagetta, V., Vitucci, D., Romano, R., Zianni, E., Napolitano, F., Marinucci, S., Di Luca, M., Calabresi, P., Fisone, G., Carta, M., Picconi, B., Gardoni, F., and Usiello, A. (2011c). Higher free D-aspartate and N-methyl-D-aspartate levels prevent striatal depotentiation and anticipate l-DOPA-induced dyskinesia. *Experimental Neurology*, 232(2), 240–250.

Errico, F., Mothet, J. P., and Usiello, A. (2015a). D-Aspartate: an endogenous NMDA receptor agonist enriched in the developing brain with potential involvement in schizophrenia. *Journal of Pharmaceutical and Biomedical Analysis*, 116, 7–17.

Errico, F., Napolitano, F., Nisticò, R., and Usiello, A. (2012). New insights on the role of free D-aspartate in the mammalian brain. *Amino Acids*, 43(5), 1861–1871.

Errico, F., Napolitano, F., Squillace, M., Vitucci, D., Blasi, G., de Bartolomeis, A., Bertolino, A., D'Aniello, A., and Usiello, A. (2013). Decreased levels of D-aspartate and NMDA in the prefrontal cortex and striatum of patients with schizophrenia. *Journal of Psychiatric Research*, 47(10), 1432–1437.

Errico, F., Nisticò, R., Napolitano, F., Mazzola, C., Astone, D., Pisapia, T., Giustizieri, M., D'Aniello, A., Mercuri, N. B., and Usiello, A. (2011b). Increased D-aspartate brain content rescues hippocampal age-related synaptic plasticity deterioration of mice. *Neurobiology of Aging*, 32(12), 2229–2243.

Errico, F., Nisticò, R., Napolitano, F., Oliva, A. B., Romano, R., Barbieri, F., Florio, T., Russo, C., Mercuri, N. B., and Usiello, A. (2011a). Persistent increase of D-aspartate in D-aspartate oxidase mutant mice induces a precocious hippocampal age-dependent synaptic plasticity and spatial memory decay. *Neurobiology of Aging*, 32(11), 2061–2074.

Errico, F., Nisticò, R., Palma, G., Federici, M., Affuso, A., Brilli, E., Topo, E., Centonze, D., Bernardi, G., Bozzi, Y., D'Aniello, A., Di Lauro, R., Mercuri, N. B., and Usiello, A. (2008a). Increased levels of D-aspartate in the hippocampus enhance LTP but do not facilitate cognitive flexibility. *Molecular and Cellular Neuroscience*, 37(2), 236–246.

Errico, F., Pirro, M. T., Affuso, A., Spinelli, P., De Felice, M., D'Aniello, A., and Di Lauro, R. (2006). A physiological mechanism to regulate D-aspartic acid and NMDA levels in mammals revealed by D-aspartate oxidase deficient mice. *Gene*, 374(1–2), 50–57.

Errico, F., Rossi, S., Napolitano, F., Catuogno, V., Topo, E., Fisone, G., D'Aniello, A., Centonze, D., and Usiello, A. (2008b). D-aspartate prevents corticostriatal long-term depression and attenuates schizophrenia-like symptoms induced by amphetamine and MK-801. *Journal of Neuroscience*, 28(41), 10404–10414.

Ewald, R. C., and Cline, H. T. (2008). NMDA receptors and brain development. *Biology of the NMDA Receptor*, 1–15.

Filali, M., and Lalonde, R. (2013). The effects of subchronic D-serine on left-right discrimination learning, social interaction, and exploratory activity in APPswe/PS1 mice. *European Journal of Pharmacology*, 701(1–3), 152–158.

Fisher, G. H., D'Aniello, A., Vetere, A., Padula, L., Cusano, G. P., and Man, E. H. (1991). Free D-aspartate and D-alanine in normal and Alzheimer brain. *Brain Research Bulletin*, 26(6), 983–985.

Fisher, G. H., Petrucelli, L., Gardner, C., Emory, C., Frey, W. H., Amaducci, L., Sorbi, S., Sorrentino, G., Borghi, M., and D'aniello, A. (1994). Free D-amino acids in human cerebrospinal fluid of alzheimer disease, multiple sclerosis, and healthy control subjects. *Molecular and Chemical Neuropathology*, 23(2–3), 115–124.

Fisher, G., Lorenzo, N., Abe, H., Fujita, E., Frey, W. H., Emory, C., Di Fiore, M. M., and D'Aniello, A. (1998). Free D- and L-amino acids in ventricular cerebrospinal fluid from Alzheimer and normal subjects. *Amino Acids*, 15(3), 263–269.

Fraaije, M. W., and Mattevi, A. (2000). Flavoenzymes: Diverse catalysts with recurrent features. *Trends in Biochemical Sciences*, 25(3), 126–132.

Fransen, M., Nordgren, M., Wang, B., and Apanasets, O. (2012). Role of peroxisomes in ROS/RNS-metabolism: Implications for human disease. *Biochimica et Biophysica Acta - Molecular Basis of Disease*, 1822(9), 1363–1373.

Friedman, M. (2010). Origin, microbiology, nutrition, and pharmacology of D-amino acids. *Chemistry and Biodiversity*, 7(6), 1491–1530.

Fuchs, S. A., Berger, R., Klomp, L. W. J., and De Koning, T. J. (2005). D-Amino acids in the central nervous system in health and disease. *Molecular Genetics and Metabolism*, 85(3), 168–180.

Furne, J., Saeed, A., and Levitt, M. D. (2008). Whole tissue hydrogen sulfide concentrations are orders of magnitude lower than presently accepted values. *American Journal of Physiology*, 295(5), 1479–1485.

Genchi, G. (2017). An overview on D-amino acids. *Amino Acids*, 49(9), 1521–1533.
Ghasemi, M., Phillips, C., Trillo, L., De Miguel, Z., Das, D., and Salehi, A. (2014). The role of NMDA receptors in the pathophysiology and treatment of mood disorders. *Neuroscience and Biobehavioral Reviews*, 47, 336–358.
Goff, D. C., and Coyle, J. T. (2001). The Emerging Role of Glutamate in the Pathophysiology and Treatment of Schizophrenia Donald. *The American Journal of Psychiatry*, 158(9), 1367–1377.
Gould, N., Doulias, P. T., Tenopoulou, M., Raju, K., and Ischiropoulos, H. (2013). Regulation of protein function and signaling by reversible cysteine s-nitrosylation. *Journal of Biological Chemistry*, 288(37), 26473–26479.
Guercio, G. D., and Panizzutti, R. (2018). Potential and challenges for the clinical use of D-serine as a cognitive enhancer. *Frontiers in Psychiatry*, 9(FEB), 1–10.
Hamase, K., Homma, H., Takigawa, Y., Fukushima, T., Santa, T., and Imai, K. (1997). Regional distribution and postnatal changes of D-amino acids in rat brain. *Biochimica et Biophysica Acta*, 1334(2–3), 214–222.
Han, H., Miyoshi, Y., Koga, R., Mita, M., Konno, R., and Hamase, K. (2015). Changes in D-aspartic acid and D-glutamic acid levels in the tissues and physiological fluids of mice with various D-aspartate oxidase activities. *Journal of Pharmaceutical and Biomedical Analysis*, 116, 47–52.
Hansen, K. B., Yi, F., Perszyk, R. E., Menniti, F. S., and Traynelis, S. F. (2017). NMDA receptors in the central nervous system. *In Methods in Molecular Biology: NMDA receptors* (Vol. 1677).
Hardingham, G. E., and Bading, H. (2003). The Yin and Yang of NMDA receptor signalling. *Trends in Neurosciences*, 26(2), 81–89.
Hashimoto, A., Kumashiro, S., Nishikawa, T., Oka, T., Takahashi, K., Mito, T., Takashima, S., Doi, N., Mizutani, Y., Yamazaki, T., Kaneko, T., and Ootomo, E. (1993). Embryonic development and postnatal changes in free D-aspartate and D-serine in the human prefrontal cortex. *Journal of Neurochemistry*, 61(1), 348–351.
Hashimoto, A., Nishikawa, T., Hayashi, T., Fujii, N., Harada, K., Oka, T., and Takahashi, K. (1992). The presence of free D-serine in rat brain. *FEBS Letters*, 296(1), 33–36.
Hashimoto, A., and Oka, T. (1997). Free D-aspartate and D-serine in the mammalian brain and periphery. *Progress in Neurobiology*, 52(4), 325–353.
Hashimoto, K., Engberg, G., Shimizu, E., Nordin, C., Lindström, L. H., and Iyo, M. (2005). Reduced D-serine to total serine ratio in the cerebrospinal fluid of drug naive schizophrenic patients. *Progress in Neuro-Psychopharmacology and Biological Psychiatry*, 29(5), 767–769.
Hashimoto, K., Fukushima, T., Shimizu, E., Komatsu, N., Watanabe, H., Shinoda, N., Nakazato, M., Kumakiri, C., Okada, S., Hasegawa, H., Imai, K., and Iyo, M. (2003). Decreased Serum Levels of D-Serine in Patients With Schizophrenia. *Archives of General Psychiatry*, 60(6), 572–576.
Holm, L., and Rosenström, P. (2010). Dali server: Conservation mapping in 3D. *Nucleic Acids Research*, 38(SUPPL. 2), 545–549.
Hu, W., MacDonald, M. L., Elswick, D. E., and Sweet, R. A. (2015). The glutamate hypothesis of schizophrenia: evidence from human brain tissue studies. *Annals of the New York Academy of Sciences*, 1338(1), 38–57.
Huang, A. S., Beigneux, A., Weil, Z. M., Kim, P. M., Molliver, M. E., Blackshaw, S., Nelson, R. J., Young, S. G., and Snyder, S. H. (2006). D-Aspartate regulates melanocortin formation and function: Behavioral alterations in D-aspartate oxidase-deficient mice. *Journal of Neuroscience*, 26(10), 2814–2819.
Huybrechts, S. J., Van Veldhoven, P. P., Brees, C., Mannaerts, G. P., Los, G. V., and Fransen, M. (2009). Peroxisome dynamics in cultured mammalian cells. *Traffic*, 10(11), 1722–1733.
Ikonomidou, C. (2009). Triggers of apoptosis in the immature brain. *Brain and Development*, 31(7), 488–492.
Jansson, L. C., and Åkerman, K. E. (2014). The role of glutamate and its receptors in the proliferation, migration, differentiation and survival of neural progenitor cells. *Journal of Neural Transmission*, 121(8), 819–836.
Javitt, D. C., Zukin, S. R., Heresco-Levy, U., and Umbricht, D. (2012). Has an angel shown the way? Etiological and therapeutic implications of the PCP/NMDA model of schizophrenia. *Schizophrenia Bulletin*, 38(5), 958–966.
Kakegawa, W., Miyoshi, Y., Hamase, K., Matsuda, S., Matsuda, K., Kohda, K., Emi, K., Motohashi, J., Konno, R., Zaitsu, K., and Yuzaki, M. (2011). D-Serine regulates cerebellar LTD and motor coordination through the δ glutamate receptor. *Nature Neuroscience*, 14(5), 603–613.

Katane, M., Furuchi, T., Sekine, M., and Homma, H. (2007). Molecular cloning of a cDNA encoding mouse D-aspartate oxidase and functional characterization of its recombinant proteins by site-directed mutagenesis. *Amino Acids*, 32(1), 69–78.

Katane, M., and Homma, H. (2010). D-aspartate oxidase: The sole catabolic enzyme acting on free D-aspartate in mammals. *Chemistry and Biodiversity*, 7(6), 1435–1449.

Katane, M., Kanazawa, R., Kobayashi, R., Oishi, M., Nakayama, K., Saitoh, Y., Miyamoto, T., Sekine, M., and Homma, H. (2017). Structure–function relationships in human D-aspartate oxidase: characterisation of variants corresponding to known single nucleotide polymorphisms. *Biochimica et Biophysica Acta - Proteins and Proteomics*, 1865(9), 1129–1140.

Katane, M., Kawata, T., Nakayama, K., Saitoh, Y., Kaneko, Y., Matsuda, S., Saitoh, Y., Miyamoto, T., Sekine, M., and Homma, H. (2015a). Characterization of the enzymatic and structural properties of human D-aspartate oxidase and comparison with those of the rat and mouse enzymes. *Biological and Pharmaceutical Bulletin*, 38(2), 298–305.

Katane, M., Kuwabara, H., Nakayama, K., Saitoh, Y., Miyamoto, T., Sekine, M., and Homma, H. (2018). Rat D-aspartate oxidase is more similar to the human enzyme than the mouse enzyme. *Biochimica et Biophysica Acta - Proteins and Proteomics*, 1866(7), 806–812.

Katane, M., Saitoh, Y., Hanai, T., Sekine, M., Furuchi, T., Koyama, N., Nakagome, I., Tomoda, H., Hirono, S., and Homma, H. (2010a). Thiolactomycin inhibits D-aspartate oxidase: a novel approach to probing the active site environment. *Biochimie*, 92(10), 1371–1378.

Katane, M., Saitoh, Y., Maeda, K., Hanai, T., Sekine, M., Furuchi, T., and Homma, H. (2011). Role of the active site residues arginine-216 and arginine-237 in the substrate specificity of mammalian D-aspartate oxidase. *Amino Acids*, 40(2), 467–476.

Katane, M., Saitoh, Y., Seida, Y., Sekine, M., Furuchi, T., and Homma, H. (2010b). Comparative characterization of three D-aspartate oxidases and one D-amino acid oxidase from Caenorhabditis elegans. *Chemistry and Biodiversity*, 7(6), 1424–1434.

Katane, M., Yamada, S., Kawaguchi, G., Chinen, M., Matsumura, M., Ando, T., Doi, I., Nakayama, K., Kaneko, Y., Matsuda, S., Saitoh, Y., Miyamoto, T., Sekine, M., Yamaotsu, N., Hirono, S., and Homma, H. (2015b). Identification of novel D-aspartate oxidase inhibitors by in silico screening and their functional and structural characterization in vitro. *Journal of Medicinal Chemistry*, 58(18), 7328–7340.

Katsuki, H., Nonaka, M., Shirakawa, H., Kume, T., and Akaike, A. (2004). Endogenous D-serine is involved in induction of neuronal death by N-methyl-D-aspartate and simulated ischemia in rat cerebrocortical slices. *Journal of Pharmacology and Experimental Therapeutics*, 311(2), 836–844.

Kawazoe, T., Tsuge, H., Pilone, M. S., and Fukui, K. (2006). Crystal structure of human D-amino acid oxidase: Context-dependent variability of the backbone conformation of the VAAGL hydrophobic stretch located at the si -face of the flavin ring . *Protein Science*, 15(12), 2708–2717.

Kera, Y., Aoyama, H., Watanabe, N., and Yamada, R. H. (1996). Distribution of D-aspartate oxidase and free D-glutamate and D-aspartate in chicken and pigeon tissues. *Comparative Biochemistry and Physiology*, 115(1), 121–126.

Kera, Y., Nagasaki, H., Iwashima, A., and Yamada, R.-H. (1992). Presence of D-aspartate oxidase and free D-aspartate in amphibian (Xenopus leavis, Cynops pyrrhogaster) tissues. *Comparative Biochemistry and Physiology*, 345–348.

Kera, Y., Nagasaki, H., Iwashima, A., and Yamada, R.-H. (1993). Gender dependence of D-aspartate oxidase activity in rat tissues. *Comp. Biochem. Physiol.*, 104(4), 739–742.

Khoury, R., and Ghossoub, E. (2019). Diagnostic biomarkers of Alzheimer's disease: A state-of-the-art review. *Biomarkers in Neuropsychiatry*, 1(November), 100005.

Kim, P. M., Duan, X., Huang, A. S., Liu, C. Y., Ming, G. L., Song, H., and Snyder, S. H. (2010). Aspartate racemase, generating neuronal D-aspartate, regulates adult neurogenesis. *Proceedings of the National Academy of Sciences of the United States of America*, 107(7), 3175–3179.

Kimura, T., Hamase, K., Miyoshi, Y., Yamamoto, R., Yasuda, K., Mita, M., Rakugi, H., Hayashi, T., and Isaka, Y. (2016). Chiral amino acid metabolomics for novel biomarker screening in the prognosis of chronic kidney disease. *Scientific Reports*, 6(May), 1–7.

Klatte, K., Kirschstein, T., Otte, D., Pothmann, L., Müller, L., Tokay, T., Kober, M., Uebachs, M., Zimmer, A., and Beck, H. (2013). Impaired D-Serine-Mediated cotransmission mediates cognitive dysfunction in epilepsy. *Journal of Neuroscience*, 33(32), 13066–13080.

Kocahan, S., and Doğan, Z. (2017). Mechanisms of Alzheimer's disease pathogenesis and prevention: The brain, neural pathology, N-methyl-D-Aspartate receptors, tau protein and other risk factors. *Clinical Psychopharmacology and Neuroscience*, 15(1), 1–8.

Krebs, H. A. (1935). Metabolism of amino-acids: deamination of amino-acids. *Biochemistry Journal*, 29(7), 1620-1644.

Le Bail, M., Martineau, M., Sacchi, S., Yatsenko, N., Radzishevsky, I., Conrod, S., Ouares, K. A., Wolosker, H., Pollegioni, L., Billard, J. M., Mothet, J. P., and Snyder, S. H. (2015). Identity of the NMDA receptor coagonist is synapse specific and developmentally regulated in the hippocampus. *Proceedings of the National Academy of Sciences of the United States of America*, 112(2), E204–E213.

Léon, S., Zhang, L., McDonald, W. H., Yates, J., Cregg, J. M., and Subramani, S. (2006). Dynamics of the peroxisomal import cycle of PpPex20p: Ubiquitin-dependent localization and regulation. *Journal of Cell Biology*, 172(1), 67–78.

Liddelow, S. A., Guttenplan, K. A., Clarke, L. E., Bennett, F. C., Bohlen, C. J., Schirmer, L., Bennett, M. L., Münch, A. E., Chung, W. S., Peterson, T. C., Wilton, D. K., Frouin, A., Napier, B. A., Panicker, N., Kumar, M., Buckwalter, M. S., Rowitch, D. H., Dawson, V. L., Dawson, T. M., … Barres, B. A. (2017). Neurotoxic reactive astrocytes are induced by activated microglia. *Nature*, 541(7638), 481–487.

Lin, C. H., Yang, H. T., and Lane, H. Y. (2019). D-glutamate, D-serine, and D-alanine differ in their roles in cognitive decline in patients with Alzheimer's disease or mild cognitive impairment. *Pharmacology Biochemistry and Behavior*, 185(2), 172760.

Liu, J., Chang, L., Song, Y., Li, H., and Wu, Y. (2019). The role of NMDA receptors in Alzheimer's disease. *Frontiers in Neuroscience*, 13(FEB), 1–22.

Madeira, C., Lourenco, M. V., Vargas-Lopes, C., Suemoto, C. K., Brandão, C. O., Reis, T., Leite, R. E. P., Laks, J., Jacob-Filho, W., Pasqualucci, C. A., Grinberg, L. T., Ferreira, S. T., and Panizzutti, R. (2015). D-serine levels in Alzheimer's disease: Implications for novel biomarker development. *Translational Psychiatry*, 5(August 2014).

Marcone, G. L., Rosini, E., Crespi, E., and Pollegioni, L. (2020). D-Amino acids in foods. *Applied Microbiology and Biotechnology*, 104(2), 555–574.

Matsuda, S., Katane, M., Maeda, K., Kaneko, Y., Saitoh, Y., Miyamoto, T., Sekine, M., and Homma, H. (2015). Biosynthesis of D-aspartate in mammals: The rat and human homologs of mouse aspartate racemase are not responsible for the biosynthesis of D-aspartate. *Amino Acids*, 47(5), 975–985.

Molinaro, G., Pietracupa, S., Di Menna, L., Pescatori, L., Usiello, A., Battaglia, G., Nicoletti, F., and Bruno, V. (2010). D-Aspartate activates mGlu receptors coupled to polyphosphoinositide hydrolysis in neonate rat brain slices. *Neuroscience Letters*, 478(3), 128–130.

Molla, G., Chaves-Sanjuan, A., Savinelli, A., Nardini, M., and Pollegioni, L. (2020). Structure and kinetic properties of human D-aspartate oxidase, the enzyme-controlling D-aspartate levels in brain. *FASEB J.*, 34(1), 1182–1197.

Molla, G., Sacchi, S., Bernasconi, M., Pilone, M. S., Fukui, K., and Pollegioni, L. (2006). Characterization of human D-amino acid oxidase. *FEBS Letters*, 580(9), 2358–2364.

Mothet, J.-P., Billard, J.-M., Pollegioni, L., Coyle, J. T., and Sweedler, J. V. (2019). Investigating brain D-serine: advocacy for good practices Jean-Pierre. *Acta Physiologica (Oxford, England)*, 226(1), e13257.

Mothet, J. P., Rouaud, E., Sinet, P. M., Potier, B., Jouvenceau, A., Dutar, P., Videau, C., Epelbaum, J., and Billard, J. M. (2006). A critical role for the glial-derived neuromodulator D-serine in the age-related deficits of cellular mechanisms of learning and memory. *Aging Cell*, 5(3), 267–274.

Mothet, J. P., Parent, A. T., Wolosker, H., Brady, R. O., Linden, D. J., Ferris, C. D., Rogawski, M. A., and Snyder, S. H. (2000). D-serine is an endogenous ligand for the glycine site of the N-methyl-D-aspartate receptor. *Proceedings of the National Academy of Sciences of the United States of America*, 97(9), 4926–4931.

Murtas, G., Sacchi, S., Valentino, M., and Pollegioni, L. (2017). Biochemical properties of human D-amino acid oxidase. *Frontiers in Molecular Biosciences*, 4(DEC), 1–11.

Mustafa, A. K., Gadalla, M. M., Sen, N., Kim, S., Mu, W., Gazi, S. K., Barrow, R. K., Yang, G., Wang, R., and Snyder, S. H. (2009). H_2S Signals Through Protein S-Sulfhydration. *Science Signaling*, 2(96), ra72.

Nagata, Y., Borghi, M., Fisher, G. H., and D'Aniello, A. (1995). Free D-serine concentration in normal and Alzheimer human brain. *Brain Research Bulletin*, 38(2), 181–183.

Nagata, Y., Horiike, K., and Maeda, T. (1994). Distribution of free D-serine in vertebrate brains. *Brain Research*, 634(2), 291–295.

Negri, A., Ceciliani, F., Tedeschi, G., Simonic, T., and Ronchi, S. (1992). The primary structure of the flavoprotein D-aspartate oxidase from beef kidney. *Journal of Biological Chemistry*, 267(17), 11865–11871.

Negri, A., Massey, V., Williams, C. H., and Schopfer, L. M. (1988). The kinetic mechanism of beef kidney D-aspartate oxidase. *Journal of Biological Chemistry*, 263(27), 13557–13563.

Negri, A., Masseyg, V., and Williams, C. H. (1987). D-Aspartate Oxidase from Beef Kidney. Purification and properties. *The Journal of Biological Chemistry*, 262(21), 10026–10034.

Negri, A., Tedeschi, G., Ceciliani, F., and Ronchi, S. (1999). Purification of beef kidney D-aspartate oxidase overexpressed in Escherichia coli and characterization of its redox potentials and oxidative activity towards agonists and antagonists of excitatory amino acid receptors. *Biochimica et Biophysica Acta - Protein Structure and Molecular Enzymology*, 1431(1), 212–222.

Nordgren, M., Wang, B., Apanasets, O., and Fransen, M. (2013). Peroxisome degradation in mammals: Mechanisms of action, recent advances, and perspectives. *Frontiers in Physiology*, 4 JUN(June), 1–12.

Nuzzo, T., Feligioni, M., Cristino, L., Pagano, I., Marcelli, S., Iannuzzi, F., Imperatore, R., D'Angelo, L., Petrella, C., Carella, M., Pollegioni, L., Sacchi, S., Punzo, D., De Girolamo, P., Errico, F., Canu, N., and Usiello, A. (2019). Free D-aspartate triggers NMDA receptor-dependent cell death in primary cortical neurons and perturbs JNK activation, Tau phosphorylation, and protein SUMOylation in the cerebral cortex of mice lacking D-aspartate oxidase activity. *Experimental Neurology*, 317(February), 51–65.

Nuzzo, T., Sacchi, S., Errico, F., Keller, S., Palumbo, O., Florio, E., Punzo, D., Napolitano, F., Copetti, M., Carella, M., Chiariotti, L., Bertolino, A., Pollegioni, L., and Usiello, A. (2017). Decreased free D-aspartate levels are linked to enhanced D-aspartate oxidase activity in the dorsolateral prefrontal cortex of schizophrenia patients. *Npj Schizophrenia*, 3(1), 1–10.

Ohide, H., Miyoshi, Y., Maruyama, R., Hamase, K., and Konno, R. (2011). D-Amino acid metabolism in mammals: Biosynthesis, degradation and analytical aspects of the metabolic study. *Journal of Chromatography B: Analytical Technologies in the Biomedical and Life Sciences*, 879(29), 3162–3168.

Oldendorf, W. H. (1973). Stereospecificity of blood-brain barrier permeability to amino acids. *American Journal of Physiology*, 224(4), 967–969.

Ota, N., Shi, T., and Sweedler, J. V. (2012). D-aspartate acts as a signaling molecule in nervous and neuroendocrine systems. *Amino Acids*, 43(5), 1873–1886.

Owen, M. J., O'Donovan, M. C., Thapar, A., and Craddock, N. (2011). Neurodevelopmental hypothesis of schizophrenia. *British Journal of Psychiatry*, 198(3), 173–175.

Panatier, A., Theodosis, D. T., Mothet, J. P., Touquet, B., Pollegioni, L., Poulain, D. A., and Oliet, S. H. R. (2006). Glia-Derived D-Serine Controls NMDA Receptor Activity and Synaptic Memory. *Cell*, 125(4), 775–784.

Parveen, Z., Large, A., Grewal, N., Lata, N., Cancio, I., Cajaraville, M. P., Perry, C. J., and Connock, M. J. (2001). D-aspartate oxidase and D-amino acid oxidase are localised in the peroxisomes of terrestrial gastropods. *European Journal of Cell Biology*, 80(10), 651–660.

Paul, B. D., and Snyder, S. H. (2015). Protein sulfhydration. *In Methods in Enzymology* (1st ed., Vol. 555). Elsevier Inc.

Pilone, M. S. (2000). D-amino acid oxidase: new findings. *Cellular and Molecular Life Sciences*, 57(12), 1732–1747.

Pollegioni, L., Piubelli, L., Sacchi, S., Pilone, M. S., and Molla, G. (2007). Physiological functions of D-amino acid oxidases: From yeast to humans. *Cellular and Molecular Life Sciences*, 64(11), 1373–1394.

Pollegioni, L., Diederichs, K., Molla, G., Umhau, S., Welte, W., Ghisla, S., and Pilone, M. S. (2002). Yeast D-amino acid oxidase: Structural basis of its catalytic properties. *Journal of Molecular Biology*, 324(3), 535–546.

Pollegioni, L., and Sacchi, S. (2010). Metabolism of the neuromodulator D-serine. *Cellular and Molecular Life Sciences*, 67(14), 2387–2404.

Pollegioni, L., Sacchi, S., and Murtas, G. (2018). Human D-amino acid oxidase: Structure, function, and regulation. *Frontiers in Molecular Biosciences*, 5(NOV), 1–14.

Powell, J. T., Vine, N., and Crossman, M. (1992). On the accumulation of D-aspartate in elastin and other proteins of the ageing aorta. *Atherosclerosis*, 97(2–3), 201–208.

Puggioni, V., Savinelli, A., Miceli, M., Molla, G., Pollegioni, L., and Sacchi, S. (2020). Biochemical characterization of mouse D-aspartate oxidase. *Biochimica et Biophysica Acta (BBA) - Proteins and Proteomics*, 1868(10), 140472.

Punzo, D., Errico, F., Cristino, L., Sacchi, S., Keller, S., Belardo, C., Luongo, L., Nuzzo, T., Imperatore, R., Florio, E., De Novellis, V., Affinito, O., Migliarini, S., Maddaloni, G., Sisalli, M. J., Pasqualetti, M., Pollegioni, L., Maione, S., Chiariotti, L., and Usiello, A. (2016). Age-related changes in D-aspartate oxidase promoter methylation control extracellular D-aspartate levels and prevent precocious cell death during brain aging. *Journal of Neuroscience*, 36(10), 3064–3078.

Riedel, G., Platt, B., and Micheau, J. (2003). Glutamate receptor function in learning and memory. *Behavioural Brain Research*, 140(1–2), 1–47.

Sacchi, S., Bernasconi, M., Martineau, M., Mothet, J. P., Ruzzene, M., Pilone, M. S., Pollegioni, L., and Molla, G. (2008). pLG72 modulates intracellular D-serine levels through its interaction with D-amino acid oxidase: Effect on schizophrenia susceptibility. *Journal of Biological Chemistry*, 283(32), 22244–22256.

Sacchi, S., Caldinelli, L., Cappelletti, P., Pollegioni, L., and Molla, G. (2012). Structure-function relationships in human D-amino acid oxidase. *Amino Acids*, 43(5), 1833–1850.

Sacchi, S., Cappelletti, P., Giovannardi, S., and Pollegioni, L. (2011). Evidence for the interaction of D-amino acid oxidase with pLG72 in a glial cell line. *Molecular and Cellular Neuroscience*, 48(1), 20–28.

Sacchi, S., Novellis, V. De, Paolone, G., Nuzzo, T., Iannotta, M., Belardo, C., Squillace, M., Bolognesi, P., Rosini, E., Motta, Z., Frassineti, M., Bertolino, A., Pollegioni, L., Morari, M., Maione, S., Errico, F., and Usiello, A. (2017). Olanzapine, but not clozapine, increases glutamate release in the prefrontal cortex of freely moving mice by inhibiting D-aspartate oxidase activity. *Scientific Reports*, 7(April 2016), 1–13.

Saitoh, Y., Katane, M., Miyamoto, T., Sekine, M., Sakamoto, T., Imai, H., and Homma, H. (2019). Secreted D-aspartate oxidase functions in C. elegans reproduction and development. *FEBS Journal*, 286(1), 124–138.

Sarower, M. G., Matsui, T., and Abe, H. (2003). Distribution and Characteristics of D-Amino Acid and D-Aspartate Oxidases in Fish Tissues. *Journal of Experimental Zoology Part A: Comparative Experimental Biology*, 295(2), 151–159.

Sasabe, J., Chiba, T., Yamada, M., Okamoto, K., Nishimoto, I., Matsuoka, M., and Aiso, S. (2007). D-Serine is a key determinant of glutamate toxicity in amyotrophic lateral sclerosis. *EMBO Journal*, 26(18), 4149–4159.

Sasabe, J., Miyoshi, Y., Rakoff-Nahoum, S., Zhang, T., Mita, M., Davis, B. M., Hamase, K., and Waldor, M. K. (2016). Interplay between microbial D-amino acids and host D-amino acid oxidase modifies murine mucosal defense and gut microbiota. *Nature Microbiology*, 1(10), 16125.

Sasabe, J., and Suzuki, M. (2019). Distinctive roles of D-Amino acids in the homochiral world: Chirality of amino acids modulates mammalian physiology and pathology. *The Keio Journal of Medicine*, 68(1), 1–16.

Schell, M. J., Cooper, O. B., and Snyder, S. H. (1997). D -aspartate localizations imply neuronal and neuroendocrine roles. *Proceedings of the National Academy of Sciences of the United States of America*, 94(March), 2013–2018.

Schell, M. J., Molliver, M. E., and Snyder, S. H. (1995). D-serine, an endogenous synaptic modulator: Localization to astrocytes and glutamate-stimulated release. *Proceedings of the National Academy of Sciences of the United States of America*, 92(9), 3948–3952.

Serrano-Pozo, A., Frosch, M. P., Masliah, E., and Hyman, B. T. (2011). Neuropathological alterations in Alzheimer disease. *Cold Spring Harbor Perspectives in Medicine*, 1(1), a006189.

Setoyama, C., and Miura, R. (1997). Structural and functional characterization of the human brain D-aspartate oxidase. *Journal of Biochemistry*, 121, 798–803.

Shleper, M., Kartvelishvily, E., and Wolosker, H. (2005). D-serine is the dominant endogenous coagonist for NMDA receptor neurotoxicity in organotypic hippocampal slices. *Journal of Neuroscience*, 25(41), 9413–9417.

Shoji, K., Mariotto, S., Ciampa, A. R., and Suzuki, H. (2006). Mutual regulation between serine and nitric oxide metabolism in human glioblastoma cells. *Neuroscience Letters*, 394(3), 163–167.

Stamler, J. S., and Hess, D. T. (2010). Nascent nitrosylases. *Nature Cell Biology*, 12(11), 1024–1026.

Still, J. L., Buell, M. V., Knox, W. E., and Green, D. E. (1949). Studies on the cyclophorase system: D-aspartic oxidase. *The Journal of Biological Chemistry*, 179(2), 831–837.

Takahashi, S., Takahashi, T., Kera, Y., Matsunaga, R., Shibuya, H., and Yamada, R. H. (2004). Cloning and expression in Escherichia coli of the D-aspartate oxidase gene from the yeast Cryptococcus humicola and characterization of the recombinant enzyme. *Journal of Biochemistry*, 135(4), 533–540.

Tanaka-Hayashi, A., Hayashi, S., Inoue, R., Ito, T., Konno, K., Yoshida, T., Watanabe, M., Yoshimura, T., and Mori, H. (2015). Is D-aspartate produced by glutamic-oxaloacetic transaminase-1 like 1 (Got1l1): A putative aspartate racemase? *Amino Acids*, 47(1), 79–86.

Tapiola, T., Alafuzoff, I., Herukka, S. K., Parkkinen, L., Hartikainen, P., Soininen, H., and Pirttilä, T. (2009). Cerebrospinal fluid β-amyloid 42 and tau proteins as biomarkers of Alzheimer-type pathologic changes in the brain. *Archives of Neurology*, 66(3), 382–389.

Topo, E., Fisher, G., Sorricelli, A., Errico, F., Usiello, A., and D'Aniell, A. (2010a). Thyroid hormones and D-aspartic acid, D-aspartate oxidase, D-aspartate racemase, H_2O_2, and ROS in rats and mice. *Chemistry and Biodiversity*, 7(6), 1467–1478.

Topo, E., Soricelli, A., Maio, A. Di, D'Aniello, E., Fiore, M. M. Di, and D'Aniello, A. (2010b). Evidence for the involvement of D-aspartic acid in learning and memory of rat. *Amino Acids*, 38(5), 1561–1569.

Van Veldhoven, P. P., Brees, C., and Mannaerts, G. P. (1991). D-Aspartate oxidase, a peroxisomal enzyme in liver of rat and man. *Biochimica et Biophysica Acta*, 1073(1), 203–208.

Wolosker, H. (2011). Serine racemase and the serine shuttle between neurons and astrocytes. *Biochimica et Biophysica Acta - Proteins and Proteomics*, 1814(11), 1558–1566.

Wolosker, H., Sheth, K. N., Takahashi, M., Mothet, J. P., Brady, R. O., Ferris, C. D., and Snyder, S. H. (1999). Purification of serine racemase: Biosynthesis of the neuromodulator D-serine. *Proceedings of the National Academy of Sciences of the United States of America*, 96(2), 721–725.

Wu, S. Z., Bodles, A. M., Porter, M. M., Griffin, W. S. T., Basile, A. S., and Barger, S. W. (2004). Induction of serine racemase expression and D-serine release from microglia by amyloid β-peptide. *Journal of Neuroinflammation*, 1(1), 2.

Xia, M., Liu, Y., Figueroa, D. J., Chiu, C. S., Wei, N., Lawlor, A. M., Lu, P., Sur, C., Koblan, K. S., and Connolly, T. M. (2004). Characterization and localization of a human serine racemase. *Molecular Brain Research*, 125(1–2), 96–104.

Yamada, R. H., Ujiie, H., Kera, Y., Nakase, T., Kitagawa, K., Imasaka, T., Arimoto, K., Takahashi, M., and Matsumura, Y. (1996). Purification and properties of D-aspartate oxidase from cryptococcus humicolus UJ1. *Biochimica et Biophysica Acta - Protein Structure and Molecular Enzymology*, 1294(2), 153–158.

Yamada, R., Nagasaki, H., Wakabayashi, Y., and Iwashima, A. (1988). Presence of D-aspartate oxidase in rat liver and mouse tissues. *Biochimica et Biophysica Acta*, 965, 202–205.

Yamamoto, A., Tanaka, H., Ishida, T., and Horiike, K. (2007). Functional and structural characterization of D-aspartate oxidase from porcine kidney: Non-Michaelis kinetics due to substrate activation. *Journal of Biochemistry*, 141(3), 363–376.

Yun, S. P., Kam, T. I., Panicker, N., Kim, S., Oh, Y., Park, J. S., Kwon, S. H., Park, Y. J., Karuppagounder, S. S., Park, H., Kim, S., Oh, N., Kim, N. A., Lee, S., Brahmachari, S., Mao, X., Lee, J. H., Kumar, M., An, D., … Ko, H. S. (2018). Block of A1 astrocyte conversion by microglia is neuroprotective in models of Parkinson's disease. *Nature Medicine*, 24(7), 931–938.

Zaar, K. (1996). Light and electron microscopic localization of D-aspartate oxidase in peroxisomes of bovine kidney and liver: An immunocytochemical study. *Journal of Histochemistry and Cytochemistry*, 44(9), 1013–1019.

Zaar, K., Köst, H. P., Schad, A., Völkl, A., Baumgart, E., and Fahimi, H. D. (2002). Cellular and subcellular distribution of D-aspartate oxidase in human and rat brain. *Journal of Comparative Neurology*, 450(3), 272–282.

Zhou, Q., and Sheng, M. (2013). NMDA receptors in nervous system diseases. *Neuropharmacology*, 74, 69–75.